Dynamic Simulation of Green Ammonia Synthesis Plant

Sampreeth Kambhampati

Delft University of Technology

TUDelft

Dynamic Simulation of Green Ammonia Synthesis Plant

by

Sampreeth Kambhampati

Student Number

5466598

to obtain the degree of Master of Science
in Mechanical Engineering
at the Delft University of Technology,
to be defended publicly on Tuesday October 31, 2023 at 10:00 AM.

Thesis Committee:	Prof. Dr. Ir. Earl Goetheer,	TU Delft
	Prof. Dr. Ir. Wiebren de Jong,	TU Delft
	Dr. Mahinder Ramdin,	TU Delft
	Dr. Gerard van Zee,	Proton Ventures B.V.
Project Duration:	January 2023 - October 2023	
Faculty:	Process & Energy Department, TU Delft	

An electronic version of this thesis is available at `http://repository.tudelft.nl/`.

TUDelft   **PROTON VENTURES**

Preface

It is with immense gratitude that I present this work, a collaboration with Proton Ventures. My time spent at this esteemed organization has been an absolute privilege which made me grow and expand my knowledge and skills in the field. Thank you for all the chocolates, biscuits and amazing conversations at the kitchen counter everyday.

I would like to extend my sincerest appreciation to my daily supervisor Dr. Gerard van Zee, who has been a source of guidance, encouragement and support throughout my project. Their expertise, coupled with their commitment to my personal and professional development, has made this experience unforgettable.

Moreover, I am deeply grateful to my professor Dr. Earl Goetheer at TU Delft who initially accepted to be my supervisor from Delft, and has been a constant source of inspiration, enlightenment and always being there during my ups and downs. Their remarkable knowledge, wisdom and insights have elevated my understanding of the subject matter to new heights. Thank you very much, Professor. I also wholeheartedly thank Prof. Wiebren de Jong and Dr. Mahinder Ramdin for being a part of the assessment committee.

In conclusion, I cannot overstate the importance of the support of my friends and family who made this journey possible. Their contributions have been vital for me me to reach this point, and for that, I am truly thankful. The two years of my time at TU Delft have been quite challenging but more fun and I am honoured to have been a part of this experience.

Sampreeth Kambhampati
Delft, October 2023

Summary

The carbon emissions from human activities are causing significant harm to the planet, leading to increased temperatures, melting of polar ice caps, rising sea levels, and other negative impacts on the environment. One promising solution is the use of green hydrogen as a fuel source, which could have a much lower carbon footprint than traditional fossil fuels. The production of hydrogen can be achieved through various methods, including the electrolysis of water, which splits water molecules into hydrogen and oxygen. To mitigate these effects and ensure a sustainable future, countries are taking various measures to reduce their carbon footprint, including increasing the use of clean energy sources and improving energy efficiency. Hydrogen storage and transportation pose major challenges since it is the one of the lightest gases leading to low energy densities.

Ammonia is emerging as a hydrogen carrier due to its high gravimetric storage densities of hydrogen. It is produced through the combination of hydrogen and nitrogen using the Haber-Bosch process. Ammonia can then be used as a clean and efficient fuel for various applications, such as transportation and power generation. Fluctuations in the hydrogen feed flow rate, resulting from variations in renewable energy sources can significantly impact the pressure and operating temperature within the system.

Morocco holds significant potential for renewable energy development due to its favorable geographic location and natural resources. The geographic location situated close to Europe makes Morocco well positioned for exporting green hydrogen to European markets. The chosen location for the ammonia plant is Boujdour in Morocco due to its excellent wind capacity factor of 67%.

Modern ammonia production plants employ control systems to maintain stable pressure. When there is a reduction in hydrogen feed flow rate, these reductions result in severe pressure reductions which would lead to metal fatigue and damage the entire production unit. Hence, these control systems respond by adjusting parameters to sustain pressure within the system. Aspen Plus Dynamics has been used in the present thesis work to model the dynamics of the ammonia synthesis plant. The varying hydrogen feed flow rate is a consequence of renewable energy fluctuations, which is served as the basis for modeling three distinct scenarios involving a 20%, 50%, and 70% reduction in hydrogen feed flow rate. Three distinct control strategies were developed where each control strategy, based on controlling the cooling duty of the condenser, manipulating the brake power of the recycle compressor, and regulating the nitrogen feed flow rate, demonstrated effective stabilization of the system's pressure, even during dynamically changing input conditions. Both linear and step reduction in hydrogen feed flow rate have been considered to gain understanding of the dynamic the behaviour of the system.

Significant outcomes were found when a reduction in hydrogen feed flow rate is imposed on all three control strategies. For a 20% reduction in hydrogen feed flow rate, the condenser's duty reduced from -1.2 MW to -1.05 MW, while the brake power of recycle compressor reduced from 12.5 kW to 5.5 kW. Furthermore, the stoichiometric ratio of $H_2:N_2$ changed from 3 to 2.8. These changes successfully stabilized the pressure in the ammonia synthesis plant under varying hydrogen input flow rate.

To determine the economic feasibility, an in-depth economic analysis was conducted, considering different renewable energy systems—solar, wind, and hybrid (solar+wind). The analysis revealed that using wind power is the optimal choice for ensuring a high capacity factor, thus making it the most feasible and sustainable energy source to power the ammonia plant achieving an annual ammonia capacity factor of 80%. It has been observed that using wind energy with oversized electrolyzer and introducing a hydrogen buffer resulted in reduction of levelized costs of ammonia (LCOA) by 11% (USD 1.3/kg to USD 1.15/kg). In conclusion, this thesis work underlines the viability of green ammonia production, emphasizing effective control strategies to adapt to renewable energy fluctuations.

Contents

List of Figures

List of Tables

<div align="right">1</div>

Introduction

1.1. Impact of Carbon Emissions

The impact of carbon emissions on the planet is significant and far-reaching. Climate change causes rising temperatures, rising sea levels, and more frequent and intense weather events such as hurricanes, droughts, and heatwaves. These changes have a negative impact on ecosystems and wildlife, and can lead to food and water scarcity, displacement of populations, and increased frequency of natural disasters.

To mitigate the impact of carbon emissions, various governments and organizations are taking steps to reduce emissions and transition to clean, renewable energy sources. This includes initiatives such as transitioning to electric vehicles, improving energy efficiency, investing in renewable energy, and implementing carbon pricing and cap-and-trade systems. In addition, the Paris Agreement, a global treaty signed by nearly 200 countries, pursues limitation of global warming to well below 2°C above pre-industrial levels and pursue efforts to limit warming to 1.5°C. [1]

The idea of sustainability refers to meeting the needs of the current generation without jeopardizing future generations' ability to meet their own needs. The use of hydrogen as a fuel and ammonia as an energy carrier are seen as important steps towards achieving a sustainable, zero carbon footprint future [2]. Hydrogen is a clean, renewable fuel that can be produced through the electrolysis of water. When burned, it produces only water and heat, making it a zero-emissions fuel. It can be used in a variety of applications, including powering vehicles and generating electricity. Together, hydrogen and ammonia have the potential to play a significant role in reducing greenhouse gas emissions and moving towards a more sustainable energy future. By using these clean, renewable energy sources, it is possible to reduce dependence on fossil fuels and contribute to a zero carbon footprint future.
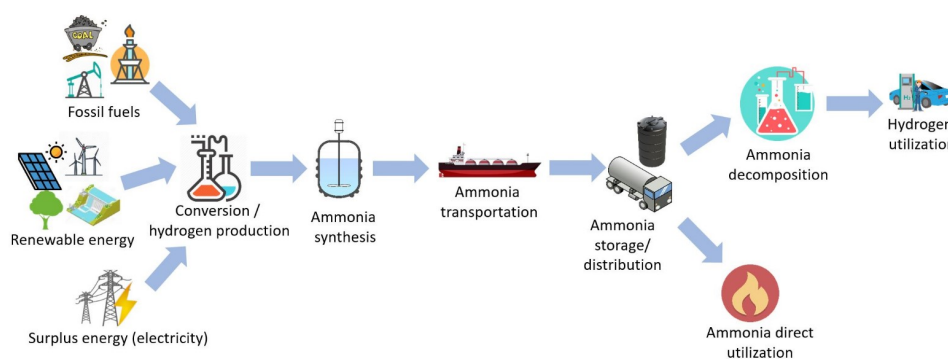
Figure 1.1: Power to Hydrogen to Ammonia to usage chain [3]

Ammonia production has a significant impact on global CO_2 emissions. It has been estimated that the largest emitting product of the chemical sector is the ammonia industry. It accounts for 1.3% of global CO_2 emissions [4]. Ammonia production is carried out by Haber-Bosch process which requires high temperatures and pressures and consumes a significant amount of power. The CO_2 emissions are projected to decrease from ammonia production from 2020 to 2050 as shown below in Figure 1.2 according to IEA [5]. These reduction in emissions could be expected due to changes in energy sector by utilizing renewable energy generated electricity, where emissions are reduced by 95% reaching net zero by 2040 and Net Zero Emissions by 2050 [4].
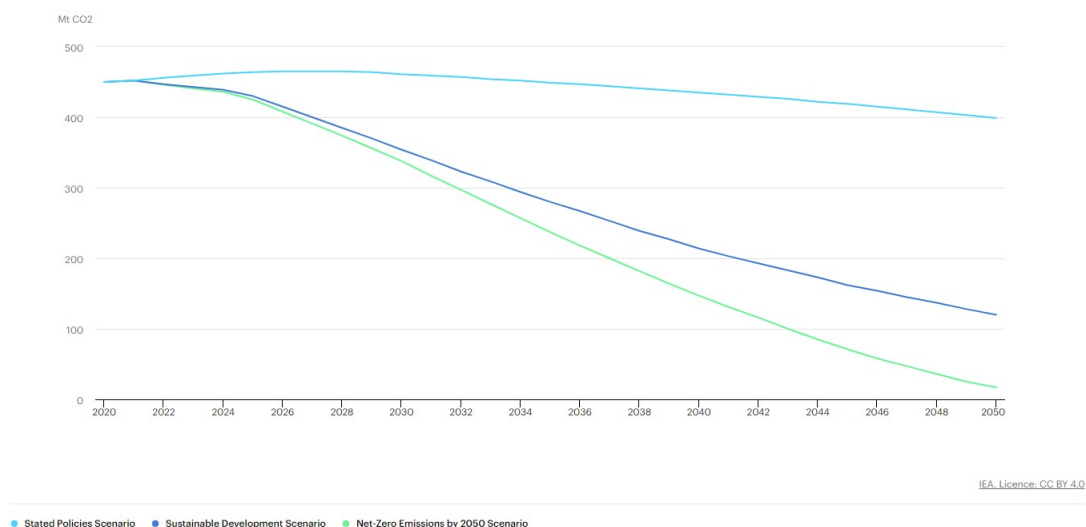
Figure 1.2: CO_2 emissions from ammonia production from 2020 to 2050 by IEA [5]

Several efforts are being made to reduce the carbon footprint from ammonia production. One way to accomplish this is to use renewable energy sources, such as solar or wind to produce hydrogen, which is used in Haber-Bosch process. Another way to reduce the impact of carbon emissions is to capture and store the CO_2 from ammonia production. This process is known as Carbon Capture and Storage (CCS). The use of CCS can reduce the CO_2 emissions from ammonia production by 90% [4].

The hydrogen produced from water electrolysis can be used as feed stock to produce ammonia. This method of ammonia production offers several benefits, including energy storage, carbon-free fertilizer production for sustainable agriculture, and reduced greenhouse gas emissions. Ammonia can be easily stored in bulk as a liquid at modest pressures or at ambient pressures if refrigerated to -33°C. Several techniques are already in place for ammonia storage and transportation from decades.

The current research project is performed in collaboration with **Proton Ventures B.V. & TU Delft**. Proton Ventures is a participant of the EU research program **ARENHA** (Advanced materials and Reactors for ENergy storage tHrough Ammonia). ARENHA is a European project with global impact seeking to develop, integrate and demonstrate key material solutions enabling the use of ammonia for flexible, safe and profitable storage and utilization of energy. One of the objectives of this program is the development of a demonstration unit for the production of ammonia from hydrogen obtained by electrolysis at varying capacity.

The production of hydrogen from renewable energy sources and subsequent production of ammonia is the central theme of the current thesis project. The thesis project focuses more in detail on dynamics in producing ammonia from renewable energy sources. The research questions and the goal of the current thesis project have been discussed in section 1.3.

1.2. Ammonia as a hydrogen carrier

Handling the intermittent nature of renewable energy production is a major challenge in the 21st century. Due to these fluctuations in space and time, energy storage techniques with high efficiencies and capacities are required. In this regard, ammonia is considered to represent as one of the promising hydrogen carriers due to its high volumetric and gravimetric hydrogen storage densities [6]. The comparison can be seen in the Figure 1.3 below.
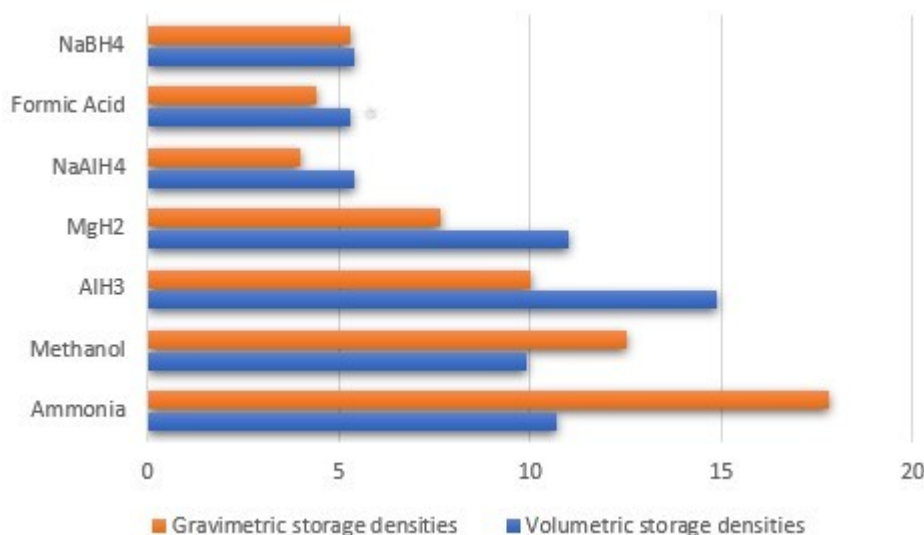
Figure 1.3: Volumetric (kg/100L) and gravimetric (wt%) hydrogen storage densities for various components

The issue of hydrogen storage and delivery opens up prospects for ammonia to be viewed as an alternative renewable energy storage medium. Ammonia is produced from Haber-Bosch process which is one of the most conventional processes in the world. Around 80% of produced ammonia is used as fertilizers in the agricultural field [7]. Production of ammonia through renewable sources is not a novel idea and isn't fully considered over methane or coal-based ammonia. As a result, ammonia can be produced via sustainable ways. Ammonia can then be transported as renewable energy from places where there is cheap/excessive renewable energy availability to those places where the renewables are limited/expensive [8]. Ammonia is a carbon free molecule and doesn't emit any carbon when burnt or decomposed into constituent gases. The boiling point of ammonia is around -33°C at atmosphieric pressures which makes it relatively easier to store and transport than compared to that of hydrogen (-253°C).

Ammonia could also be compressed to liquid at a mild pressure of 10 bar and atmospheric temperatures. Ammonia is also the second most produced chemical in world after sulfuric acid in the world, with 180 million tonnes of ammonia being produced per year [9]. Many infrastructures and engineering practices are already in place for the production, storage and transportation of ammonia. Ammonia has a distinct odour that is clearly detectable by human nose at extremely low quantities, allowing preventative steps to be implemented promptly. Furthermore, Ammonia is also non-flammable, with a comparatively low explosive limit (16-25% in air). The likelihood of ammonia causing combustion and explosion is thought to be lower than that of other gas and liquid fuels [9].

Some of the advantages of implementing ammonia as a hydrogen carrier are [10] [11]:

- High gravimetric hydrogen storage densities
- Mature technology of production and the second most produced chemical in the world
- Zero-carbon chemical
- Easy liquefaction by compression making it easy for transportation and storage
- Production, transportation and storage technologies already in place

1.3. Research Questions

The following research questions form the basis of the current project:

- How can a stable ammonia synthesis process be maintained under varying hydrogen feed flow rates?

    - How can the dynamic behaviour of the system be modelled?
    - What are the suitable control philosophies to maintain pressure under dynamic input?

- How can the complete ammonia plant be optimized by introducing a hydrogen buffer for realistic renewable power availability scenarios?

    - What renewable power source can be considered to ensure ammonia production with reduced levelized cost of ammonia?
    - What is the optimum amount of hydrogen storage capacity required for the selected ammonia production capacity?

1.4. Objective & Scope

The major goal of the present study is to examine the dynamic response of an ammonia synthesis process to variations in the hydrogen feed flow rate. The source of these variations is due to the renewable power provided to an electrolyzer for hydrogen production. The goal of this project is to demonstrate operation of an ammonia plant capable of generating 25 tonnes of ammonia per day. This scale was selected as the plant's capacity because it represents a scale at which the ammonia production process can be effectively integrated with renewable energy. The feasibility and practicality of green ammonia production is investigated for this selected scale size.

In particular, **Boujdour in Morocco** was chosen as the intended area of operation for the present ammonia synthesis facility because it has excellent access to solar and wind energy resources [12], which is consistent with a highly competitive large-scale manufacturing industry utilizing its close proximity to the European Union.

The project merely comprises of an ammonia synthesis loop assuming that the hydrogen input is produced by an electrolyzer unit. The primary focus of the research is to create a model which can accommodate dynamic fluctuations in hydrogen feed flow rate by implementation of control philosophies to stabilize pressure in the system. The storage and transportation of produced liquid ammonia is not modelled as it is out of scope.

Capacity	25 tonnes/day
Operating Pressure	150 bar
Feed conditions	$25°C$ and 80 bar
NH$_3$ Separation Method	Cryogenic Condensation
Pressure Drop	3.5 bar

Table 1.1: Characteristics of ammonia synthesis unit for present thesis work

The predominant purpose of the research is to produce liquid ammonia, which may subsequently be utilized to transport energy from one location to another. The classic condensation method was chosen because it is consistent with the overall goal of the study and its potential influence on energy transportation and other sectors.

An overall schematic of the process is shown in Figure 1.4. The scope of this thesis work is limited to the dynamics of ammonia synthesis unit. Therefore, the production of hydrogen and nitrogen are not modelled in the current thesis work and the red dashed line represents the scope boundary for modelling of production unit.
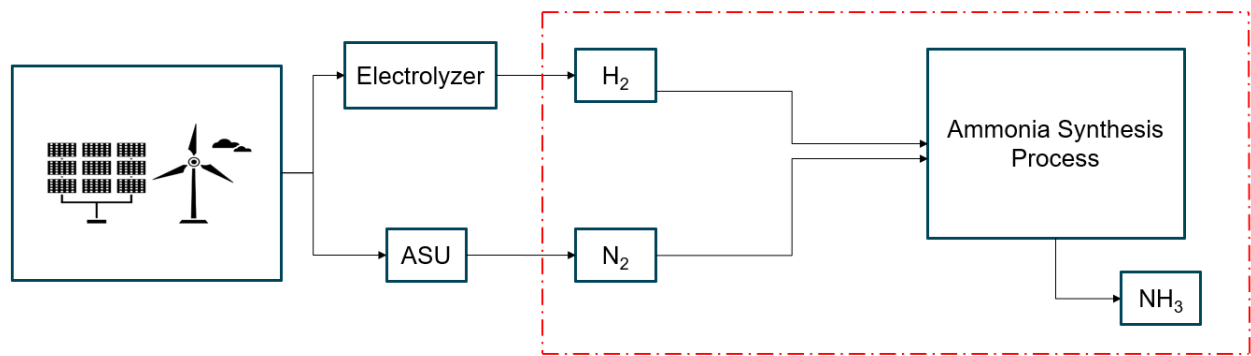
Figure 1.4: Complete schematic of Power-to-Ammonia process

Figure 1.5 shows the process flow diagram of the ammonia synthesis plant that is modelled for the current thesis project.
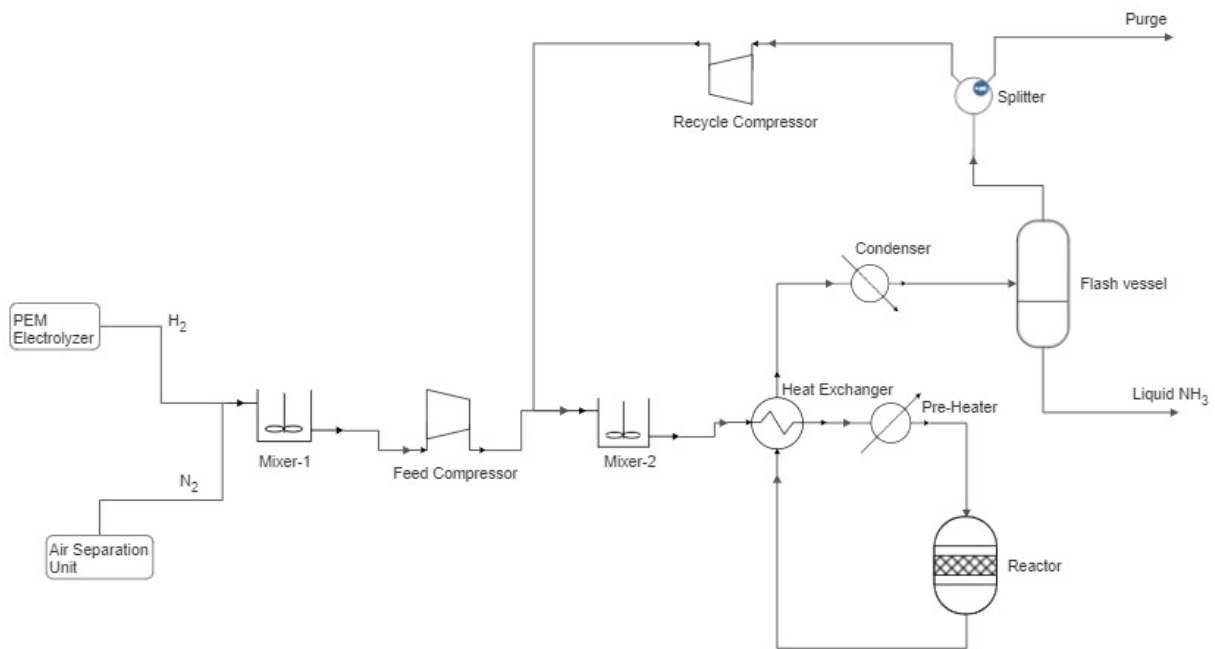
Figure 1.5: Ammonia Synthesis Plant Flowsheet

1.5. Approach

The following approach has been used to carry out the current thesis project as shown in Figure 1.6. The figure below describes each step followed during the project.

Figure 1.6: Overview of Approach

The three main elements of the performed research are:

1. **Steady State Simulation**

   • Process design is carried out during the initial design phase in Aspen Plus
   • The optimal operating conditions, equipment sizes and configurations are determined
   • The cooling and heating requirements of the plant have been evaluated.

2. **Dynamic Simulation**

   • The effect of change in hydrogen feed flow rate is examined
   • Three different control strategies are developed to control the change in pressure in the process
   • Amount of excess hydrogen required and size of storage tank are determined

3. **Economic Evaluation**: A brief cost estimation is carried out using HySupply hydrogen and ammonia cost tools [13] by using different sources of renewables (solar, wind and hybrid) and the complete value chain of power-ammonia is assessed.

1.6. Organization of this document

The following section gives a brief description of each chapter that is included in this report:

Chapter 2: "Literature Review" - This chapter provides an overview of the literature study that has been carried out in the initial phase of the thesis project.

Chapter 3: "Methodology" - This chapter focuses on the scenarios, assumptions made and the softwares used for the current thesis project.

Chapter 4: "Steady State Simulation" - This chapter gives an overview about the working of steady state model and different components selected for the chemical plant.

Chapter 5: "Dynamic simulation" - This chapter outlines the effect of variation in hydrogen feed flow rate on the entire ammonia synthesis plant. The current chapter also covers different strategies used to control the pressure.

Chapter 6: "Economic Evaluation" - This chapter provides a brief overview of cost estimate of the ammonia synthesis plant.

Chapter 7: "Results and Conclusion" - This chapter highlights the answers to the research questions and recommendations for the future work.
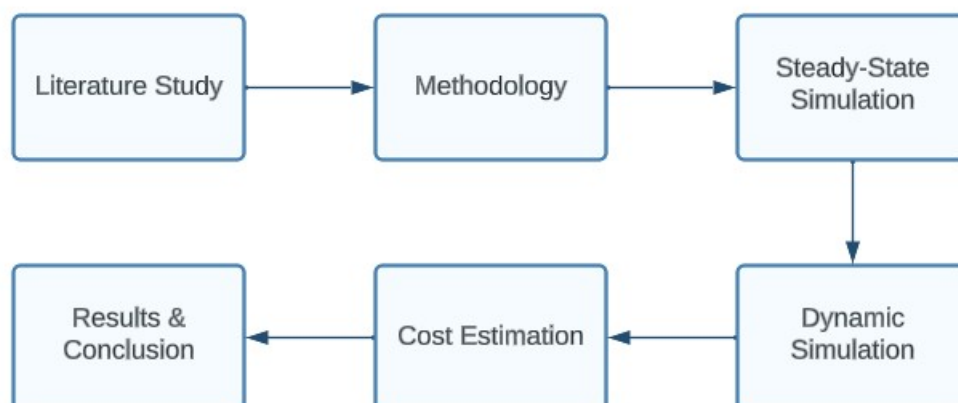
Figure 1.7: Organization of the Report

2

Literature Study

2.1. Fluctuations in solar and wind energy

The reduction of greenhouse gases is by far one of the biggest challenges ongoing. The primary reasons associated behind the emission of these greenhouse gases are power generation, transportation and industrial activities [14]. Several initiatives are being taken by various sectors and one of the most promising and an effective action is to use the energy from renewable sources. These renewable sources are comprised of hydropower, wind power, solar power, and geothermal power.

Renewable energy sources and their percentage in power production have steadily expanded, owing mostly to energy regulations, markets, and environmental concerns. Wind power and photovoltaics (Solar) are two of the most important renewable energy sources [15]. Despite the numerous advantages of renewable energy sources, several shortcomings remain, such as: output discontinuity owing to seasonal changes since most renewable energy supplies are climate-dependent, necessitating sophisticated design, planning, and control optimization approaches. Intermittent renewables are difficult to implement because they disrupt traditional techniques of planning the daily functioning of the electric grid. For example, because solar energy is only accessible during the day, the grid operator must modify the day-ahead plan to include units that can swiftly alter their power output to compensate for the increase and decrease in solar generation [16].

On top of this, there are additional fluctuations during the day caused by the clouds. Therefore it is more difficult for the grid operator to control the whole unit operation because of the variability by clouds. Similarly, intra hourly fluctuations in wind energy are caused due to fluctuations in wind speed and atmospheric instability. As a result, to maximize the utilization of the renewable energy, it requires grid power optimizations along with energy storage technology [14]. Another promising solution is to deploy solar/wind combined renewable energy production site in such a way that wind power compensates the deficiency of electricity output from solar power.

Boujdour located in the Western Sahara to south-west of Morocco is chosen to be the best location for the current thesis project because of exceptional wind energy production efficiencies. Figure 2.1 illustrates the wind speed of 10 m/s for 100m tall wind turbines. Figure 2.2 and Figure 2.3 show the fluctuations in solar and wind energy powered electricity generation. The optimum year round tilt angle for the solar panels is $24.4°$ from horizontal according to [17]. For the selected region, the mean capacity factor is 22.4%. Using Siemens Gamesa SG 4.5 145 turbine at 107m hub height [18], the total mean capacity factor is 66.7%. All the above values were obtained from renewables.ninja [19]. Mean capacity factor is defined as the ratio of actual electricity output by maximum possible output.
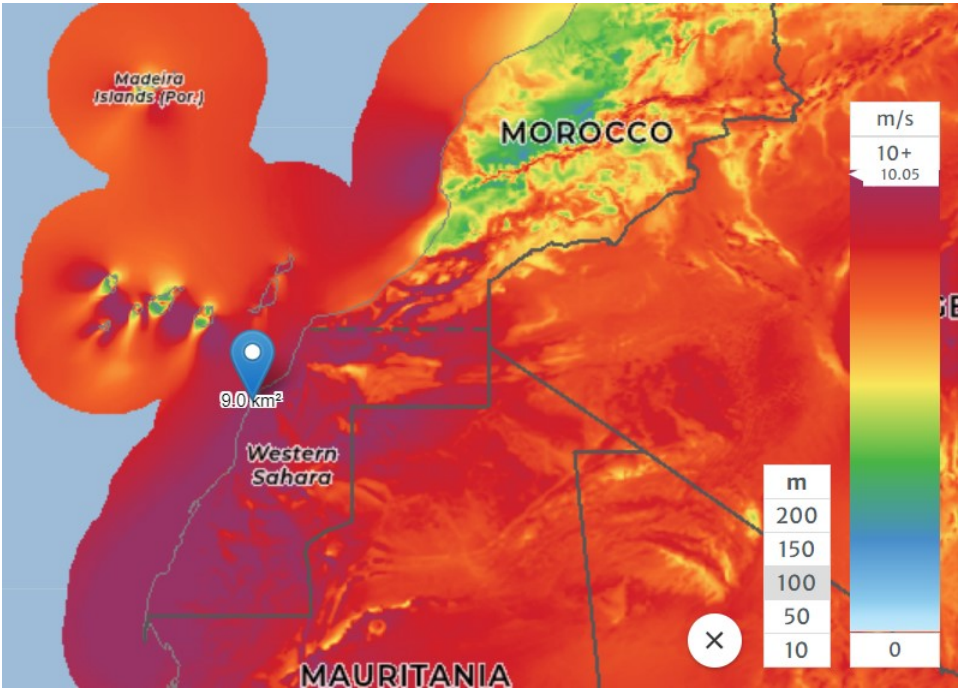
Figure 2.1: Illustration of wind speed in Boujdour, Morocco [12]

Figure 2.2: Solar energy powered electricity generation profile in Boujdour, Morocco [19]

Figure 2.3: Wind energy powered electricity generation profile in Boujdour, Morocco [19]

2.2. Hydrogen Production & Storage

Hydrogen is produced from various sources. Hydrogen is classified into three categories, can be identified by distinct colors, based on the environmental friendliness of the manufacturing method. The colors used for classification are green, grey and blue and depend on the primary resources used for the production of the gas [20]. The hydrogen produced from renewable energy sources is called Green Hydrogen. The hydrogen produced from fossil fuels is called Grey Hydrogen. The hydrogen produced from fossil fuels with capturing and storing CO_2 is called Blue Hydrogen [21].

Hydrogen can be created using a variety of renewable and non renewable energy sources. These include fossil fuels, particularly steam methane reforming, oil reforming, coal gasification, biomass gasification, various biological sources, and water electrolysis [22].

Nevertheless, natural gas steam reforming has been the most frequently utilized hydrogen generation process in recent years, accounting for around 50% of hydrogen products, followed by oil reforming and coal gasification. This classification is shown in the Figure 2.4 below:
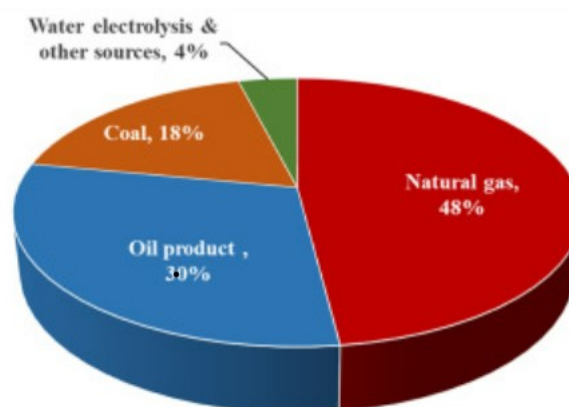
Figure 2.4: Comparison of various hydrogen production sources [20]

Water electrolysis is a technique which is used to split water into hydrogen and oxygen gases. The process uses electricity from renewable energy sources. The current research is mainly focused on various techniques of electrolysis because the end goal is to produce ammonia using renewable energy sources. The different electrolysis technologies addressed in the current thesis project are:

- Alkaline Water Electrolysis
- Proton Exchange Membrane Electrolysis
- Solid Oxide Electrolysis

2.2.1. Alkaline Water Electrolysis

The process generally consists of an anode and a cathode connected to an external power supply and are immersed in a conducting electrolyte. The alkaline water electrolyser is made of an electrolyte in aqueous solution which consists of either NaOH or KOH in a 20-40 wt % [23]. The operating conditions typically range from temperatures of 50-90 °C and pressure upto 30 bar. The specific energy consumption of the system is around 4.2 - 4.8 kWh / Nm^3 H$_2$.

The electrode material chosen for the anode and cathode should be corrosion resistant, have high conductivity, have a high catalytic effect, and be inexpensive. Although stainless steel and lead were mentioned as inexpensive electrode materials with low overpotentials, they cannot withstand strongly alkaline conditions. Noble metals were discovered to be prohibitively costly for usage as bulk electrode materials. Therefore, Nickel was later identified as an electroactive material with high corrosion resistance in alkaline solutions [24].

The reactions (Equation 2.1) & (Equation 2.2) occurring at anode and cathode are called Oxygen Evolution Reaction (OER) and Hydrogen Evolution Reaction (HER) respectively. Hydrogen is generated at the cathode while oxygen is generated at the cathode.

$$Anode: 2OH^- \longrightarrow 2H_2O + \frac{1}{2}O_2 + 2e^- \tag{2.1}$$

$$Cathode: 2H_2O + 2e^- \longrightarrow 2OH^- + H_2 \tag{2.2}$$
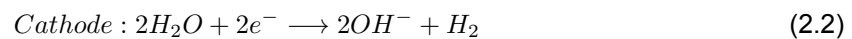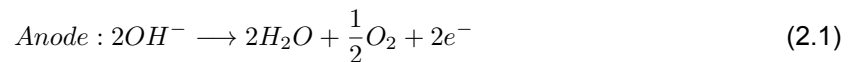
The overall cell reaction of the water electrolysis process is shown in Equation 2.3

$$H_2O \longrightarrow H_2 + \frac{1}{2}O_2 \tag{2.3}$$

A basic schematic of alkaline water electrolyzer is shown below in Figure 2.5
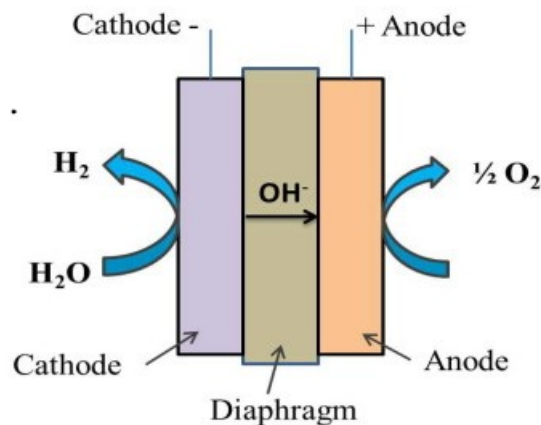
Figure 2.5: Alkaline Electrolyzer [22]

A diaphragm separates two compartments in an alkaline water electrolyzer. Typically, this diaphragm is constructed of asbestos or polyphenylene sulphide. When a direct current (DC) current is supplied through the unit, electrons go from the DC power source to the cathode. These electrons are consumed by the hydroxide ions to generate hydrogen gas [25]. Normally, these hydroxide ions travel from the cathode to the anode via the diaphragm. As a result, the hydrogen and oxygen gases which are formed at the cathode and anode respectively are collected and stored/utilized for further applications.

The minimum required cell voltage for the electrochemical reaction can be determined by thermodynamics. The energy required to decompose one mole of water is related to enthalpy of formation of one mole of water. The minimum amount of enthalpy that has to be applied as electrical energy is the change in Gibbs free energy [23]. This change in Gibbs free energy is represented in terms of change in enthalpy of reaction, entropy of reaction and the reaction temperature as shown in the Equation 2.4

$$\Delta G_{reac} = \Delta H_{reac} - T \Delta S_{reac} \tag{2.4}$$

At standard temperature and pressure, the reversible cell voltage (U_{rev}) is 1.23V. It is the minimum voltage needed for the electrolysis when the reaction occurs ideally. This reversible voltage is usually expressed by Nernst equation in terms of change in Gibbs free energy and the Faraday's constant [26] as shown in Equation 2.5

$$U_{rev} = \frac{\Delta_R G}{n\ F} \tag{2.5}$$

where, n is the equivalent number of material (n=2) and F is Faraday's constant (F = 96500 C/mole)

There are advantages and disadvantages associated with usage of alkaline water electrolysis for the production of hydrogen. Some of the advantages are [27]:

- It is a well established technology and has long term stability
- Relatively low manufacturing cost
- Usage of non noble catalysts

Some of the disadvantages are [28]:

- Low current densities and possibility of gas crossover
- Slow start-up and corrosion problems due to the electrolyte
- Complicated maintenance because of many components in the device

2.2.2. Proton Exchange Membrane (PEM) Electrolysis

The first PEM electrolyser was introduced by General Electric in the early 1960s through the work of Thomas Grubb and Leonard Niedrach. The fundamental difference between the PEM electrolyzer and the alkaline water electrolyzer is the employment of a thin-film electrode assembly (membrane electrode) to generate a zero pole spacing [28]. The specific energy consumption of the system is around 4.4 - 5.0 kWh / Nm^3 H_2. This technology of PEM electrolysis was invented to overcome the drawbacks that were being faced whilst using alkaline water electrolyzer.

PEM electrolyzers consist of solid polysulfonated membranes (Nafion,fumapem) as an electrolyte which conducts protons. The usage of membranes have various advantages such as lower gas permeability, high proton conductivity, lower thickness and high pressure operations [22]. PEM electrolyzers can be operated at a current density of 10000-20000 A/m^2 which is around 5 times more than that of an alkaline water electrolyzer. The operating temperatures are around 50-80°C and operating pressures are around 80 bar. A typical schematic of a PEM electrolyzer is shown below in Figure 2.6
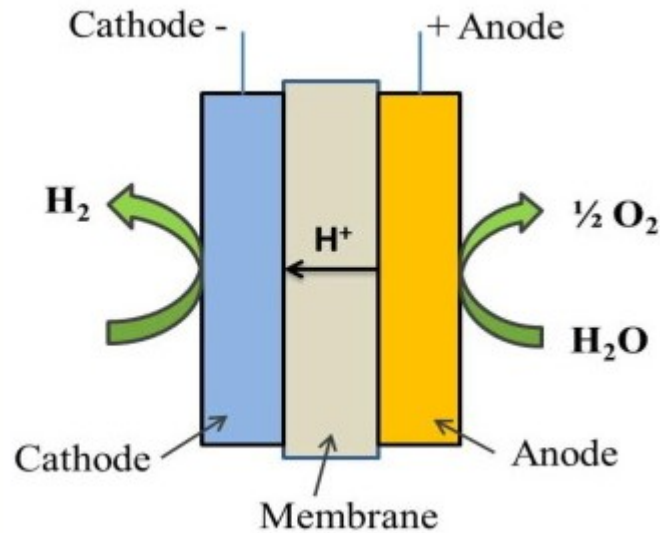
Figure 2.6: PEM Electrolyzer [22]

In the working of PEM electrolyzer, the deionized water is only sent to the anode side unlike the alkaline electrolysis. The water is split into oxygen, hydrogen ions and electrons. These hydrogen ions move to the cathode side through the proton conducting membrane. The electrons escape the anode through the external power circuit, which provides the reaction's driving force (cell voltage). At the cathode side, the hydrogen ions and electrons re-combine to produce hydrogen gas. The following half-cell reactions at the anode and cathode are shown below in Equation 2.6 & Equation 2.7 respectively [22].

$$H_2O \longrightarrow 2H^+ + \frac{1}{2}O_2 + 2e^- \tag{2.6}$$

$$2H^+ + 2e^- \longrightarrow H_2 \tag{2.7}$$

The membrane separates hydrogen from oxygen and therefore the gases are sent to further treatment and stored in later on stages.

The PEM electrolyzer has various advantages and disadvantages. Some of the advantages are:

- The system can be operated at high pressures
- The method has high energy efficiency due to the usage of a membrane and the absence of solution voltage drop
- High dynamic operation i.e., certain to handling fluctuations in the electricity input
- High purity hydrogen due to high current densities
- the system has a rapid response time and corrosion-free environment

Some of the disadvantages associated are [27]:

- High costs of components due to usage of noble and scarce metal elements like iridium as catalyst
- Acidic environment since the Nafion tubing absorbs the OH^- groups and leaves the excess H^+ in the water causing the pH to decrease
- Low durability of the equipment

2.2.3. Solid Oxide Electrolysis

The working principle of Solid Oxide Electrolytic Cell is similar to that of Solid Oxide Fuel Cell (SOFC). In a typical SOFC, the cell is used to generate electricity by directly transforming the chemical energy in the fuel to electrical energy [29]. Whereas, a solid oxide electrolytic cell (SOEC) is a regenerative solid oxide fuel cell that electrolyzes water using a solid oxide, or ceramic electrolyte to create hydrogen gas

and oxygen. These electrolyzers operate at very high temperatures. The specific energy consumption of the system is around 2.5 - 3.5 kWh / Nm^3 H_2. A typical schematic of SOEC is shown below in Figure 2.7.
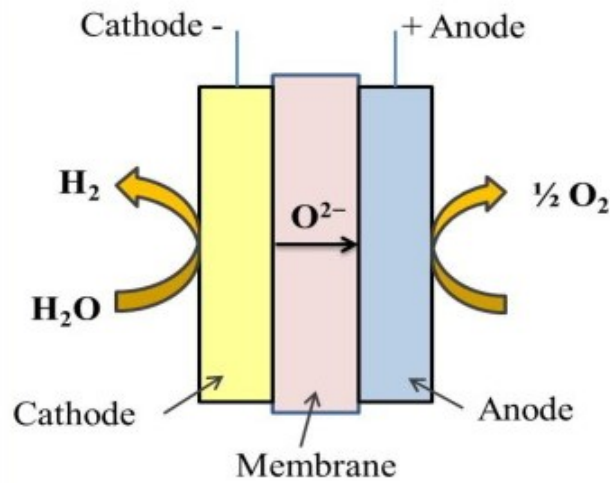
Figure 2.7: Schematic of solid oxide electrolysis [22]

SOECs consist of three components, a solid electrolyte and two porous electrodes. The most commonly used electrolyte is Yttrium Stabilized Zirconia (YSZ). YSZ consists of zirconium dioxide doped with 8 mol% of yttrium oxide. This material is mainly used since it has properties that make it suitable for high temperature processes. YSZ has high strength, high melting temperature and excellent corrosion resistance. On top of that, it enables oxygen ion conduction while blocking electronic conduction [30]. The high resistance of YSZ electrolytes limits the electrolysis performance when the temperatures are below 500°C and hence this process is carried out at high temperatures.

The operating temperatures of SOECs range from 500-850°C. Since the operating temperatures are quite high, the water is fed in the form of steam to the porous cathode. When a voltage is applied to the cell, the steam moves towards the cathode-electrolyte interface and is reduced to form pure hydrogen gas and oxygen ions. These oxygen ions are sent to the anodic side of the cell through the dense electrolyte and thereafter oxygen gas and electrons are produced. The produced electrons are again sent back from the anode to the cathode by external power supply as a driving force [31]. The electrolyte must be dense enough such that the steam and hydrogen gas cannot diffuse through thereby leading to recombination of the H_2 and O^{2-}. The hydrogen evolution reaction and the oxygen evolution reaction occurring at cathode and anode are given by (Equation 2.8) & (Equation 2.9) respectively.

$$H_2O + 2e^- \longrightarrow H_2 + O^{2-} \tag{2.8}$$

$$O^{2-} \longrightarrow \frac{1}{2}O_2 + 2e^- \tag{2.9}$$
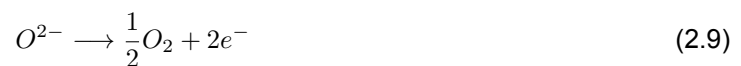
There are advantages and disadvantages as well which are associated with using SOECs for hydrogen production. Some of the advantages are [32]:

- The need for electrolyte loss maintenance and electrode corrosion is eliminated because of all the components being solid in the cell
- Expensive catalysts are usually avoided since the electrolyzers work at high operating temperatures
- These cells usually have a better ability to tolerate the presence of impurities
- Because of high operating temperatures, faster kinetics and more favorable thermodynamics are achieved

- High efficiency of hydrogen gas can be produced
- Very efficient when there is a source for steam available

Some of the drawbacks associated with SOECs are [33]:

- The materials used for components are thermally challenged and the material deterioration rate is noticeable because of high operating temperatures
- Incompatibility to intermittent power resources (takes time to heat up the cell and to start the process)
- Material fabrication is rather expensive and complicated

2.2.4. Comparison of different electrolysis techniques

Factors	Alkaline Electrolysis	PEM Electrolysis	Solid Oxide Electrolysis
Electrolyte	KOH/NaOH	Solid Polymer Electrolyte (Eg: Nafion)	Yttrium Stabilized Zirconia (YSZ)
Operating Temperatures (C)	60-90	50-80	500-1000
Current Density (A/cm2)	0.2-0.8	1-2	0.3-1
Electrolysis Efficiency	50-78%	50-85%	90% (laboratoy)
Pressure (bar)	1-30	10-200	1-25
Hydrogen Purity	99.5-99.9998%	99.9-99.9999%	99.9%
Capital Costs (USD/kW)	500-1000	700-1400	>2000
Lifetime (Stack) (hr)	60000	50000-80000	20000
Technology Readiness Level	9	8-9	5-6

Figure 2.8: Comparison of different electrolysis techniques [34] [35] [36]

2.2.5. Hydrogen Storage

To store hydrogen there are various technologies available. The three main categories associated with the storage of hydrogen are shown in Figure 2.9: (1) hydrogen can be stored in pure form, molecular gas or liquid with no extensive physical or chemical connection to other materials; (2) hydrogen molecules are adsorbed onto a material which are held by weak Van der Walls bonds; (3) hydrogen molecules can be chemically bonded [37]. Moreover, the chemical storage is divided into two subcategories based on the chemical bonding: metal hydrides and chemical hydrides.

Since hydrogen gas has a very low density (*1kg of hydrogen gas occupies 11 m^3 at standard conditions*), it is therefore difficult to store with high efficiency. Hence the storage density of hydrogen must be increased to make the storage of hydrogen remunerative. Due to the intermittency in the renewable energy sources (wind and solar), it is therefore necessary for surplus hydrogen to make sure that the entire ammonia plant operates continuously [38].
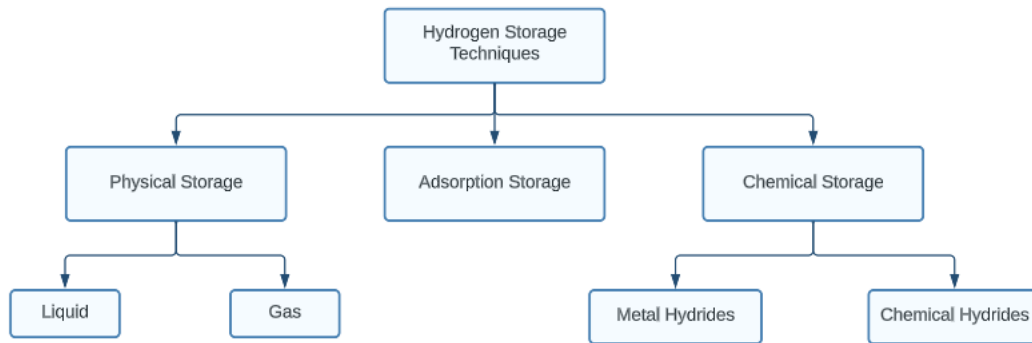
Figure 2.9: Different Technologies for hydrogen storage

Physical Storage

Physical hydrogen storage methods are primarily based on the compression and cooling/liquefaction of hydrogen. The process is carried out by cooling down the hydrogen gas using heat exchangers. The hydrogen gas is then stored in liquid hydrogen tanks, or in compressed gaseous hydrogen tanks where the gas is compressed to high pressures [37]. Both of the technologies require infrastructure - a compressor system for pressurization and cryogenics for liquefaction. Cryo-compressed hydrogen storage system is a combination of liquid hydrogen and compressed gaseous hydrogen storage systems. The cryo-compressed storage system was first launched by BMW in 2012 and allows a relatively high volumetric density (at 20K, from 70g/L at 1 bar to 87g/L at 240 bar) [39].

Compressed hydrogen gas storage

The compressed hydrogen gas storage system typically consists of two major components: the compressors necessary to raise the pressure of the gas in order for the gas to be stored, and the storage chambers. This technology of compressing the gas and storing is one of the most common technique used to store hydrogen. The storage tanks are pressurized up to a pressure of 700 bars [38]. The approach for high pressure compression is reasonably mature and easy in comparison to other techniques. However the system's weight and cost must be reduced more in the future.

The compressed gas can be stored either above ground or underground (below ground level). The storage above the ground requires sophisticated infrastructure and therefore it is quite expensive in terms of investment costs. As a result, it is possible to store the compressed gas underground by the means of salt caverns [38]. A basic schematic of how a salt cavern storage facility looks like can be seen in Figure 2.10.
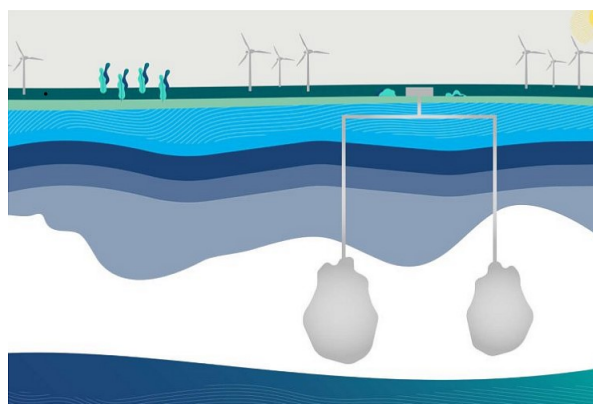
Figure 2.10: Underground H_2 storage facility [40]

Metal containers are generally used to store natural gas but could also be applied for the storage of hydrogen. Three different types of metallic containers are used for natural gas storage. They are:

- Gas holders, with storage pressures just above the atmospheric pressure
- Spherical pressure vessels, with storage pressures approximately up to 20 bar
- Pipe storages, with storage pressures up to approximately 100 bar [38]

Some of the advantages and disadvantages of storing hydrogen in compressed gaseous form are:

- \+ Well established technology and commercially available
- \- High energy input required because of use of compressors
- \- The storage densities are low leading to need for large storage specific volumes of storage tanks
- \- High investment costs and expensive to store high pressure gas

2.3. Nitrogen Production & Storage

The air in the atmosphere is composed of a mixture of several gases. The most important of these are nitrogen (N_2) and oxygen (O_2), which account for approximately 99.03% of the total sample volume. There are few other gases present in trace amounts due to natural processes and human activities. Water vapour is also present in the air. The water content of air fluctuates significantly with local ambient conditions. Dry air contains around 78.10% nitrogen, 20.90% oxygen, and 0.933% argon by volume along with traces of other gases like hydrogen, helium, neon, krypton, xenon, carbon dioxide etc [41]. The production of oxygen and nitrogen is accomplished by an air separation process, which involves the separation of air into a stream containing mostly nitrogen and an oxygen enriched stream.

Air separation is typically classified as cryogenic and non-cryogenic. The non-cryogenic methods include pressure swing adsorption and membrane separation. A detailed description of each process type is given in the following subsections.

2.3.1. Cryogenic Distillation

Gases such as oxygen, nitrogen, and argon are created from the air that surrounds us. Separation of the naturally occurring air components allows us to develop their particular features and employ them in a variety of applications. These gases are usually produced in Air Separation Units (ASUs) that use cryogenic distillation. Cryogenic distillation is a process where the gases are cooled down to extremely low temperatures therefore separating them in the form of liquid [42].

The plant consists of a collection of equipment such as

- Distillation columns
- Heat exchangers
- Adsorbers
- Gas and liquid compressors
- Turbine and supporting apparatus for control

As per the requirement, the component gases are sold and delivered to clients for a wide range of industrial, medicinal, and other specialized uses. The core technique for large-scale air separation has stayed stable for decades, however equipment orientation will alter depending on process needs. A basic overview of various steps associated with the cryogenic distillation process is shown below in Figure 2.11 based on [43].
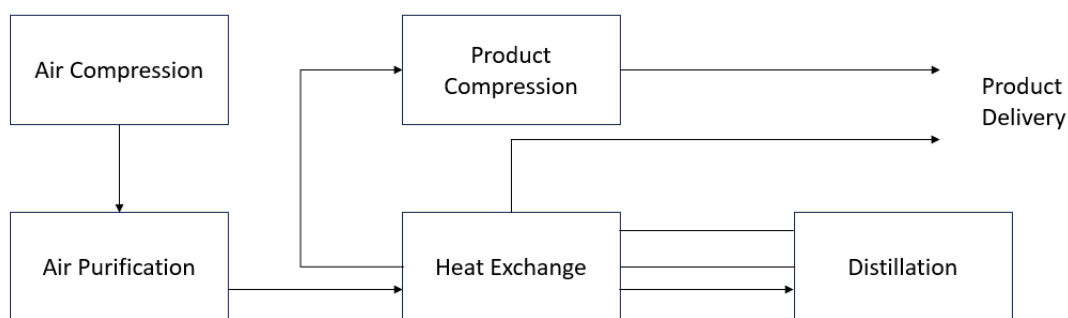
Figure 2.11: Overview of cryogenic distillation

The various steps involved in cryogenic distillation of air are:

- Pre-treatment, Compression and cooling of air
- Removal of carbon dioxide
- Heat exchange to reduce the temperature of feed air to cryogenic temperatures
- Distillation of air

Pre-treatment, compressing and cooling the feed air is the first step in cryo-distillation air separation unit. Air is first purified by sending it through filtration devices for removal of dirt. The feed air is then compressed till 5-10 bar and is then sent to the next step [44]. The compression of air is a necessary step in order to ensure the efficiency of the system and increasing the purity of air. Thereafter, the compressed air is sent to several stages of intercoolers for cooling and much of the water vapour is condensed and removed.

Removal of Carbon dioxide and Water vapour is a critical step to do before releasing the air downstream. This is done because at low temperatures, carbon dioxide and water would ultimately freeze and block the apparatus. As a result, remaining water vapour and carbon dioxide must be eliminated to match the product's specifications. The most widely used purification technology is molecular sieve adsorption, in which water and carbon dioxide molecules are adsorbed onto the surface of a molecular sieve at near-ambient temperatures. [44].

Additional heat exchange is carried out against the cold product and waste gas streams to bring the air feed to cryogenic temperatures. The cooling is performed by the use of Brazed Aluminum heat exchangers, which are utilized to cool the incoming air flow to a temperature adequate for downstream components (boiling point of nitrogen is 77 K). The outgoing gas streams are warmed to a temperature close to that of ambient air. The heat exchange between feed and product streams reduces the plant's net refrigeration load and, as a result, energy consumption.

Distillation of air is done after the heat exchange. Part of the air liquefies to form a liquid that is enriched in oxygen after the heat exchange. The remaining gas that is richer in nitrogen is distilled to almost pure nitrogen in a distillation column. In order to separate nitrogen usually one distillation column is needed but if the required purity of Nitrogen is very high then two distillation columns are used.

There are some advantages and disadvantages associated with using cryogenic distillation for nitrogen production. Some of the advantages are [45]:

- Most efficient process for large scale production of gases compared to membrane separation and pressure swing adsorption
- Yields high purity products
- Liquid forms of cryogenic gases are easier and cheaper to transport

However, the major drawbacks associated with cryogenic distillation are [46]:

- Large scale utility and space required for economic feasibility
- High capital costs
- Longer time required for start-up or shut down
- High energy costs to cryogenically cool gases
- Indirectly causes the release of significant quantity of greenhouse gases due to huge power consumption

2.3.2. Pressure Swing Adsorption

Pressure Swing Adsorption (PSA) is a non-cryogenic process used for the extraction of nitrogen from air. These systems work on the principle of adsorption by trapping the oxygen molecules from compressed air to produce nitrogen. The most commonly used adsorbent is Carbon Molecular sieve (CMS) for PSA applications. Carbon molecular sieves have pores of molecular dimensions which provide a relatively high adsorption capacity and kinetic selectivity for various gases. The PSA approach is based on the difference in kinetics of oxygen and nitrogen adsorption, with oxygen adsorption being substantially quicker than nitrogen adsorption [47]. Three different stages are involved in this process and are shown below in Figure 2.12
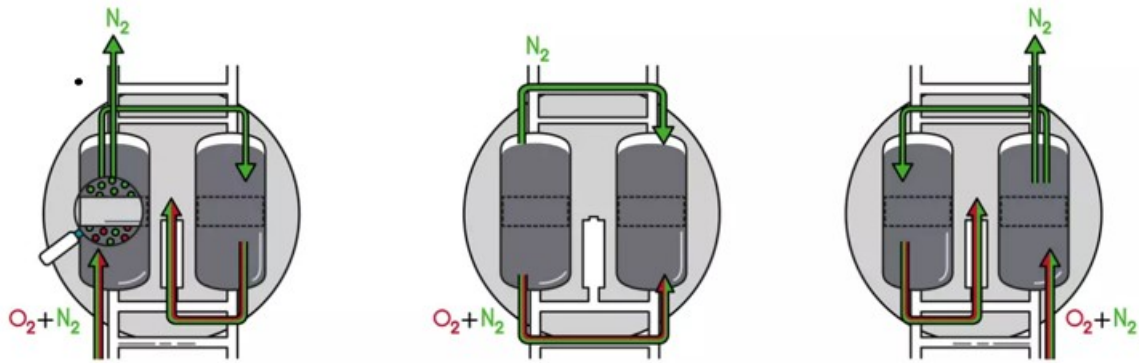
Figure 2.12: Pressure Swing Adsorption [48]

When compressed air passes over the material, oxygen molecules are adsorbed into the pores. At some point the carbon molecular sieve is saturated and the gas separation stops. As a result, PSA generators are always equipped with two or more adsorption columns to ensure that the process is continuous. These two vessels undergo switch between the separation process and regeneration processes. The clean and dry compressed air enters the first tower (First part of Figure 2.12) and since the oxygen molecules are smaller than nitrogen molecules, the oxygen molecules will enter the pores of carbon sieve. Nitrogen molecules on the other hand cannot fit into the pores so they will bypass the carbon molecular sieve. As a result, nitrogen of desired purity is obtained. This phase of separation of nitrogen is called the adsorption or separation phase. However, the process does not stop here. Most of the nitrogen produced in the first vessel exits the system which is ready for direct use or storage. A small portion of the generated nitrogen is led to the second vessel from the top [49].

This flow of nitrogen into the second vessel is required to push out the oxygen that was captured in the previous adsorption phase of second vessel. By releasing the pressure in second vessel, the carbon molecular sieves lose their ability to hold the oxygen molecules. The process occurs in the second part of Figure 2.12. The oxygen molecules will detach from the sieves and get carried away through the exhaust by the small nitrogen flow coming from first tower. Hence the system makes room for new oxygen molecules to attach to the sieves in a next adsorption phase. The process of removing saturated oxygen particles from the tower as regeneration process [50]. After the regenerative process,

the pressure in both towers will equalize and they change stages from regenerating to adsorbing and vice versa. The CMS in first tower gets saturated, while in second tower due to depressurization is able to start the adsorption process again as seen in the third part of Figure 2.12.

Some of the advantages of using pressure swing adsorption for nitrogen separation are [51]:

- Low to average capital investment costs
- Easy installation and start up of the equipment
- Relatively high purity
- Low operation costs
- Easy scale-up by adding extra unit columns and the process doesn't require any chemicals or solvent

Some of the drawbacks associated with PSAs are [46]:

- Large maintenance equipment and production capacity is limited
- Slow cycle times can give high losses and can cause the rate change of inlet flow, leading to the unstable pressure in the column during the plant operation [52]
- Usually requires a buffer storage vessel thus increasing the costs associated with it

2.3.3. Membrane Separation

Membrane separation is a method that separates nitrogen from air by using a selective membrane in the form of a polymer membrane which is the heart of equipment. It is based on the notion of selective permeation of gases through a porous medium. The membrane is made up of thousands of hollow fibers that allow compressed air to flow through. Gas molecules can pass through the walls of each fiber, however some gases pass through more easily than others [51]. Permeability and separation selectivity (α) are the two main criteria used to evaluate membrane performance for gas separations.

The permeability of glassy polymeric membranes is affected by pressure and temperature when large input flow rates and membrane surfaces are utilized. The vapor pressure and density, which also impact permeability, are very vulnerable to temperature fluctuations [53]. The purity of the nitrogen gas that is usually extracted from the outlet of the separator highly depends on the pore size of the membrane. A typical schematic of membrane separation technique is shown below in Figure 2.13
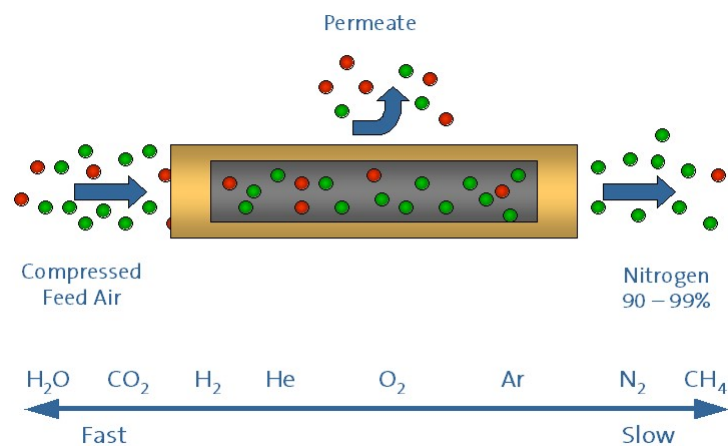
Figure 2.13: Schematic of Membrane Separation nitrogen production [54]

The figure above shows the classification between fast and slow gases. Fast gases, such as oxygen, CO_2, H_2, and water vapour, flow through the fiber walls and are vented into the environment. The slow gas, nitrogen, moves significantly slower through the fiber wall, resulting in a high purity nitrogen

stream at the membrane exit. In the membrane separation process, there are no moving parts to the membrane. As a result, high purity nitrogen can be obtained by controlling the pressure and flow rate of compressed air through the membrane [55].

Some of the advantages associated with using membrane separators for nitrogen production are:

- The capital cost is inexpensive in comparison to the purity level that the generator will create, and the generator is ready to perform the task and begin operating in a matter of seconds
- Since there are no moving parts, it is easy to control and maintain
- Can be easily expanded and no regeneration process required [56]

However, some of the drawbacks associated with the technique are:

- May cause clogging due to impurities in the gas stream thus high periodic maintenance costs
- Not suitable for very high purity outputs (99.9%)

2.3.4. Comparison of different air separation techniques

Factors	Cryogenic Distillation	Pressure Swing Adsorption (PSA)	Membrane Separation
Operating Principle	Separation based on boiling point differences	Separation based on adsorption affinity	Separation based on selective permeation through a membrane
Operating Temperatures (C)	-195 to -170	20-35	40-60
Pressure (bar)	1-10	6-10	6-25
Purity (%)	99.999	99.8	99.5
Energy Consumption (kWh/kg N2)	0.1	0.2-0.3	0.2-0.6
Investment Cost (k€/tpd NH3)	<8	4-25	25-45
Technology Readiness Level	9	9	8-9
Capacity Range (Nm3/h)	250-50000	25-3000	3-3000

Figure 2.14: Various air separation techniques comparison [51] [36]

2.3.5. Nitrogen Storage

Nitrogen is usually stored in the liquid form since it can be transported relatively easily. Dewar vessels and vacuum insulation were originally produced for the storage and transport of small quantities of liquid nitrogen. A dewar is a specialized type of an insulated container which is used for storing cryogens. All dewar vessels have multiple layers of walls and a high vacuum is maintained between the walls. The presence of vacuum ensures that the vessel is properly insulated and no heat transfer takes place between the interior of the vessel and surroundings. The vacuum insulation is done to reduce the boil off rate of liquid nitrogen [57]. A general overview of how dewar vessels look like can be seen in the Figure 2.15 below.

Figure 2.15: Dewar vessels for storage of cryogens [58]

2.4. Ammonia Production: Haber-Bosch Process

The Haber-Bosch process which is also referred to as Haber process is the primary method applied to in the manufacturing of ammonia. The process is named after the two German chemists, Fritz Haber and Carl Bosch, who invented the process in early 1900s [59]. Fritz Haber first developed the process and later this process was purchased by a German company BASF (Badische Anilin & Soda Fabrik with headquarters in Ludwigshafen, Germany).

Later the process was scaled-up by Carl Bosch and succeeded in 1910. The main idea of the process is that it converts nitrogen to ammonia with the presence of hydrogen under extremely high pressures and temperatures in the presence of a metal catalyst. The reaction carried out at equilibrium is shown below.

$$N_2 + 3H_2 \longrightarrow 2NH_3 \quad \Delta H° = -91.8 \ KJ/mol$$

The reaction scheme for the catalytic ammonia synthesis comprises of number of primary steps. According to Ertl [60], the series of reactions are:

$$H_2 + 2* \Longleftrightarrow 2H_{ad}$$

$$N_2 + 2* \Longleftrightarrow 2N_{ad}$$

$$N_{ad} + H_{ad} \Longleftrightarrow NH_{ad} + *$$

$$NH_{ad} + H_{ad} \Longleftrightarrow NH_{2,ad} + *$$

$$NH_{2,ad} + H_{ad} \Longleftrightarrow NH_{3,ad} + *$$

$$NH_{3,ad} \Longleftrightarrow NH_3 + *$$
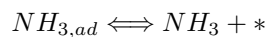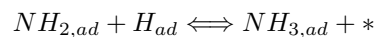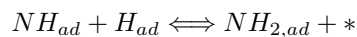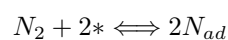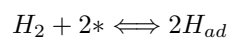
A general overview of Haber-Bosch process is expressed as a block diagram in Figure 2.16

The below diagram represents the production of green ammonia which refers to using hydrogen produced from renewable energy sources. The process of production of ammonia is typically carried out at pressures more than 100 bar and temperatures ranging from 400-500°C and are passed over beds of catalyst. The recycle of the unreacted gases enhances the conversion rate to around 97% [61].

Nitrogen shares a triple covalent bond and has a very high stability. Due to the high stability, the bond between the nitrogen molecules is strong which keeps the nitrogen molecules (N_2) together. Therefore, high dissociation energy of 942 KJ/mol is required to break the triple $N \equiv N$ bond. As a result, a catalyst is required to break the bonding between nitrogen molecules. Without a catalyst the process would require very high temperatures and pressure thereby reducing the efficiency of the plant [62]. Heterogeneous catalysts are used where solid catalyst is in contact with gaseous reactants. To make the process happen in an efficient way, iron based catalysts are used in Haber-Bosch process. Iron-based catalysts are used to increase the speed of the reaction and are cheap.

These iron based catalysts consist of promoters which usually are aluminium oxide, potassium hydroxide, calcium oxide, magnesium oxide etc. These promoters are used to boost the effectiveness of the catalyst in the process and to keep the surface area of the catalysts stable. The promoters are usually unreactive with hydrogen and therefore do not cause any harm to the reaction [63].
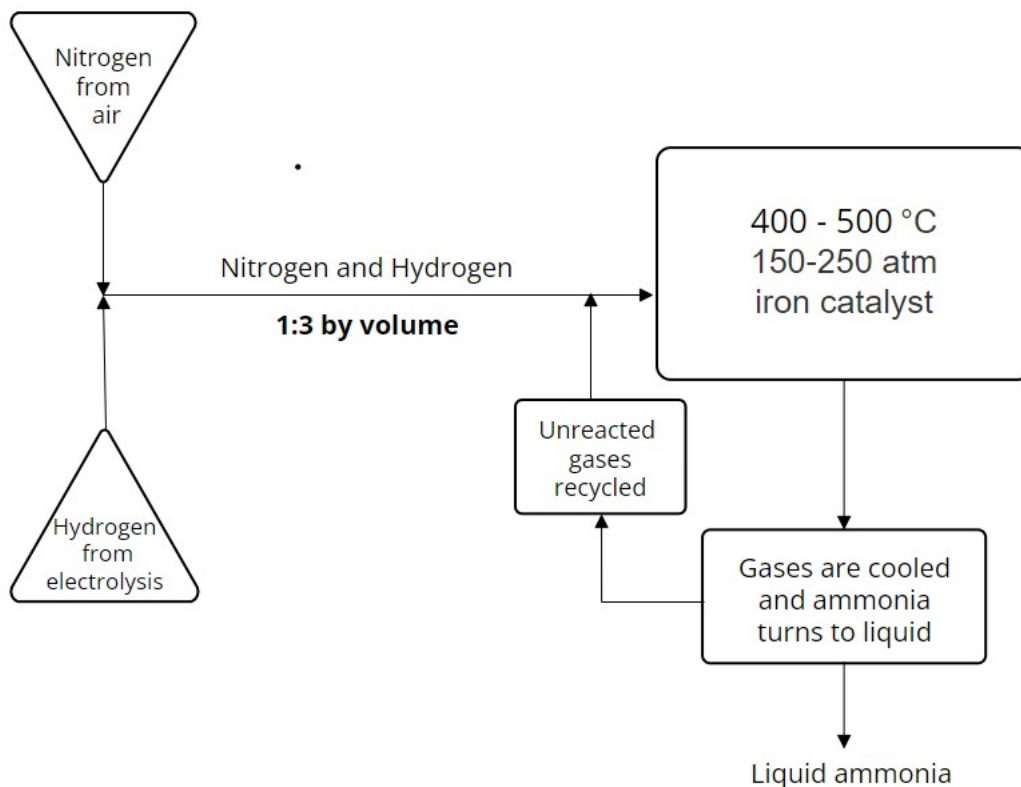
Figure 2.16: Schematic route of Haber-Bosch process

The reaction is a reversible reaction, that is, it can proceed both in forward direction (ammonia synthesis) and in backward direction (ammonia decomposition). The Le Chatlier's Principle explains the temperature and pressure dependency on the reaction and why the pressure should be high for efficient reaction.

- **Pressure:** For gaseous reactions, gas pressure is related to the number of gas particles in the system. Increasing the pressure on the equilibrium system will result in shift of equilibrium towards the side with fewer molecules. Therefore, increasing the pressure gives rise to higher mole fraction of ammonia.
- **Temperature:** The effect of change in temperature depends on whether the reaction is exothermic or endothermic. In case of ammonia synthesis reaction (exothermic), increasing the temperature will result in shifting the equilibrium position to the right. Therefore, the ammonia mole fraction decreases as the temperature is increased.

- **Concentration:** If the concentration of the reactant is increased, the equilibrium position shifts to use up the added reactants by producing more products.

The pressure and temperature dependency on ammonia mole fraction is shown in Figure 2.17
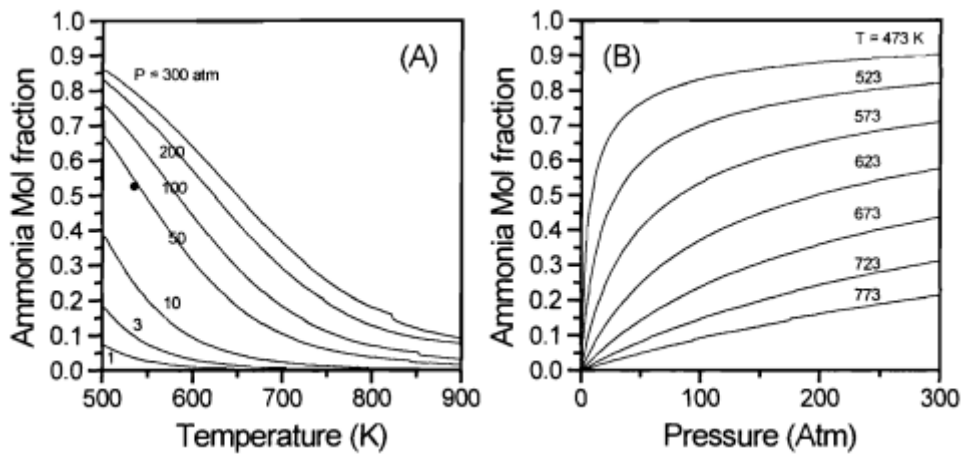
Figure 2.17: Mole fraction of ammonia at equilibrium as a function of temperature and pressure (1:3 mixture of N_2/ H_2) [64]

Ammonia Recovery

Ammonia recovery is a process where ammonia is separated from the unreacted gases (i.e., hydrogen and nitrogen) after the well known Haber-Bosch process. Two different ways to recover ammonia are discussed in the current thesis report. One of the most commonly used method to recover ammonia is by condensation, and the other way to recover ammonia is by absorption. The latter is still in development phase and an extensive research is being carried out. A general overview on both the processes is given below.

Ammonia recovery by Condensation

Ammonia recovery by condensation is one of the commonly used method to separate ammonia from the unreacted gases in the ammonia synthesis loop. Ammonia recovery by condensation is usually carried out by cooling the gases coming out of the reactor to temperatures ranging from -25°C to -33°C with pressures around 140 bar [7]. The unreacted gases (H_2 & N_2) are recycled back to the reactor after being compressed back to the reaction conditions. The mole fraction of the ammonia recovered highly depends on the condensation temperature. The phase diagram of ammonia as shown in Figure 2.18 depicts the pressure dependency on temperature [65].
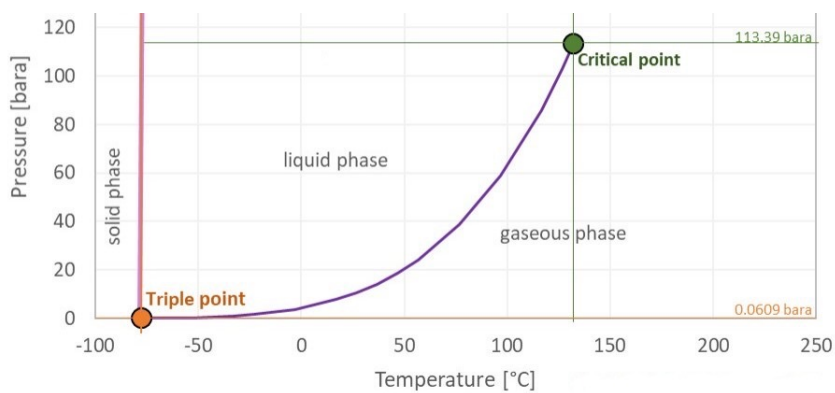
Figure 2.18: Phase diagram of ammonia [65]

The critical point of ammonia is at 132.25°C and 113.39 bar. The partial pressure is expressed in terms of total pressure and mole fraction as:

$$p_i = p_a \times X_i \tag{2.10}$$

where p_a is the total pressure of the system and X_i is the mole fraction of the component.

The recovery rate of ammonia depends on the ammonia partial pressure and the saturation pressure. As a result, if the total pressure is high and the saturation pressure is low, the conversion of ammonia increases. This saturation pressure depends on temperature and the only way to reduce the pressure is by reducing the temperature. Therefore, the plants are usually run at -25°C to -33°C [7] thereby reducing the ammonia yield in the recycle stream.

Ammonia recovery by absorption

A recovery unit of ammonia consists of a condenser after the reactor where it is cooled down to very low temperatures as discussed in Figure 2.4. Another alternative that can replace the condenser and is widely being researched is the use of solid absorbents [66] [67] [68] [69]. An absorbent that collects ammonia in a solid crystal is preferable in such a way that it can be done even at high temperatures [66]. However, the absorption might take longer to achieve its full capacity compared to cryogenic condensation.

The solid absorbent material used is responsible for the selectivity of the absorption where ammonia is absorbed but the hydrogen and nitrogen gases are not. These absorbents incorporate molecules into the crystal lattice thereby offering high capacity and being more stable at high temperatures [67]. Because of their ability to retain multiple moles of ammonia per mole of salt, metal halide salts such as magnesium chloride or strontium chloride have been proven to be viable candidates for NH_3 storage materials.

3

Methodology

3.1. Scenarios

The ammonia production rate of a green electricity powered plant is subjected to fluctuations due to variations in hydrogen availability. These fluctuations in hydrogen availability are caused by intermittency of renewable power supply to the electrolyzer. Due to these fluctuations in hydrogen feed flow rate, a stable and efficient production process cannot be achieved. Changes in hydrogen feed flow rate has a direct impact on the pressure within the ammonia synthesis loop. A reduction in the hydrogen feed flow rate can lead to a reduction in pressure and these extreme changes in pressures lead to metal fatigue and result in damaging the components in the production unit. Therefore, the key goal of the current thesis project is to test potentially effective control strategies that can stabilize pressure within the ammonia synthesis loop under varying hydrogen feed flow rate.

Under various conditions, three distinct control methods and the effect of change in hydrogen feed flow rate on the ammonia synthesis plant are examined. The effect of these variations in hydrogen feed flow rate on ammonia synthesis plant are discussed in detail in chapter 5.

The electrolyzer and the ammonia synthesis unit are powered by renewable energy sources in order to produce green ammonia. Three different scenarios are considered where the effect of solar, wind and hybrid (solar+wind) on the ammonia production are studied and a cost evaluation is carried out. These scenarios are explained in detail in chapter 6. A brief cost estimation is carried out using the HySupply open source tool and the levelized cost of ammonia is determined for each of the selected scenarios. The effect of introduction of hydrogen buffer on ammonia production capacity factor and levelized costs are also examined further.

3.2. Assumptions

The following assumptions have been made for construction of the model:

- The electrolyzer is assumed to be handling the power fluctuations efficiently
- Frictional pressure drop in the synthesis loop is assumed to be constant at 3 bar
- Hydrogen coming out of the electrolyzer is assumed to be pure hydrogen
- The production and storage of feed components (H_2 & N_2) is not modelled in the simulation
- The storage of ammonia is not modelled in the present study
- An electric heater is integrated in the ammonia synthesis reactor

3.3. Modeling and Simulation Software

For the current thesis project, Aspen Plus, Aspen Plus Dynamics and HySupply Open Source Tools [13] were used for modeling and simulation purposes. Aspen Plus and Aspen Plus Dynamics are part of AspenTech (Aspen Technology) who is a provider of software and services for process industries.

Aspen Plus is primarily used for steady-state modeling and incorporates a comprehensive thermodynamic property database enabling users to select appropriate models for reaction kinetics and physical property calculations.

Aspen Plus Dynamics focuses on dynamic simulation where it allows users to model and simulate processes over time, taking into account the transient behaviour, start-up, shut-down and control strategies.

HySupply is a collaboration between Germany and Australia to investigate the feasibility of exporting renewable energy in the form of hydrogen. As part of feasibility study, HySupply Australia developed a series of open-source and open-access costing tools to assess the viability of the supply chain. For the current research project, HySupply Hydrogen Analysis Tool and HySupply Ammonia Analysis Tool were used to calculate the levelized costs of hydrogen and ammonia using renewable energy sources as primary electricity input.

<div align="right">

4

</div>

Steady State Simulation

The aim of the steady-state model is to find the thermodynamic limitations and sizing of the components in the ammonia synthesis plant.

4.1. Model

The reaction kinetics and sizing of various equipment have been included in the current steady state model. In addition to these, the heating duty, cooling duty, and heat integration possibility are investigated and provided in the simulation. This specific model was built with dynamics of each component considered along with addition of valves as necessary. Thereafter, the steady state model is sent to the dynamic environment for simulations in Aspen Plus Dynamics. Figure 4.1 shows the conceptual design of the ammonia synthesis unit.
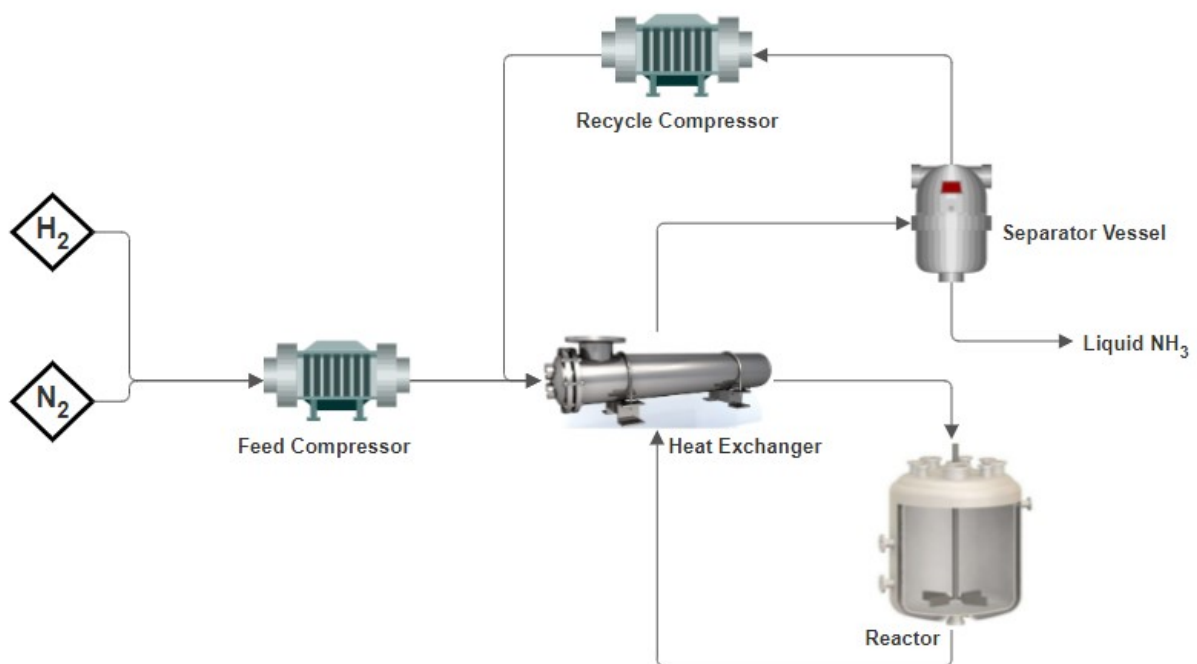
Figure 4.1: Conceptual Design of Ammonia Synthesis Plant

The following Figure 4.2 shows the modelled conceptual ammonia synthesis plant that was simulated in Aspen Plus and the configuration of each of the components shown in the figure below are described in the following sections.
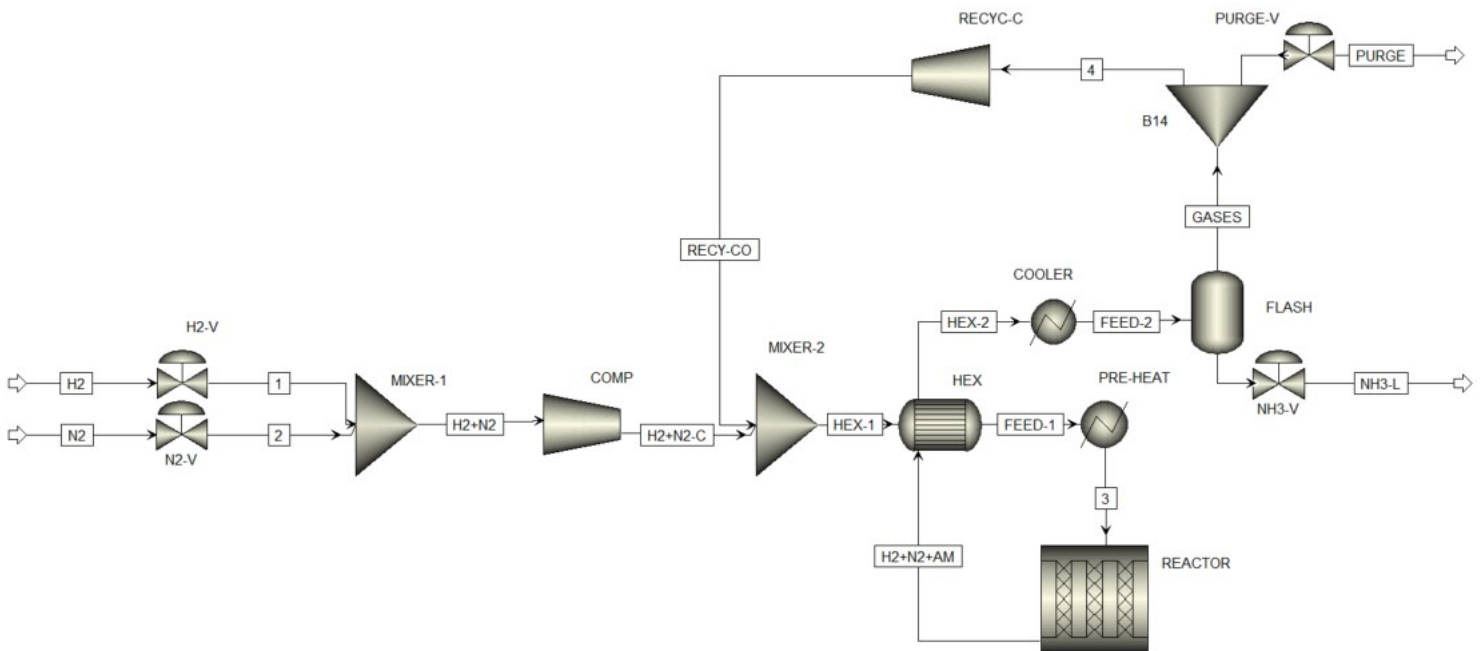
Figure 4.2: Steady-State Model from Aspen Plus

4.2. Reactor Configuration

For the current work, R-PLUG reactor is used in Aspen Plus to model the ammonia synthesis reactor. This specific type of reactor is used since it enables the user to model the catalyst bed. Ammonia synthesis is a process which is carried out under the presence of an Iron based catalyst. The reaction kinetics have been provided by Proton Ventures B.V. and the same have been implemented in the current project work. For this purpose, Langmuir-Hinshelwood-Hougen-Watson model has been used and the reaction kinetics are derived from [68]. For the sake of simplicity, the ratio of reactor length to diameter is taken as 8 based on data from Proton Ventures B.V. since the reactor modelling was out of the scope for the present work.

A sensitivity analysis has been performed on the reactor to determine the optimal length of the reactor based on the selected flow rate as shown in Figure 4.3 and Figure 4.4.
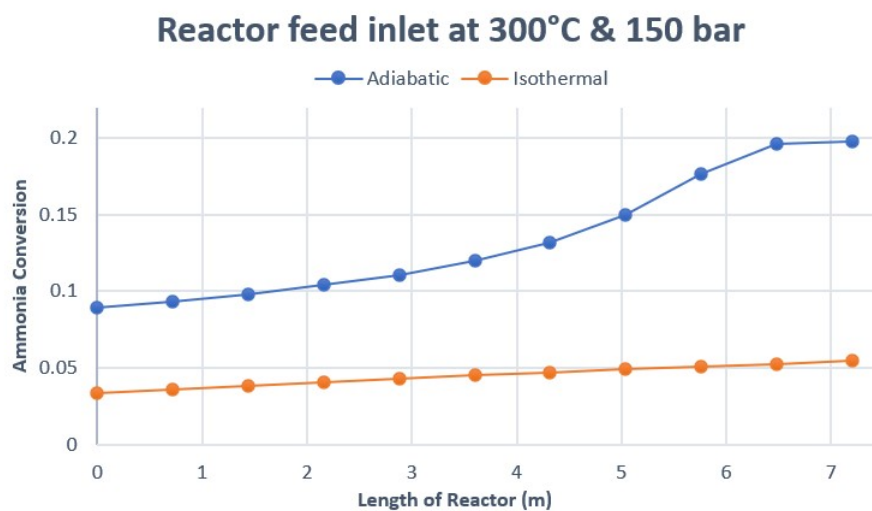
Figure 4.3: Sensitivity analysis of R-PLUG reactor at $300°C$ and 150 bar
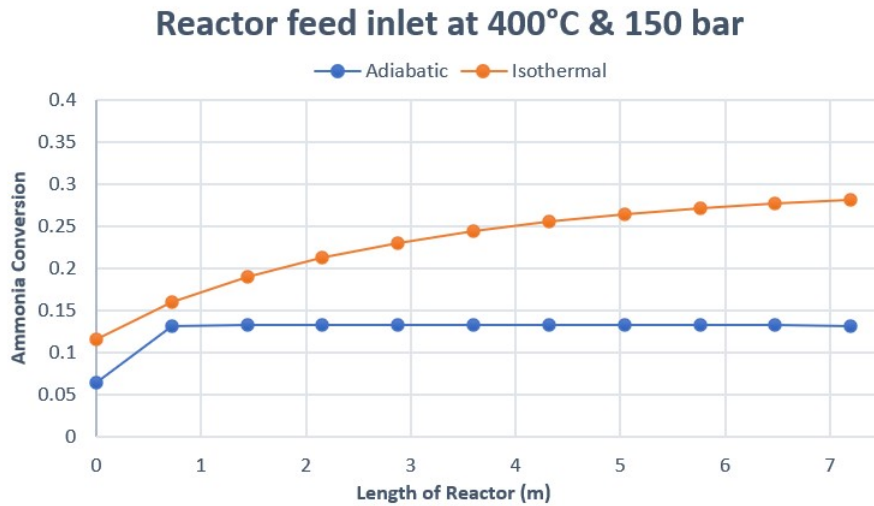
Figure 4.4: Sensitivity analysis of R-PLUG reactor at $400°C$ and 150 bar

The sensitivity analysis provides the following observations.

• Adiabatic reactor reaches the conversion much faster than isothermal reactor. This is because there is a thermodynamic equilibrium of heat and the temperature increases in the reactor. Due to this increase in temperature, the reaction goes faster.

• At higher temperatures, the isothermal reactor performs better due to the influence of temperature on ammonia synthesis kinetics, whereas the adiabatic reactor performs better at lower temperatures.

• The inlet temperature of the feed going into the reactor plays a major role in determining the conversion of ammonia.

For the present work, adiabatic reactor is chosen for the reactor configuration since isothermal configuration is difficult to achieve and maintain. The inlet temperature of the feed is taken as $300°$ C and the length and diameter of the reactor considered are 7.2m and 0.9m respectively from the sensitivity analysis where a conversion of 19.7% is achieved thereby, validating the model according to [70] which states that a single pass conversion of 18-20% is achieved.

The catalyst used for the present work is Ferrous Oxide based catalyst (ZA-5) since it has a lower activation temperature of $300°C$ and high heat resistance (temperatures till $500°C$) [68]. By using ZA-5 catalyst under the conditions of 8 MPa of pressure and reaction temperatures at the inlet and exit of the reactor of 215 °C and 363 °C, respectively, the net value of ammonia is more than 10% in the industrial process of high-purity ammonia, which has met the economic requirement for net value of ammonia in industry [71]. Further, a bed voidage of 0.33 and particle density of 2200 kg/m^3 were considered based on literature [72].

4.3. Flash Vessel

The flash vessel which is used as a separator to separate gas from liquid is modelled for the present work. The dimensions of the flash vessel have been calculated as it was observed that the dimensions play a crucial role in dynamic simulation of the model. In order to calculate the dimensions, the terminal velocity (u_t) must be known. The terminal velocity of the stream is expressed as Equation 4.1:

$$u_t = \sqrt{\frac{4 \times g \times d\,(\rho_l - \rho_v)}{3 \times C_D \times \rho_v}}$$

(4.1)

Bent Wiencke [73] suggested various expressions for drag coefficient (C_D) but for the present work, the equation suggested by Brown and Lawler has been considered as shown in Equation 4.2.

$$C_D = \frac{24}{Re_p}(1 + 0.150Re_p^{0.681}) \; + \; \frac{0.407}{1 + \frac{8710}{Re_p}} \quad for \;\; Re \leq 2 \times 10^5 \tag{4.2}$$

To perform the calculations, the density of vapor going into the separating vessel is taken from Aspen Plus. The diameter of the droplet of ammonia is assumed to be $100\mu m$ based on the range of 50-100 μm as stated in [8]. The viscosity of the gas is calculated based on the molar composition of the gases in the stream. Further, the volumetric flow rate of the feed stream to the vessel is also taken from Aspen Plus.

In order to determine the Reynolds' number, an initial guess of terminal velocity is done in order to calculate the drag coefficient (C_D). After calculating the drag coefficient, the value is used to find the actual terminal velocity. This process is carried out till both the predicted terminal velocity and the actual terminal velocity match. The terminal velocity is found to be 0.083 m/s.

Once the terminal velocity is found, the diameter of the vessel is calculated by using the Equation 4.3

$$D = \sqrt{\frac{4 \times \dot{Q}}{\pi \times u_t}} \tag{4.3}$$

From the above values and calculations, the diameter of the vessel is found out to be 0.54m. As a rule of thumb, the Length:Diameter ratio for separator vessels is in the range of 3-5 [74]. For the current project, a length-to-diameter ratio of 4 is considered. Hence, the height of the vessel is 2.16m.

(a) Horizontal Vessel   **(b)** Vertical Vessel
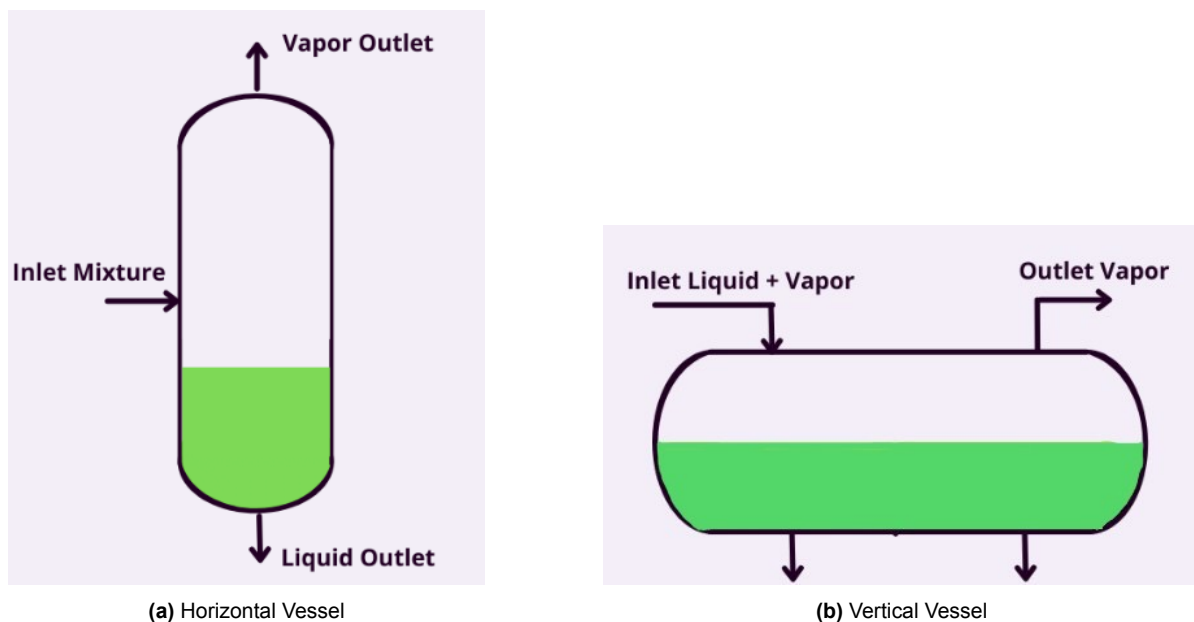
Figure 4.5: Schematic of types of separator vessels

Figure 4.5 represents the basic schematic of different types of vessels. Horizontal separation vessels are usually used when the liquid flow rate is dominant compared to the gas flow rate. In the present work, vertical separator has been used because of liquid flow rate being less dominant and is more efficient in terms of separation since the densities difference between the liquid ammonia and gases is high.

The specifications of the flash vessel are described in the Table 4.1 below:

Parameter	Value
Duty	0 kW
Pressure Drop	0 bar
Phases	Vapor-Liquid
Vessel Type	Vertical & Elliptical
Length	2.1642 m
Diameter	0.54106 m
Heat Transfer Type	Constant Duty
Liquid Volume Fraction	0.35

Table 4.1: Flash Vessel Specifications

4.4. Heat Exchanger

Heat exchangers are one of the key components to realistically represent the working of the production plants. A shell and tube exchanger is commonly used in industries to transfer heat between two pressurized fluids while keeping them physically separate. Two fluids are involved in the process known as the "hot fluid" and the "cold fluid".

The cold fluid outlet temperature is specified as $300°$C in design type calculation mode. In steady-state modelling, the heat exchanger area is calculated. The calculated heat exchanger area is 11.708 m^2. This value of heat exchanger area is used as input for dynamic model. The calculation mode is selected as simulation and the evaluated heat exchanger area is specified as unit specification for dynamic simulation.

Based on the literature [75], the allowable pressure drop for gases is taken as 0.1 bar on both the cold and hot side of heat exchanger. Table 4.2 shows the results obtained from steady-state simulation of heat exchanger.

Parameter	Value	Unit
Heat Exchange Area	11.708	m^2
Heat Transfer Coefficient	850	W/m^2K
Heat Duty	1500	kW
Cold Stream Outlet Temperature	300	$°C$
Hot Stream Outlet Temperature	190	$°C$

Table 4.2: Heat Exchanger Results

4.5. Compressors

Two different compressors are used for the current ammonia synthesis plant. A reciprocating compressor is used to compress the hydrogen and nitrogen feed gases. This reciprocating compressor is used for make-up gas compression since it has better performance with high pressure ratios and intermittent operations compared to centrifugal compressor. The make-up gas is compressed from 80 bar to 150 bar. The compressor model is selected as isentropic compressor and a pressure ratio is specified as the input for the make-up gas compressor. The outlet temperature of the compressor is found out to be $105°$C and therefore, only a single stage compression is used. This is because the maximum allowable discharge temperature of the compressor is usually less than $150°$C due to durability of the seal and thermal stress on the compressor. The results of the make-up gas compressor are shown below in Table 4.3.

Parameter	Value	Unit
Brake Power	87.7	kW
Isentropic Efficiency	0.72	
Compressor Outlet Temperature	105	°C
Pressure Ratio	1.88	
Outlet Pressure	150	bar

Table 4.3: Make-Up Gas Compressor Results

A centrifugal compressor is used for the recycle stream compression to bring the pressure back to the system pressure (150 bar). A centrifugal compressor is used as it is effective for low to medium pressure ratios and for high flow rates. The unit specification for the recycle compressor is isentropic type and the discharge pressure has been specified as 150 bar. The brake horsepower of the compressor is determined from the steady-state simulation as 12.5kW.

4.6. Valves

Valves are mechanical devices which are used to control the flow of fluids through a system. For the present work, valves are used to regulate the flow rates of the fluids within the system. By adjusting the position of the valve, the amount of fluid flowing through the pipeline can be controlled.

From Figure 4.2, H2-V and N2-V are used to control the flow rates of hydrogen and nitrogen respectively in dynamic simulation. NH3-V is used to regulate the liquid level in the flash vessel. The PURGE-V is used to send impurities from the system to the flare where they are burnt off. Each valve have their own specification and are discussed in the Table 4.4 below. The calculation type used for all the valves is adiabatic flash for specified outlet pressure (pressure changer).

Valve	Specification	Value (bar)
H2-V	Pressure Drop	0.5
N2-V	Pressure Drop	0.5
NH3-V	Outlet Pressure	50
PURGE-V	Pressure Drop	0.5

Table 4.4: Valves Specification

4.7. Condenser

A condenser is a device which is used in various chemical plants to convert a vapor or gas into liquid state by releasing heat from the hot stream. In the present work, the condenser cools the ammonia into liquid form to -20°C. The specifications for the condenser are temperature and pressure. In the dynamic operation, the heater type selected is instantaneous and the heat transfer option is selected as constant process temperature. A detailed specification of condenser can be seen in the Table 4.5 below.

Parameter	Value
Temperature	$-20°$C
Pressure Drop	0.1 bar
Cooling Duty	-1209 kW
Heat Transfer	Constant Process Temperature
Heater Type	Instantaneous

Table 4.5: Condenser Specifications

4.8. Other elements in MODEL-2

Mixer-1 & Mixer-2: These mixers are assumed to be instantaneous in response and no other specifications have been provided. The pressure drop along the mixers is assumed to be 0 bar. The valid phases input specification for both the mixers is specified as Vapor-Only.

Pre-Heater: The pre-heater before the reactor is placed to make sure that the reactor inlet temperature of the stream is maintained at $300°$C. A pressure drop of 0.1 bar is specified with a vapor-only valid phase. The heater type is assumed to be instantaneous and the heat transfer option chosen was constant process temperature.

Splitter: A splitter is used to split the purge stream from the recycle stream. This splitter has a specified split fraction to the purge stream as 1% of the recycle stream. The pressure drop is assumed to be 0 bar and the valid phases specification is selected as vapor-only.

<div style="text-align: right; font-size: 4em;">5</div>

Dynamic Simulation

The current chapter describes various control strategies implemented in Aspen Plus Dynamics and the results obtained from each of them. The steady state model was used as the starting point and is sent to dynamic simulation.

5.1. Scenarios

The three different scenarios that were modelled for dynamic simulation in the current thesis project are 20% reduction, 50% reduction and 70% reduction in hydrogen feed flow rate. These scenarios are considered to be extreme and is stopped at 70% since it is considered to be the highest ramp-down that the compressors can handle. It is observed that there is a reduction in pressure in the system and therefore the goal is to control the pressure back to the original value even if there is a reduction in feed flow rates. The three different control strategies implemented are:

- Pressure control by controlling the cooling duty of the condenser
- Pressure control by controlling the brake power of the recycle compressor
- Pressure control by changing the stoichiometric ratio of $N_2 : H_2$ feed

The response of the three control strategies to 50% and 70% reduction in hydrogen feed flow rate can be found in Appendix A, Appendix B and Appendix C.

For the present work, two different types of change in hydrogen feed flow rate are implemented in Aspen Plus dynamics i.e., step-change and linear change (ramp). Step change is a sudden and instantaneous change in a process variable. This abrupt change is often used to simulate disturbances that can occur due to equipment malfunctions, sudden variations in feed conditions, or operator interventions. Step changes can help evaluate how well the control system responds to sudden disturbances and how quickly the system returns to a new steady state. In the current thesis work, a step-change is carried out by changing the set point in the controller and running the simulation. The simulation is carried out for 100 minutes when hydrogen feed flow rate is reduced as a step-change.

A ramp change, on the other hand, involves gradually changing a process variable over time. Instead of an instantaneous jump, the variable is adjusted at a constant rate. Ramp changes can represent scenarios where a certain parameter is slowly changing due to external factors. This type of disturbance is useful for studying the dynamic response of the control system to more gradual disturbances. For the current simulations, timedata in aspen plus dynamics is used to model the linear changes in hydrogen feed flow rate. Table 5.1 shows the timeline of the dynamic linear change simulations. Four distinct phases in time are incorporated and they are labelled as A, B, C, D in each of the plot.

<div style="text-align: center;">34</div>

Time (min)	Action
0-30	Hydrogen feed is linearly ramped down
30-90	New steady state value is maintained for 60 min
90-120	Hydrogen feed is linearly ramped up back to original value
120-150	Simulation ends at 150 min

Table 5.1: Timeline of Simulation for Linear Change

5.2. Dynamic Simulation Preparation

The first step in the dynamic model preparation is to turn on dynamic mode in Aspen Plus and specifying pressure drops at each and every component. There are two different types of dynamic simulations, Flow-Driven Simulation & Pressure-Driven Simulation. For the current project, pressure-driven simulation has been selected since manipulation of pressure is considered to be the primary concern.

5.3. Control Philosophy-1

The operational principle of control philosophy-1 is to change the condenser's cooling duty in order to maintain system pressure. The controller measures the downstream pressure of the reactor and adjusts the condenser's cooling duty to retain the pressure back to its initial value. In addition to the pressure controller, a ratio controller is used to maintain the stoichiometric ratio of H_2:N_2 at a value of 3. Figure 5.1 depicts the process flow diagram and controller addition, while Table 5.2 describes and parameters of controllers employed in the current control philosophy.
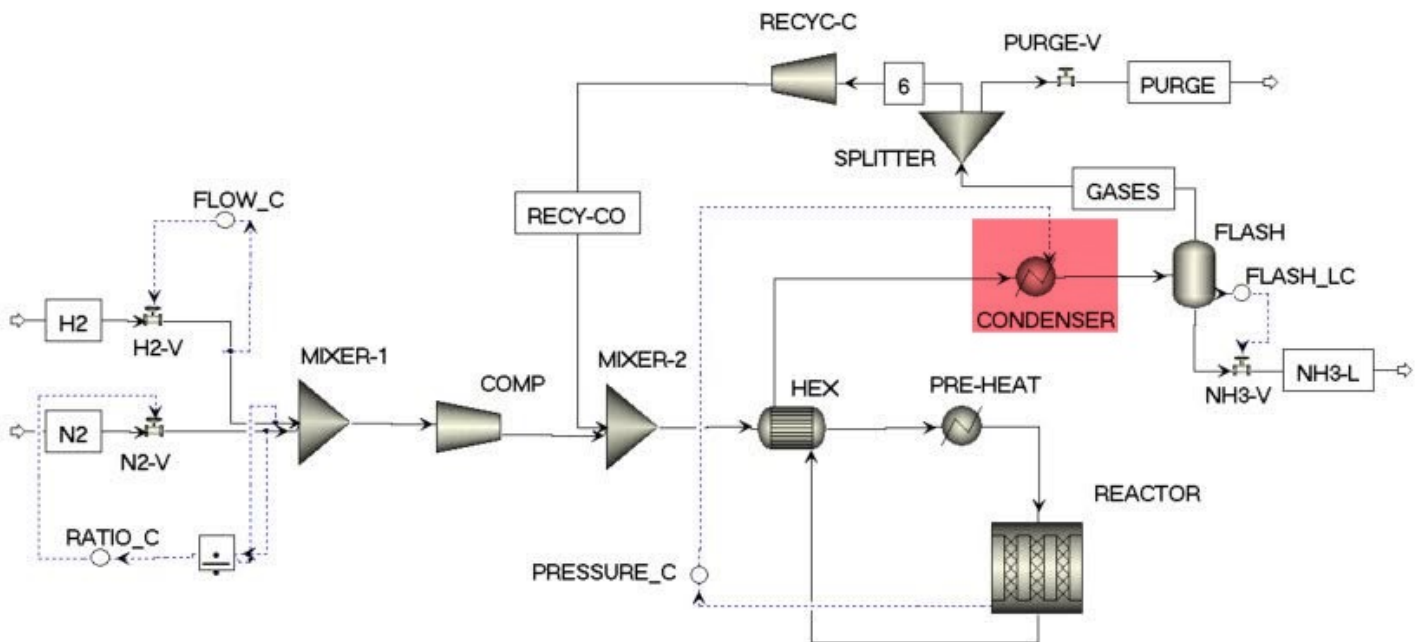
Figure 5.1: Control Philosophy-1 from Aspen Plus Dynamics

	Proportional Gain (%/%)	Integral Time (min)	Controller Action	Controlled Variable	Manipulated Variable
FLOW-C	1	1	Reverse	Hydrogen Feed Flow Rate	H2-V Opening
PRESSURE-C	1	1	Reverse	Downstream Pressure of Reactor	Condenser Duty (MW)
FLASH-LC	10	1	Direct	Flash Liquid Level	NH3-V Opening
RATIO-C	1	1	Reverse	Stoichiometric Ratio	N2-V Opening

Table 5.2: Control Philosophy-1 controller parameters and details

5.3.1. Step-Change in Hydrogen Feed to Control Philosophy-1

In the current section, an extreme scenario is assumed where there is a sudden reduction in hydrogen production. In this scenario, it is assumed that there is no hydrogen buffer and there is an instant reduction of hydrogen feed flow rate to the ammonia synthesis plant. Therefore, to understand the effect of instant reduction of hydrogen, a sudden reduction in electrolyzer's hydrogen generation capacity to 80%, 50% and 30% were assumed. These scenarios were modelled as 20%, 50% and 70% of hydrogen feed flow rate reduction.

Figure 5.2 illustrates different parameters plotted for 20% reduction in hydrogen feed flow rate. The response is as follows:
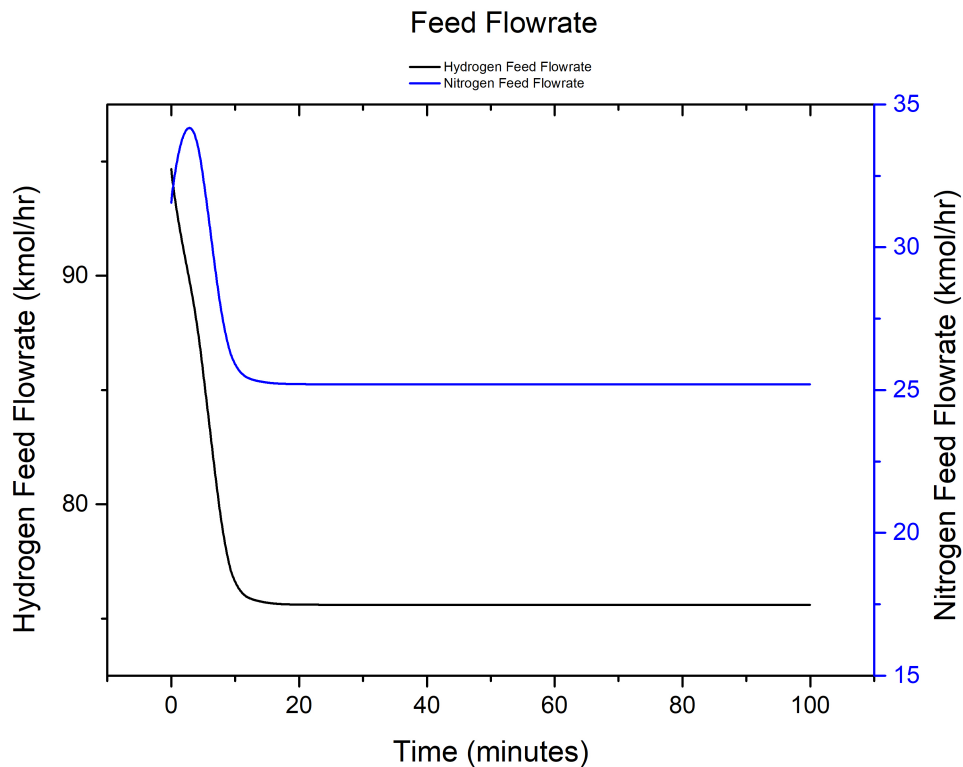
(a) 20% Reduction in Hydrogen and Nitrogen Feed Flow Rates
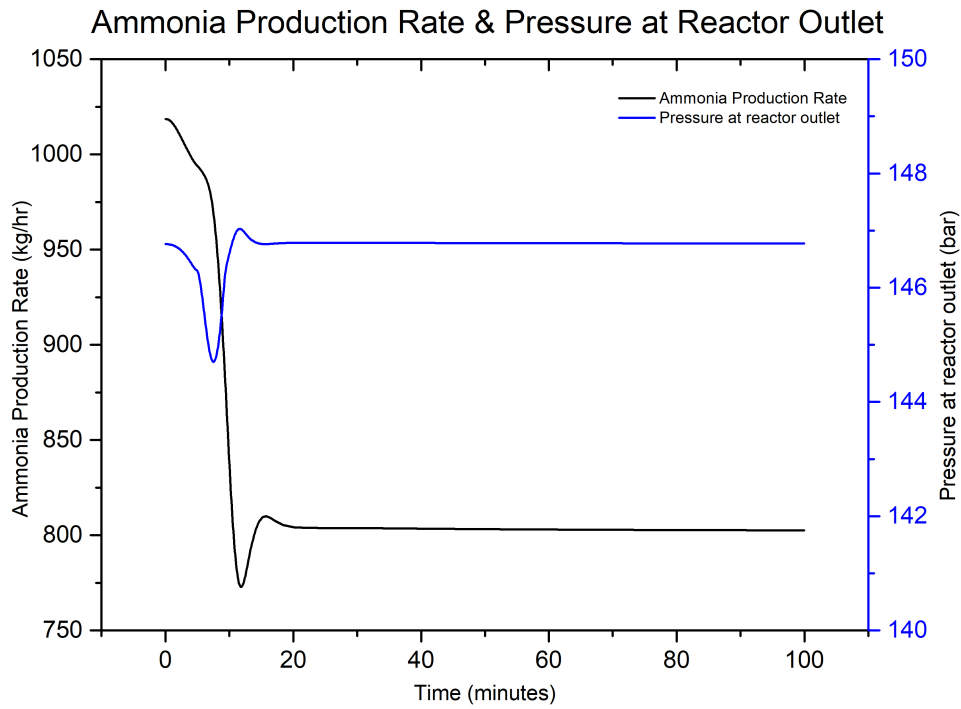
(b) Effect of 20% Reduction of Hydrogen Feed Flow Rate on Ammonia Production Rate and Pressure at Reactor Outlet
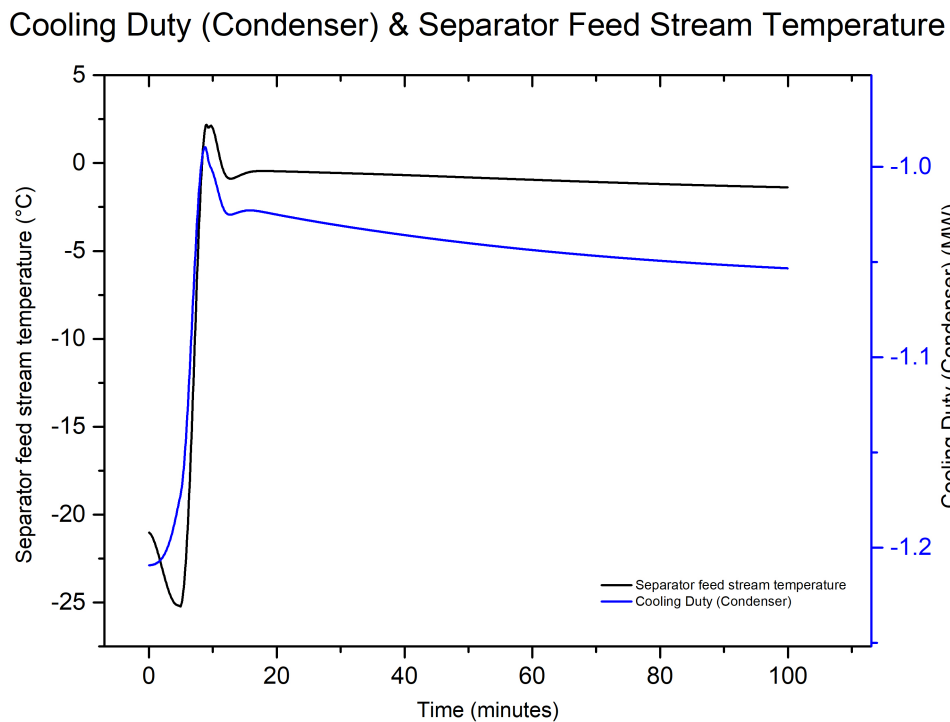
(c) Effect of 20% Reduction in Feed Flow Rate on Cooling Duty of Condenser and Temperature of Condenser Outlet Stream

Figure 5.2: Control Philosophy-1 response to 20% step change in hydrogen feed flow rate

Results:

- Figure 5.2 (a) depicts the dynamic interaction between hydrogen and nitrogen feed flow rates throughout a 100-minute time interval. The interaction between these two variables in response to variations in the hydrogen feed rate is the key observation from this graph. As the hydrogen feed rate falls, the ratio controller actively adjusts the nitrogen feed rate to maintain a constant stoichiometric hydrogen-to-nitrogen ratio. This real-time control technique ensures that the system maintains the proper chemical composition even when hydrogen input rates fluctuate.

- Figure 5.2 (b) depicts the relationship between ammonia production rate and the effect of reducing the hydrogen input flow rate on system pressure. Notably, introducing a 20% reduction in hydrogen feed flow rate into the system results in a corresponding 20% reduction in ammonia production rate. This relationship emphasizes the system's sensitivity to variations in the hydrogen feed rate, which affects reactant availability for ammonia production. Furthermore, the graph shows an immediate pressure reduction of 2 bar, which corresponds to a decrease in hydrogen supply rate. However, the control system reacts quickly to this pressure drop, and the system successfully stabilizes the pressure at the reactor exit in about 20 minutes.

- Figure 5.2 (c) depicts the relationship between the condenser's cooling duty and the temperature of the stream leaving the condenser. The major goal here is to control the system pressure by adjusting the condenser's cooling duty. The inverse relationship between cooling duty and temperature of condenser's outlet stream is shown in this graph. As the cooling duty is reduced from -1.2 MW to -1.05 MW, the temperature of the outlet stream rises noticeably, from -20°C to -1°C. Pressure is projected to decrease as the hydrogen input flow rate decreases. As a result, the pressure control senses the deviation in pressure from the set point. Therefore, the pressure controller reduces the cooling duty, resulting in a rise in the temperature of the outlet condenser stream. The thermodynamic link between pressure and temperature is responsible for this phenomena where increase in temperature resulted in increase in pressure.

5.3.2. Linear-Change in Hydrogen Feed to Control Philosophy-1

The incorporation of buffer storage between the electrolyzer and the ammonia synthesis plant represents a pivotal advancement in the approach. It serves as a crucial mechanism for gradually reducing the hydrogen supply. In this particular section, simulations were carried out in which hydrogen feed flow rate is lowered linearly, while observing how the system responded under the influence of control philosophy-1.

The following Figure 5.3 shows the control philosophy-1 response to 20% reduction in hydrogen feed flow rate linearly.
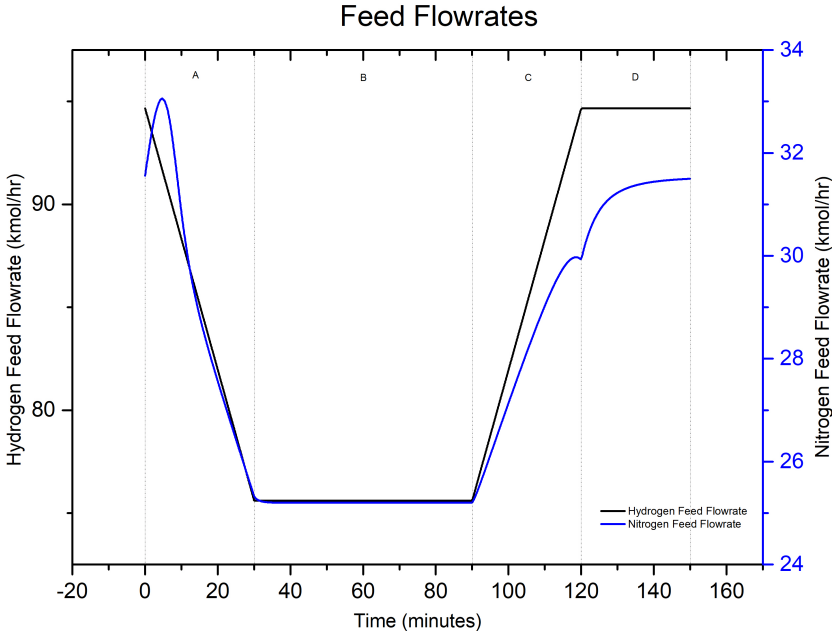
(a) Effect of 20% Linear Reduction of Hydrogen Feed Flow Rate on Nitrogen Feed Flow Rates
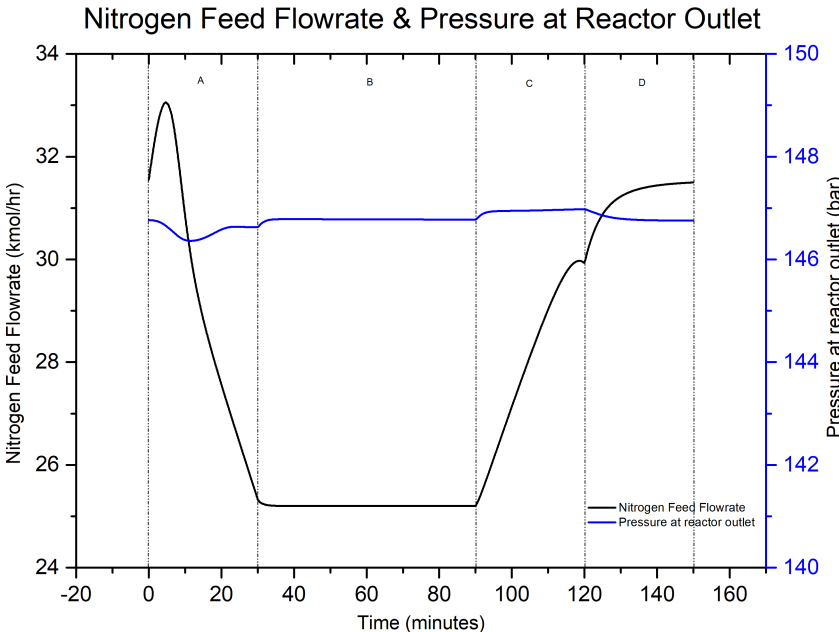
(b) Effect of 20% Linear Reduction of Hydrogen on Pressure at Reactor Outlet

Discussion:

- **Region A:** The hydrogen supply flow rate is gradually reduced during a 30-minute time period. When the controller senses a change in the ratio, it instantly closes the nitrogen valve, causing the nitrogen supply flow rate to drop. A minor peak in the nitrogen feed flow rate is detected, which could be attributed to a slight delay in the controller's response to changes in the stoichiometric ratio. It is important to note that the greatest pressure reduction observed due to change in hydrogen feed flow rate is essentially negligible.

- **Region B:** A consistent feed flow rate is maintained for 60 minutes during this simulation phase, allowing the system to create a new steady-state equilibrium. As a result, the nitrogen and hydrogen feed flow rates remain constant during this time, maintaining a stoichiometric ratio of 3 ($H_2 : N_2$) while the system pressure remains constant. The controller responded quickly to any disturbances or oscillations in the system, ensuring quick and efficient control.

- **Region C:** For a 30-minute time interval, the hydrogen feed flow rate is gradually increased back to its initial value. To maintain the stoichiometric ratio, the nitrogen input flow rate increases correspondingly during this process. As a result of increasing input flow rates, there is relatively small pressure fluctuation from the set point.

- **Region D:** The simulation was carried out for another 30 minutes, allowing the system to gradually revert to its original steady-state characteristics. During this time, the system's pressure was kept constant, ensuring that it remained stable. After 30 minutes, the simulation was terminated.
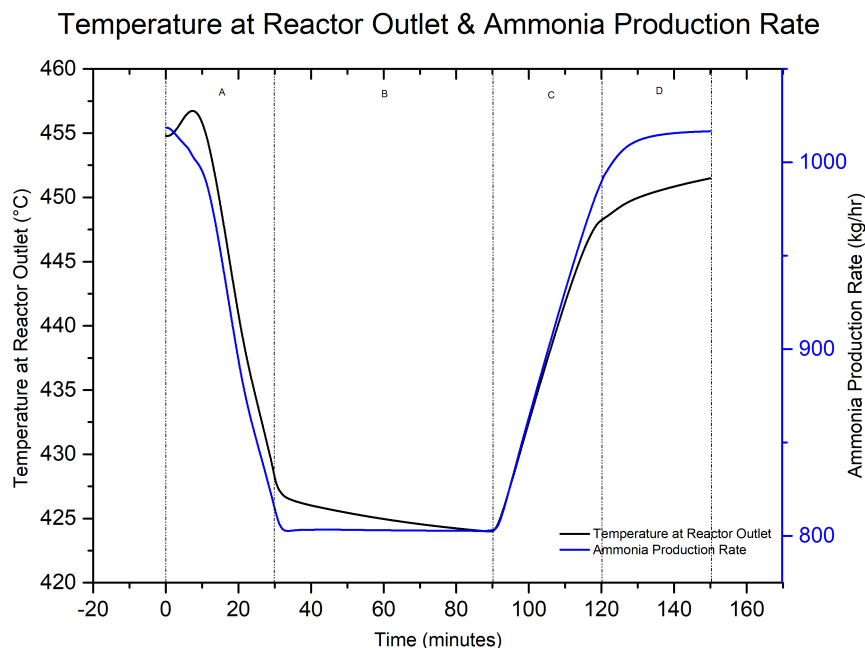
Temperature at Reactor Outlet & Ammonia Production Rate

(c) Ammonia Production Rate and Temperature at Reactor Outlet
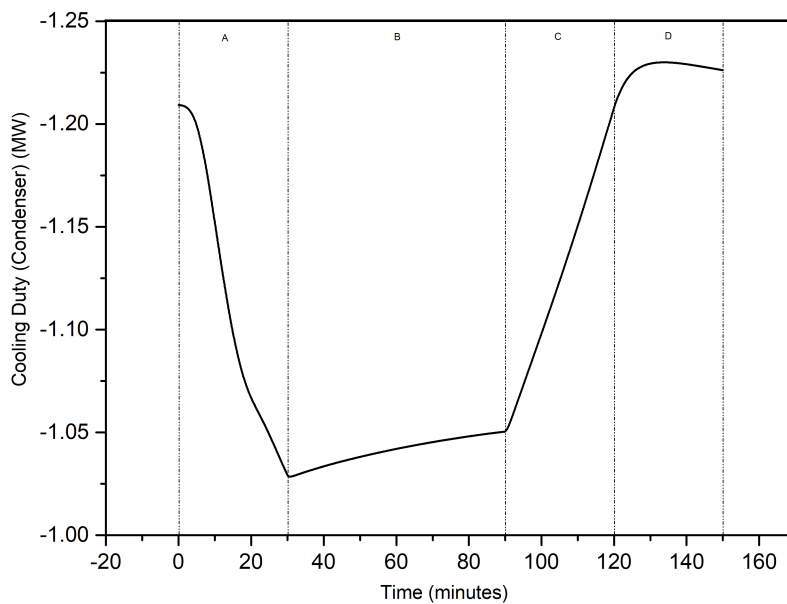
(d) Cooling Duty of Condenser

Figure 5.3: Control Philosophy-1 response to 20% linear change in hydrogen feed flow rate

Discussion:

- **Region A:** Because there were fewer reactants available during the steady ramp-down in hydrogen supply flow rate, the ammonia production rate reduced by 20%. Because the reactants are reduced, less heat is emitted in the exothermic ammonia synthesis reaction, and thus the temperature at the adiabatic reactor's outlet stream lowers. The cooling duty of the condenser is reduced to restore the pressure to its initial amount. This raises the temperature of the stream leaving the condenser, and thus the pressure.

- **Region B, C & D:** The ammonia production rate and the temperature at the reactor exit remain constant when the feed flow rates are kept constant. As the hydrogen feed flow rate is increased back to its prior value, the heat emitted from the exothermic process increases, so does the rate of ammonia generation. As a result of the higher feed flow rate, the pressure rises, and the cooling duty rises to reduce the pressure. The simulation is continued for another 30 minutes before being terminated at the 150-minute mark.

Results and Conclusion:

1. **Hydrogen Flow Rate and Nitrogen flow Rate:**

   - The hydrogen input flow rate clearly follows a linear decline pattern across all conditions. Simultaneously, the nitrogen input flow rate is reduced linearly to maintain the stoichiometric ratio constant.

2. **Pressure Control:**

   - Even when the hydrogen input fluctuates, the system successfully maintains constant pressure levels. This demonstrates the usefulness of control philosophy-1, particularly in situations where hydrogen supply may be limited. As a result of this configuration, the controller

responded quickly to any disturbances or oscillations in the system, ensuring quick and efficient control.

- The maximum recorded pressure reduction was 2 bar, which occurred when the hydrogen input flow rate was reduced by 70%.

3. **Reactor Outlet Temperature and Ammonia Production:**

- The output temperature of the reactor's discharge stream decreases noticeably in all cases. This drop is due to reduced heat release from the exothermic reaction as a result of reactant scarcity. Furthermore, the ammonia production rate falls in direct proportion to the reduction in hydrogen feed flow rate.

4. **Condenser Outlet Stream Properties:**

- The temperature of the condenser's exit stream rises, resulting in higher vapor mole fractions and lower liquid mole fractions of ammonia. As a result, the ammonia flow rate within the recycle stream increases.

5. **Hydrogen Buffer Importance:**

- It is essential to provide a hydrogen buffer between the electrolysis and ammonia production processes. This buffer reduces abrupt pressure reductions caused by quick fluctuations in renewable electricity output. This displays the model's capacity to deal with modest changes in feed flow rates.

6. **Model Performance and Limitations:**

- When the hydrogen feed flow rate is increased back to its initial value, the system pressure reaches the same value by the end of 150 minutes. However, other parameters such as nitrogen feed flow rate, condenser cooling duty, and so on do not return to their initial conditions. This demonstrates that the model takes more than 30 minutes to stabilize. However, no limitations in the model's operation have been discovered till 70% reduction in hydrogen feed flow rate.

5.4. Control Philosophy-2

The primary idea of control philosophy-2 is handling of the recycle compressor's brake power as a way of maintaining system pressure. It essentially aims to control the flow rate of the recycle stream in order to keep system pressure constant. This is accomplished by adjusting the brake power, which in turn exerts indirect control over the flow rate of the recycle stream, ensuring steady pressure within the loop. In addition to the pressure controller, a ratio controller has been included to maintain the stoichiometric ratio. The process flow diagram is visually illustrated in Figure 5.4, which has been improved by the integration of various controllers within Aspen Plus Dynamics. Table 5.3 provides broad information and parameters for an in-depth understanding of the controllers used in control philosophy-2.
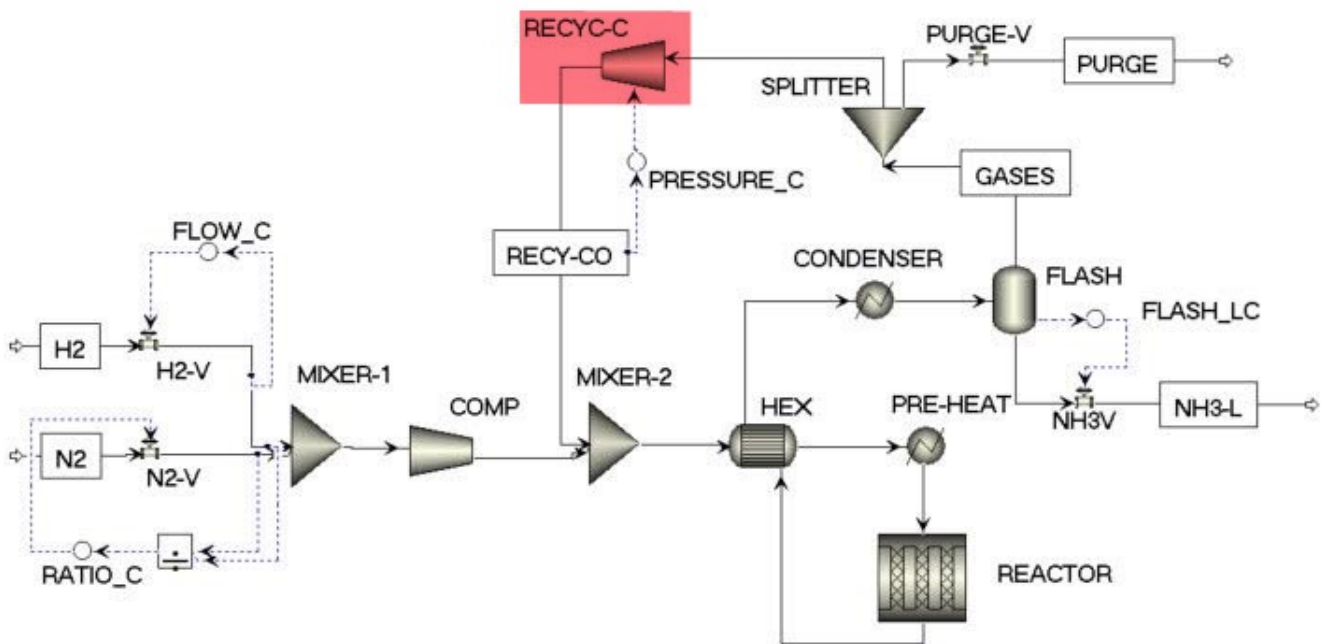
Figure 5.4: Control Philosophy-2 from Aspen Plus Dynamics

	Proportional Gain (%/%)	Integral Time (min)	Controller Action	Controlled Variable	Manipulated Variable
FLOW-C	1	1	Reverse	Hydrogen Feed Flow Rate	H2-V Opening
PRESSURE-C	1	1	Direct	Recycle Stream Pressure	Brake Power (kW)
FLASH-LC	10	1	Direct	Flash Liquid Level	NH3-V Opening
RATIO-C	1	1	Reverse	Stoichiometric Ratio	N2-V Opening

Table 5.3: Control Philosophy-2 controller parameters and details

For the control philosophy-2, a step-change and linear-change of hydrogen feed flow rate is implemented similar to control philosophy-1. The results are shown in the following sections.

5.4.1. Step-Change in Hydrogen Feed Flow Rate to Control Philosophy-2

A step-change in hydrogen feed flow rate is implemented similar to what was discussed in section 5.3. The following plots show the response of control philosophy-2 to sudden reduction in hydrogen feed flow rate.

Figure 5.5 (b) shows the response of the recycle compressor brake power and the pressure of outlet stream of recycle compressor.
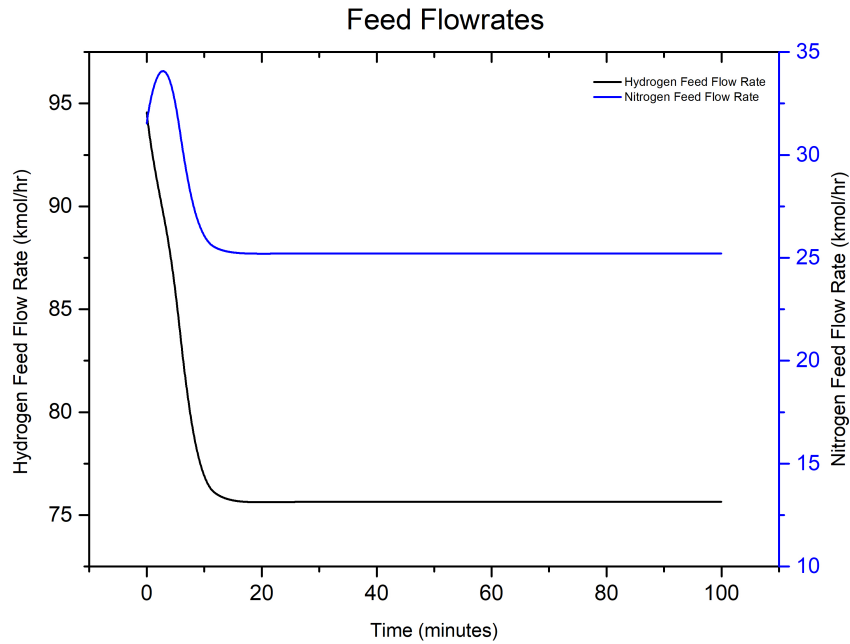
Feed Flowrates

(a) Hydrogen and Nitrogen Feed Flow Rate

Recycle Stream Pressure and Recycle Compressor Brake Power
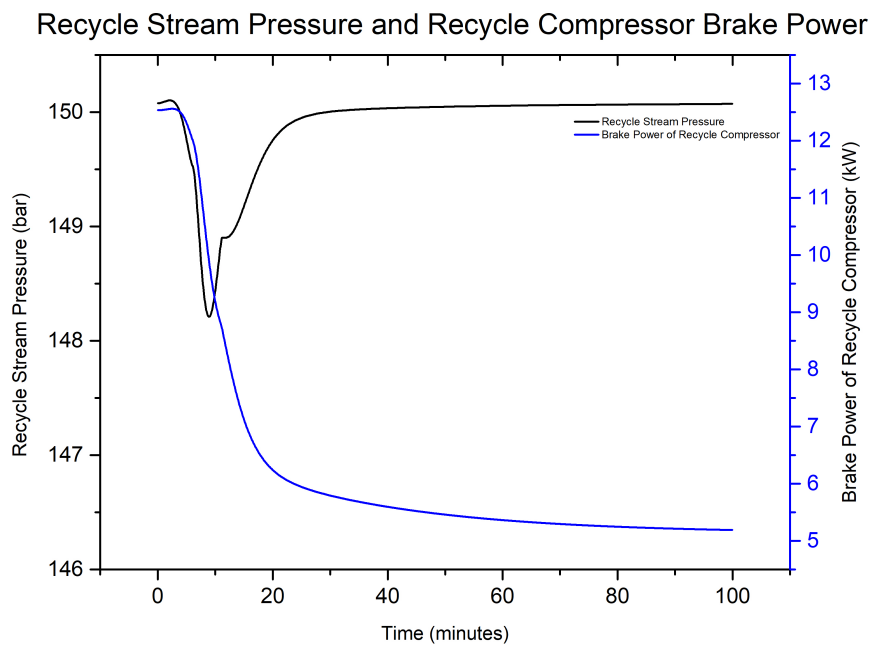
(b) Recycle Compressor Outlet Pressure and Brake Power

Figure 5.5: Control Philosophy-2 response to 20% step change in hydrogen feed flow rate

Results:

- It demonstrates that control philosophy-2 is a successful method for restoring system pressure to its initial level when the hydrogen feed flow rate is reduced. When the hydrogen input flow rate is reduced by 20%, an immediate pressure reeduction of 2 bar is noticed.

- The controller detects a deviation in set point, and the system is able to return to a stable and desired steady-state condition after around 25 minutes. However, it should be noted that response time is affected by control parameter adjustment.

- The recycle compressor's brake power was lowered from 12.5kW to 5.25kW throughout the pressure recovery operation. This reduction in recycle compressor brake power eventually reduces the mass flow rate of the recycle stream.

- Because of the mass balance at the inlet of the synthesis loop and recycle, the pressure returns to its original value. To maintain a stoichiometric inlet feed flow rate ratio of 3 ($H_2 : N_2$), a ratio controller is also employed.

To get a more insightful findings about the system behaviour, a gradual change of hydrogen feed flow rate is implemented and is discussed in the subsection below.

5.4.2. Linear Change of Hydrogen Feed Flow Rate to Control Philosophy-2

The following Figure 5.6 represents the response of control philosophy-2 to a gradual reduction in hydrogen feed. Similar to linear reduction in hydrogen feed in Control Philosophy-1, four regions can be observed in the plots and each region (A, B, C, D) represents similar action done as described in Table 5.1. The results and findings are discussed after the response shown for each of the scenarios.
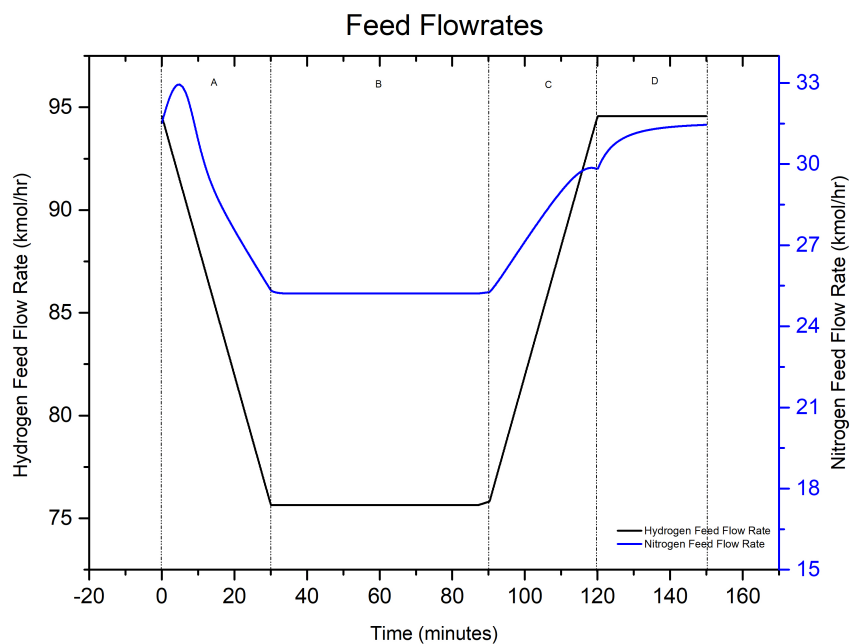
(a) Hydrogen and Nitrogen Feed Flow Rates
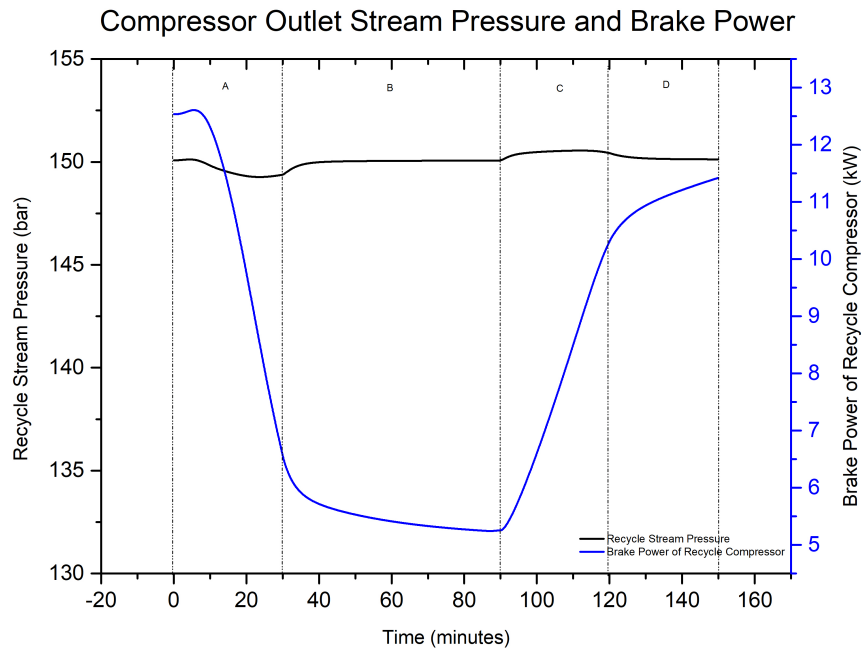
Compressor Outlet Stream Pressure and Brake Power

(b) Compressor Outlet Pressure and Brake Power

Recycle Flowrate and Ammonia Production Rate
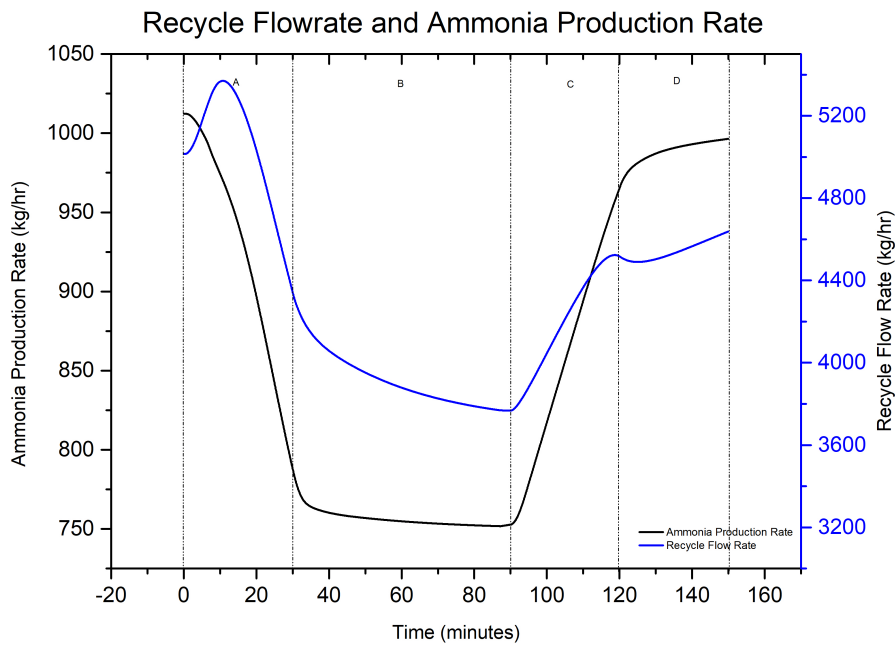
(c) Recycle stream Flow Rate and Ammonia Production Rate

Figure 5.6: Control Philosophy-2 response to 20% linear change in hydrogen feed flow rate

Results:

- **Region A:** A similar trend has been identified when observing reduction in hydrogen and nitrogen flow rates, as depicted in Figure 5.3 of control philosophy-1. The compressor brake power gradually decreases throughout the period of reduced hydrogen feed flow rate. This decrease in compressor power corresponds to a decrease in flow rate, resulting in less gas entering the system. As a result, the decrease in system pressure is small and exhibits only minor oscillations. As expected, the reduction in reactants reduces ammonia production.

- **Region B:** The hydrogen and nitrogen feed flow rates were kept constant for 60 minutes in order for the system to reach its new steady-state. During this simulation phase, the system pressure remains constant, but the recycle flow rate does not reach a steady-state value. This demonstrates that the system takes more than 60 minutes to achieve new steady-state conditions.

- **Region C:** The hydrogen supply is linearly scaled up to its initial value for 30 minutes. The recycle flow rate increases as the flow rate increases. As a result, the compressor's braking power increases in order to compress more gas. The system's pressure does not shift abruptly. As a result of the increased reactant feed flow rate, the ammonia production rate rises.

- **Region D:** The system is left for 30 minutes after the linear ramp-up of the hydrogen feed flow rate to reach its original steady-state values. Because steady-state conditions are not met, the current model takes longer than 150 minutes.

Conclusion:

1. **Compressor Brake Power:**

   - The model includes a recycle compressor, which is critical to the system. The compressor's brake power is a crucial characteristic that influences the level of gas compression. Reduced brake power results in lower gas compression. This causes a reduction in flow rate, which balances the recycle flow rate with the reduced feed flow rate. The result is that the pressure is retained its initial level.

2. **Ammonia Production:**

   - The model additionally tracks ammonia synthesis, which is an immediate consequence of the hydrogen-nitrogen reaction process. The models provided useful insights into the temporal variability in ammonia production rates when feed flow rates are changed. As the availability of reactants decreased, the production rates gradually decreased over time.

3. **Model Performance and Limitations:**

   - The model successfully runs until the hydrogen supply flow rate is reduced by 70%, and no restrictions have been discovered. However, the brake power of the compressor is not as flexible as it is assumed to be in Aspen Plus dynamics. When the brake power is too low, the compressor does not work, resulting in instability in the production unit.

4. **Pressure Control:**

   - The model includes a feedback mechanism that continuously checks the system's pressure. The model can respond quickly to pressure variations, ensuring that pressure fluctuations are addressed. Based on the pressure feedback, the controller adjusts the recycle compressor's brake power to maintain a steady pressure under varying input feed flow rates.

5.5. Control Philosophy-3

The operating principle of control philosophy-3 is to replace the deficient hydrogen with surplus nitrogen thereby changing the stoichiometric ratio of H_2:N_2. The pressure controller measures the downstream pressure of the reactor and is connected to the nitrogen valve. This controller opens/closes the nitrogen valve to reach the set-point of pressure. Figure 5.7 shows the control philosophy-3 from Aspen Plus Dynamics and Table 5.4 illustrates the details and parameters of the controllers used for the current philosophy 3.
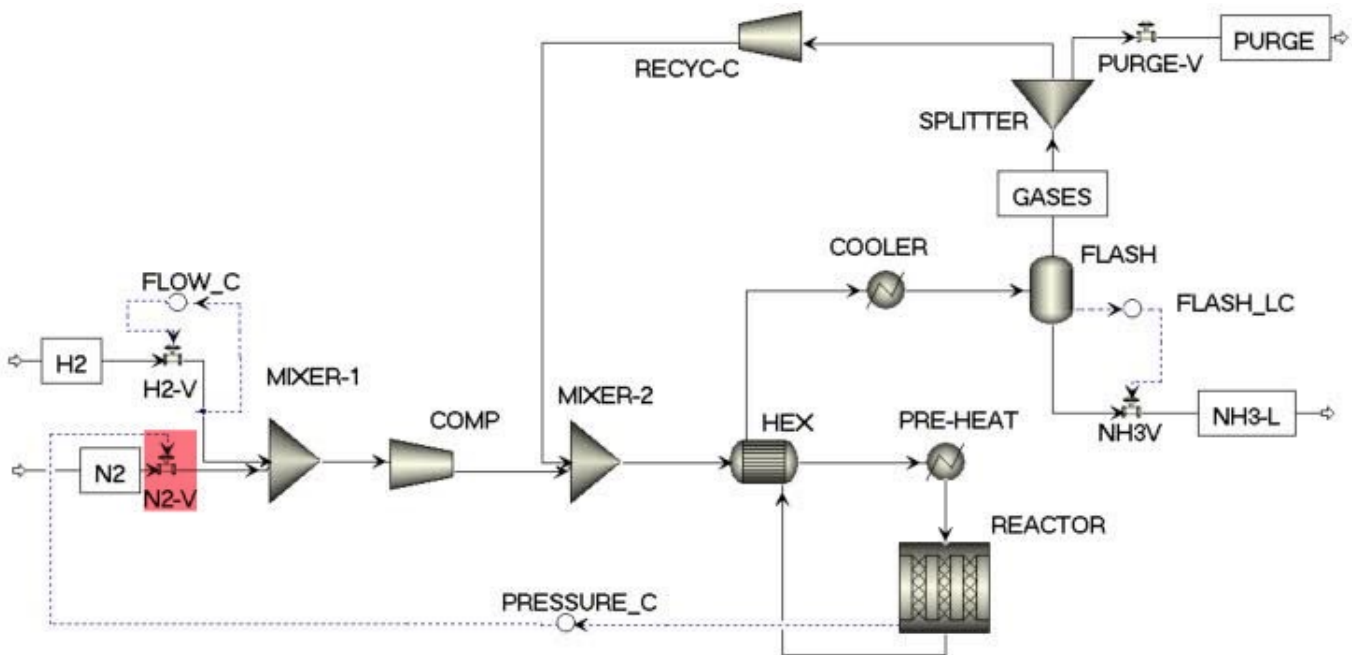
Figure 5.7: Control Philosophy-3 from Aspen Plus Dynamics

	Proportional Gain (%/%)	Integral Time (min)	Controller Action	Controlled Variable	Manipulated Variable
FLOW-C	1	1	Reverse	Hydrogen Feed Flow Rate	H2-V Opening
PRESSURE-C	1	1	Reverse	Downstream Pressure of Reactor	N2-V Opening
FLASH-LC	10	1	Direct	Flash Liquid Level	NH3-V Opening

Table 5.4: Control Philosophy-3 controller parameters and details

5.5.1. Step-Change in Hydrogen Feed Flow Rate to Control Philosophy-3

Similar to Control Philosophy 1 & 2, a step-change in reduction of hydrogen feed flow rate is implemented to examine the behaviour of the system. The response time of the controller and the effect of control action are noticed and plotted below in Figure 5.8.
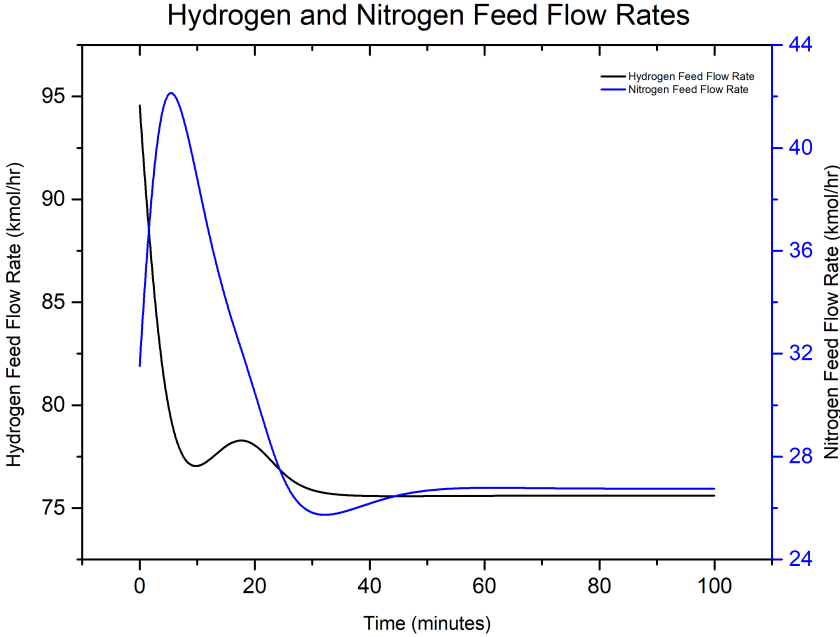
(a) Hydrogen and Nitrogen Feed Flow Rates
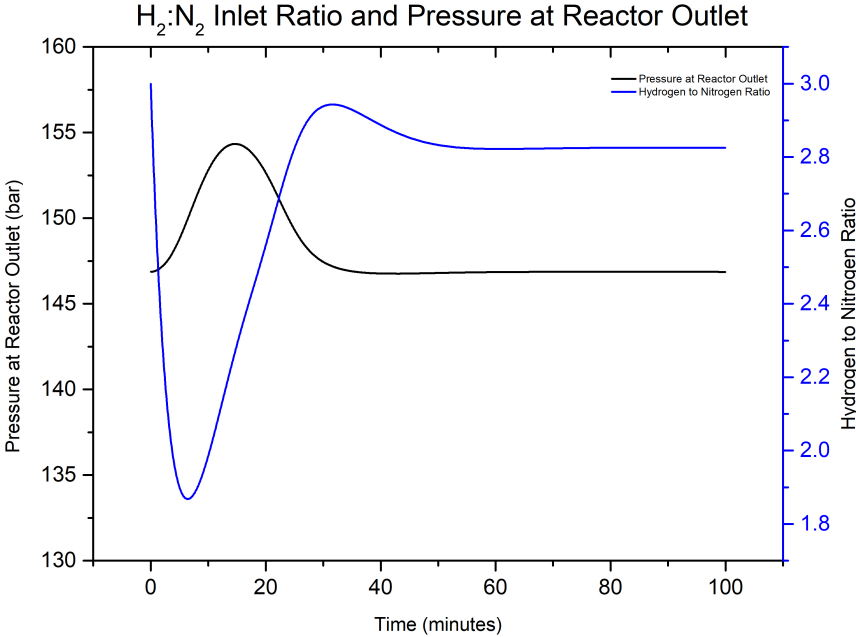
(b) Inlet Feed Ratio and Pressure at Reactor Outlet
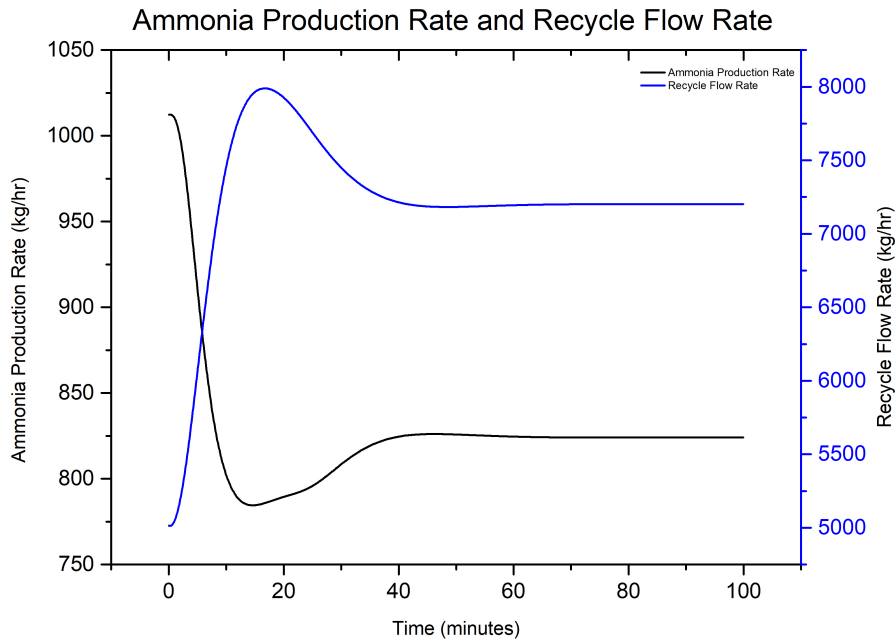
(c) Recycle stream Flow Rate and Ammonia Production Rate

Figure 5.8: Control Philosophy-3 response to 20% step change in hydrogen feed flow rate

Results:

- **Hydrogen and Nitrogen Feed Flow Rates:**

  – A 20% reduction in hydrogen input flow rate causes the system to respond dynamically. The nitrogen flow rate peaks at a given point and then gradually decreases over time. One probable explanation is that the controller initially uses nitrogen as a substitute to replace the deficit hydrogen feed flow rate and then gradually declines when the systems gets adapted to reduces hydrogen feed flow rate. The pressure controller adjusts the nitrogen feed flow rate to keep the system pressure stable.

- **Inlet Ratio and Pressure at Reactor Outlet:**

  – The drop in hydrogen feed flow rate has an immediate effect on the stoichiometric $H_2 : N_2$ ratio, generating an initial decrease due to the addition of extra nitrogen. When the system responds to changes in feed conditions, the ratio settles down to around 2.8.

  – When the hydrogen input flow rate is reduced, the pressure at the reactor outlet rises due to unreacted nitrogen in the reactor. An initial pressure increase of 6 bar is observed, but the pressure gradually recovers to its initial value over time.

- **Ammonia Production Rate and Recycle Flow Rate:**

  – The recycle flow rate has increased significantly. This is because there is more nitrogen in the system than usual, and because the density of nitrogen is higher, the recycling flow rate increases. This impact is caused by a decrease in the stoichiometric inlet ratio. Hydrogen becomes the limiting reactant in ammonia production, hence a decrease in hydrogen leads to a decrease in ammonia production rate.

5.5.2. Linear-Change in Hydrogen Feed Flow Rate to Control Philosophy-3

Instant increase in pressure was observed when there is an instant reduction in hydrogen feed flow rate. To mitigate this, a hydrogen buffer could be added and therefore, the hydrogen ramp-down is done linearly. The effect of the gradual reduction in hydrogen feed flow rate is shown below in Figure 5.9.
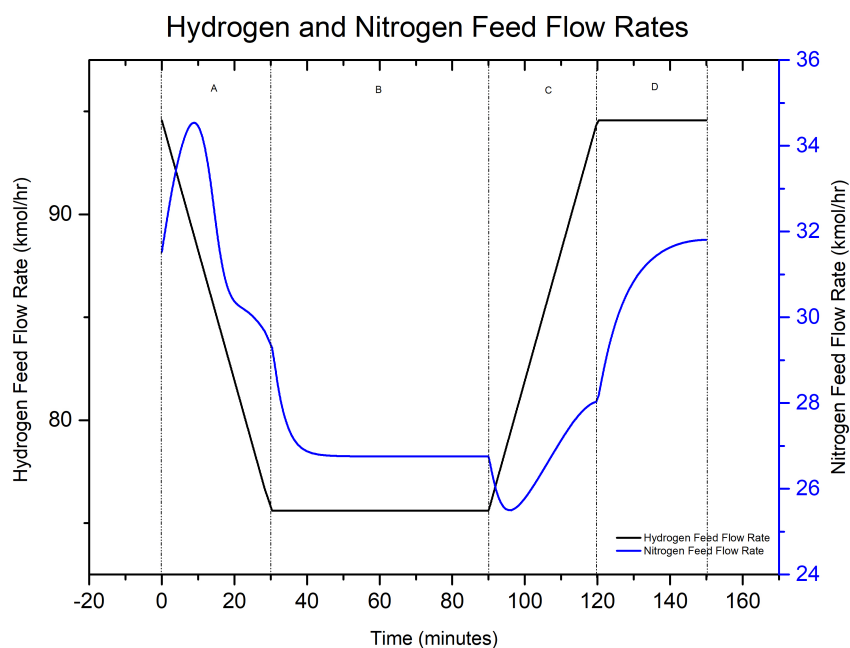
(a) Hydrogen and Nitrogen Feed Flow Rates

Discussion:

- **Region A:** During the first 30 minutes, the nitrogen feed flow rate increases while the hydrogen feed flow rate is linearly lowered. To compensate for the system's lack of hydrogen, the controller pumps nitrogen. This behavior was also observed when the hydrogen input flow rate was abruptly lowered, as illustrated in Figure 5.8 (a). As the system gets adjusted to the changing hydrogen flow rate, the nitrogen flow rate decreases, indicating a dynamic adjustment period.

- **Region B:** The simulation is carried out for 60 minutes to bring the model to a new steady-state. The hydrogen feed flow rate stabilizes but the nitrogen feed flow rate remains constant after ~ 40 minutes. This time period represents the formation of a new equilibrium under different hydrogen feed conditions.

- **Region C:** For 30 minutes, the hydrogen feed flow rate is linearly ramped up to the original value, and a minor dip in the nitrogen feed flow rate is noticed. As a result of the increased hydrogen feed flow rate, the controller reduces the nitrogen to compensate for any pressure increase caused by the increased hydrogen flow rate. The nitrogen input flow rate gradually increases.

- **Region D:** The model is run for the final 30 minutes to recover its original steady state settings. By the end of the 150-minute simulation, the hydrogen feed flow rate is constant, and the nitrogen feed flow rate is nearly constant.
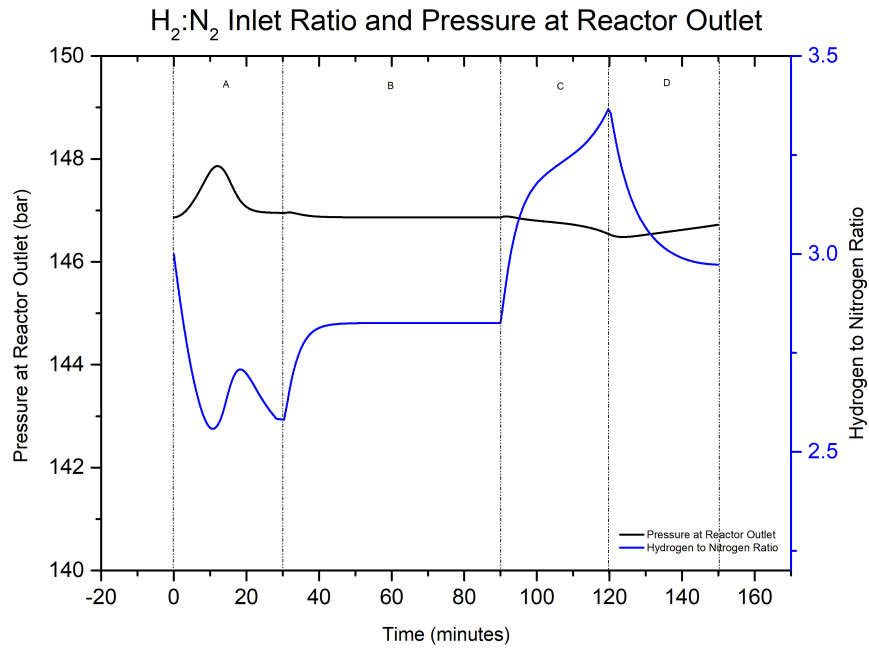
H$_2$:N$_2$ Inlet Ratio and Pressure at Reactor Outlet

(b) Inlet $H_2 : N_2$ Ratio and Pressure at Reactor Outlet

Recycle Flow Rate and Purge Flow Rate
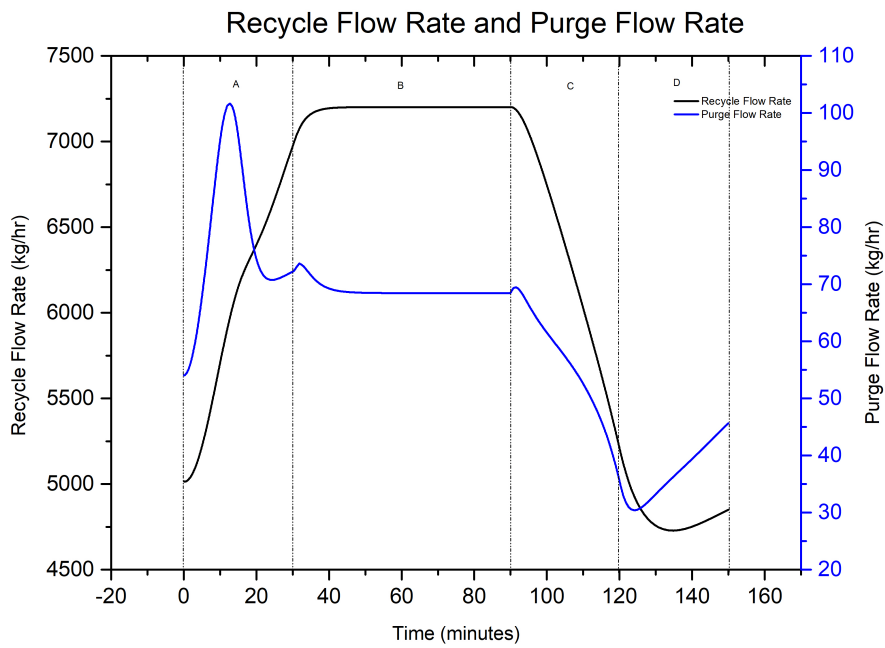
(c) Recycle stream Flow Rate and Purge Flow Rate

Figure 5.9: Control Philosophy-3 response to 20% linear change in hydrogen feed flow rate

Discussion:

- **Region A:** A 1 bar increase in pressure is seen at first, followed by a return to its original value. The stoichiometric ratio of $H_2 : N_2$ fluctuates, which is controlled by nitrogen feed rate variability. Because of the increase in nitrogen gas in the system, both recycle and purge flow rates increase significantly.
- **Region B:** When the feed is kept at a steady rate, the pressure in the system remains constant, suggesting a stable system response. The input hydrogen to nitrogen ratio stabilizes at 2.8. The recycle and purge flow rates are also constant, resulting in a 45% increase in the recycling flow rate.
- **Region C:** With only a minor decrease in pressure, the pressure practically remains constant. The inlet ratio rises from 2.8 to 3.3, indicating an adjustment to the changing hydrogen supply flow rate. Both the recycle and purge flow rates drop in reaction to the increasing hydrogen feed flow rate.
- **Region D:** The pressure remains constant at the end of the 150-minute experiment, showing the system's stability. The ratio attained a value of 3. However the recycling and purge flow rates did not reach a steady-state value, indicating that more time is needed to stabilize under the current control parameters.

Conclusion:

1. **Response to Hydrogen Reduction**

    - When the hydrogen feed flow rate is reduced by 20%, the nitrogen feed flow rate increases. This spike could be the result of the pressure controller's response, which alters the nitrogen feed flow rate to maintain system pressure.

2. **Shift in Inlet Stoichiometric Ratio**

    - Reduced hydrogen feed flow rate has a direct impact on the inlet stoichiometric ratio of hydrogen to nitrogen, resulting in an initial abrupt fall. When the hydrogen supply is reduced by 20%, the ratio settles to 2.8, stabilizing the system pressure.

3. **Recycle Flow Rate Increase**

    - When the hydrogen feed flow rate is lowered, the recycle flow rate increases significantly. This is because a greater amount of nitrogen is pumped into the system to compensate for the lack of hydrogen. This rise in recycle flow rates poses issues to the manufacturing unit.

4. **Model Performance and Limitations**

    - The model successfully runs until the hydrogen supply flow rate is reduced by 70%, and no restrictions have been discovered. However, these reduced flow rates pose a significant issue when managing with higher recycle flow rates.

6

Economic Evaluation

An economic evaluation has been carried out using **HySupply** open-source tools [13] to see the behaviour and the costs associated with the ammonia production plant under different scenarios. Four different tools have been developed by the professors from the University of New South Wales. For the current thesis project, HySupply Cost Analysis Tool and HySupply Ammonia Tool have been used to calculate the total investment costs of the entire ammonia production unit under various conditions. The HySupply Cost Tool is used to model the hydrogen production unit and determine the levelized cost of hydrogen (LCOH). HySupply Ammonia Tool is used for cost analysis of ammonia plant by determining the levelized cost of ammonia (LCOA). Different scenarios are considered and are shown in section 6.1 below.

6.1. Scenarios

Five different scenarios have been considered to determine the overall costs and the feasibility of working of the ammonia production unit. They are:

- Solar PV generator connected to electrolyzer and Haber-Bosch unit
- Wind generator connected to electrolyzer and Haber-Bosch unit
- Hybrid (Solar+Wind) generator connected to electrolyzer and Haber-Bosch unit
- Grid connected wind generator to electrolyzer and Haber-Bosch unit
- Wind generator connected to electrolyzer, Haber-Bosch unit and Battery

Due to the fluctuations in the sun and wind, generation of electricity from renewables is fluctuating. These fluctuations depend on several factors and thus, a back-up power source is necessary in order to maintain the ammonia synthesis plant running. Therefore, a balancing technology has to be used in order to stabilize these fluctuations. For the sake of simplicity, the balancing technologies used for the current thesis project are batteries and grid connected electricity. A cost analysis is carried out for the presented scenarios. Several other scenarios could be considered depending on the desired output. Some of the options that are generally considered are:
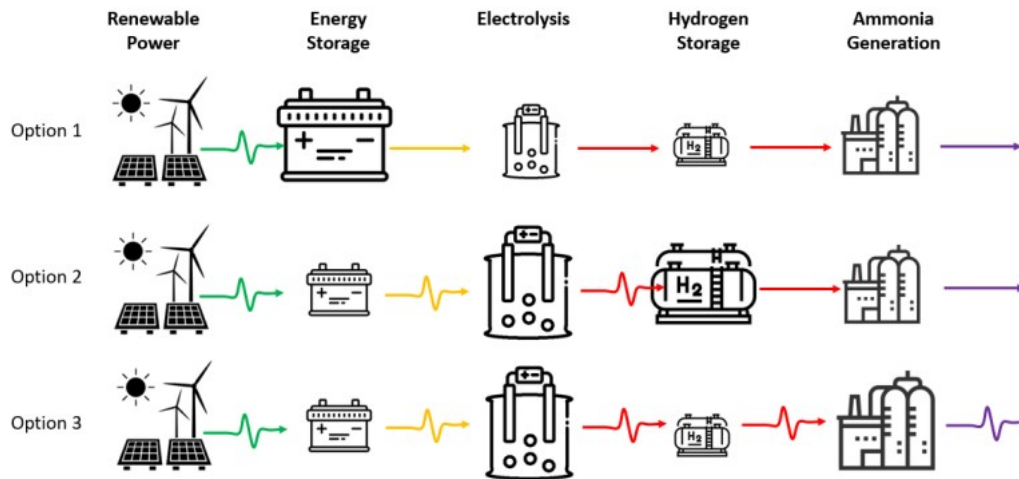
Figure 6.1: Three Different Options for Green Ammonia Production

As illustrated in the Figure 6.1, the three possibilities for manufacturing ammonia from renewable energy sources are large scale energy storage, hydrogen storage, and flexible ammonia synthesis reactor. Option 1 employs battery/grid electricity storage to smooth out variable electric power. This battery or grid is used to generate uniform electric power in order to continually manufacture hydrogen, which is then fed into the ammonia synthesis reactor, which functions on a uniform scale. Option 2 generates hydrogen using various amounts of renewable energy and then stores it in huge, compressed gas tanks. This stored hydrogen is utilized to balance out the fluctuating hydrogen production rate, maintaining a steady supply of hydrogen to the ammonia synthesis unit. Option 3 uses multiple ammonia synthesis reactors in parallel where each of the reactor is configured differently. In this way of configuration, the ammonia production is flexible.

For the current thesis project, option 2 is considered where the effect of over sizing of electrolyzer and introduction of hydrogen buffer storage on the levelized costs of ammonia are studied.

6.2. Input Data to the Tools

Several assumptions have been made in the cost analysis tools and are given as input to the models in order to calculate the costs associated with each of the scenario. Some of the assumptions/input data provided are based on the data from Open-Source tool [13]. For all the scenarios, the solar and wind data have been extracted from renewables.ninja [19] and were exported to the custom column in the analysis tools.

- The operational year of the plant is considered as 2030.
- The power consumption of the electrolyzer for the balance of the plant has been assumed to be 54.3 kWh/kg$_{H_2}$ [76].
- An 8 hours of hydrogen buffer storage at rated electrolyzer power for all configurations has been reported [76] and therefore, the hydrogen buffer used for the current project is 8 hours but it is highly dependant on location and availability of renewable power resources.
- The stack lifetime is assumed to be 80000 hours with a stack degradation of 1%/year.
- Electrolyzer cost is considered as USD 785/kW from the data provided by Proton Ventures B.V.
- Installation costs are 200% of CAPEX for electrolyzer, 400% for ammonia synthesis unit according to Lange factor [77].
- Solar PV farm equipment cost is considered as USD 480/kW and Wind farm cost as USD 740/kW (values from Proton Ventures B.V.) with a USD 15000/MW/year OPEX for solar [78] and USD 40000/MW/year OPEX for wind [79].

- The cost of batteries is considered as USD 152/kW according to BloombergNEF [80] with a lifetime of 10 years.
- The SEC of Ammonia plant is considered as 0.41 kWh/kg$_{NH_3}$ and the SEC of air separation unit is 0.23 kWh/kg$_{N_2}$ [13].
- The ammonia synthesis unit cost is USD 378/T$_{NH_3}$ and air separation unit cost as USD182/T$_{N_2}$ [13].
- The operating costs for electrolyzer is 2%/year of electrolyzer purchase cost. The operating costs for ammonia synthesis unit and air separation unit are considered to be 2% of CAPEX.
- For HVAC transmission lines, a cost of USD 323000/km [81] is considered by taking 3.6% inflation rate per year with an installation cost of 10% of CAPEX.
- According to Global Petrol Prices [82], the cost of all components of the electricity bill such as cost of power, distribution and taxes in Morocco is taken as USD106/MWh.
- Depreciation time is taken as 20 years and a discount rate of 7% per annum for calculation of levelized costs.

6.3. Solar PV generator with Electrolyzer and Haber-Bosch unit

In the first scenario, a solar farm is connected to the electrolyzer, air separation unit and Haber-Bosch unit. The size of the solar farm is determined by the total amount of electricity required for each of the processes. A calculation is made to determine the amount of solar electricity required.

Electrolyzer Capacity:

The amount of hydrogen required to produce 25 tonnes of ammonia per day is 190 kg/hr. Therefore, the total amount of electricity required is 10.31 MW

$$Capacity = 190 \times 54.3 = 10317 \; kW = 10.317 \; MW$$

Ammonia Synthesis Unit Energy Consumption:

The ammonia synthesis unit is less energy intensive process as compared to hydrogen production. As stated in inputs that the SEC of ammonia synthesis is 0.41 kWh/kg of ammonia produced, the total electricity requirement for the Haber-Bosch process is 0.42MW.

$$Required \; Electricity = \frac{Annual Ammonia Production}{8760} \times \frac{SEC_{NH_3}}{1000}$$

$$= \frac{9000000}{8760} \times \frac{0.41}{1000}$$

$$= 4212 \; kW \; = \; 0.42 MW$$

In a similar way, the power demand of air separation unit is also calculated and found to be 0.19 MW.

Therefore, the total capacity of the solar farm is modelled as 11 MW.

Electrolyzer Response to Solar PV generator:

Based on the input data provided to the cost analysis tool, the following response of electrolyzer is observed. Figure 6.2 below shows the capacity factor of electrolyzer as a function of time for the enitre year.
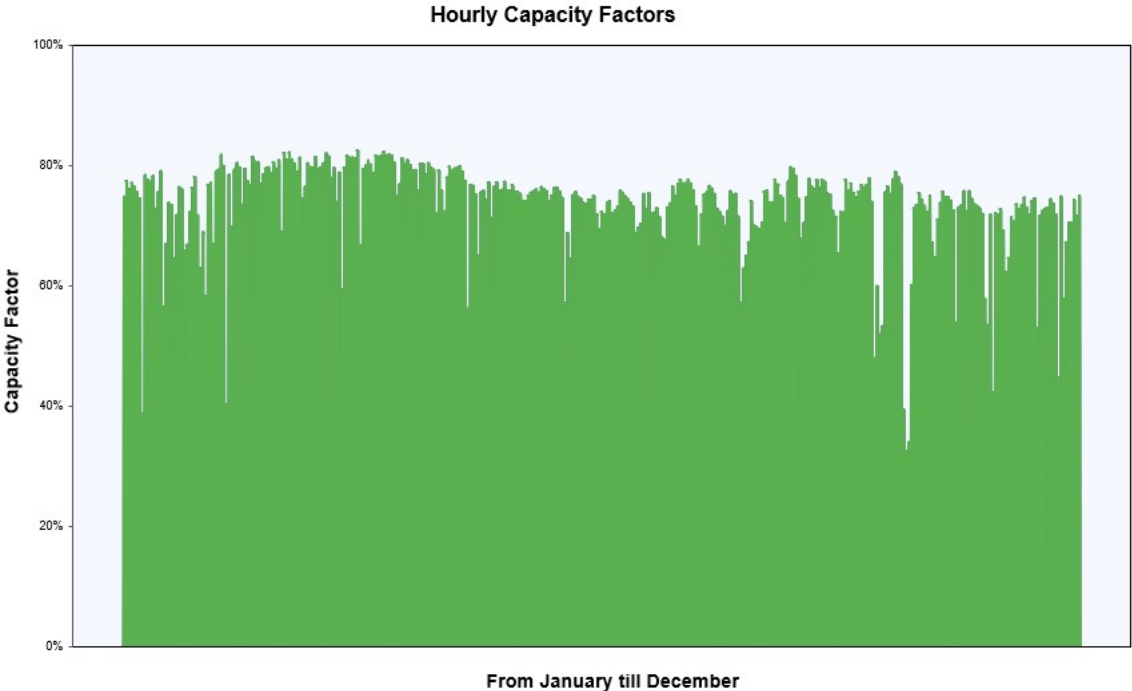
(a) Capaciity Factor of Electrolyzer as a function of time

To get a clear understanding of the performance of the electrolyzer, the Figure 6.2 shows the capacity factor of electrolyzer for 30 days.
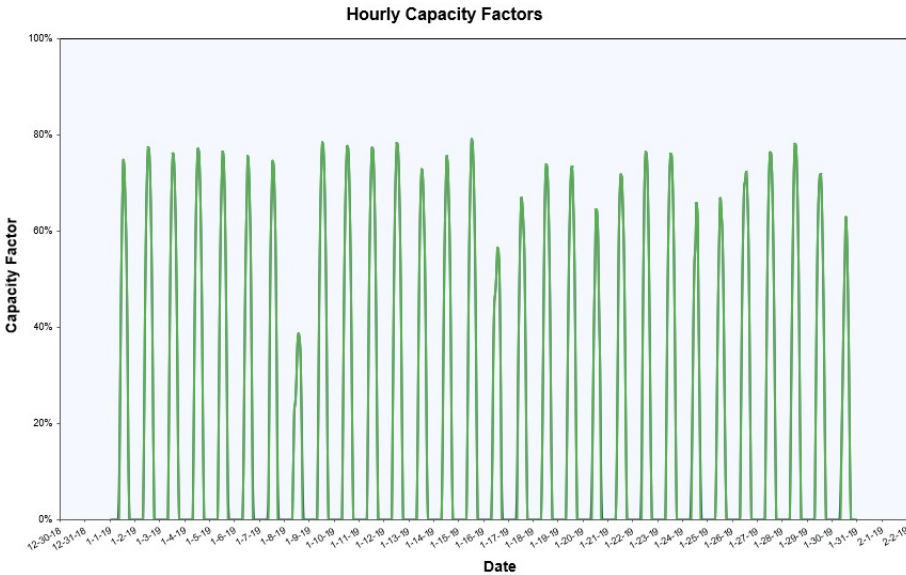
(b) Hourly Capacity Factor of Electrolyzer for 30 days

Figure 6.2: Capacity Factor vs Time for Solar PV connected Electrolyzer

It can be observed from the graph above that the capacity of the electrolyzer drops to 0 when there is a lack of sunlight (during the night). The capacity factor of an electrolyzer is highly influenced by the intermittent nature of solar PV. During cloudy days, during the night, or at times in less solar irradiation, the electrolyzer's operation is affected leading to a lower capacity factor. This is also clear that the lack of energy storage systems or energy supply impacted the performance of electrolyzer. The key results

obtained form the analysis tool are given in the Table 6.1 below.

Parameter	Value
Total Time Electrolyzer is Operating	43%
Electrolyzer Capacity Factor Achieved	23%
Energy Consumed by Electrolyzer (MW/yr)	21000
Hydrogen Output (TPA)	325
LCOH (USD/kg)	7.2

Table 6.1: Solar PV connected Electrolyzer results

Haber-Bosch unit response to Solar PV generator:

The current section presents an analysis of ammonia production unit integrated with solar PV generator. The hourly performance graphs indicate the dynamics between solar power generation and ammonia production. The below Figure 6.3 show the real-time relationship between solar energy availability and its impact on ammonia production efficiency throughout the year. The Figure 6.4 shows the performance of ammonia production unit for 30 days.
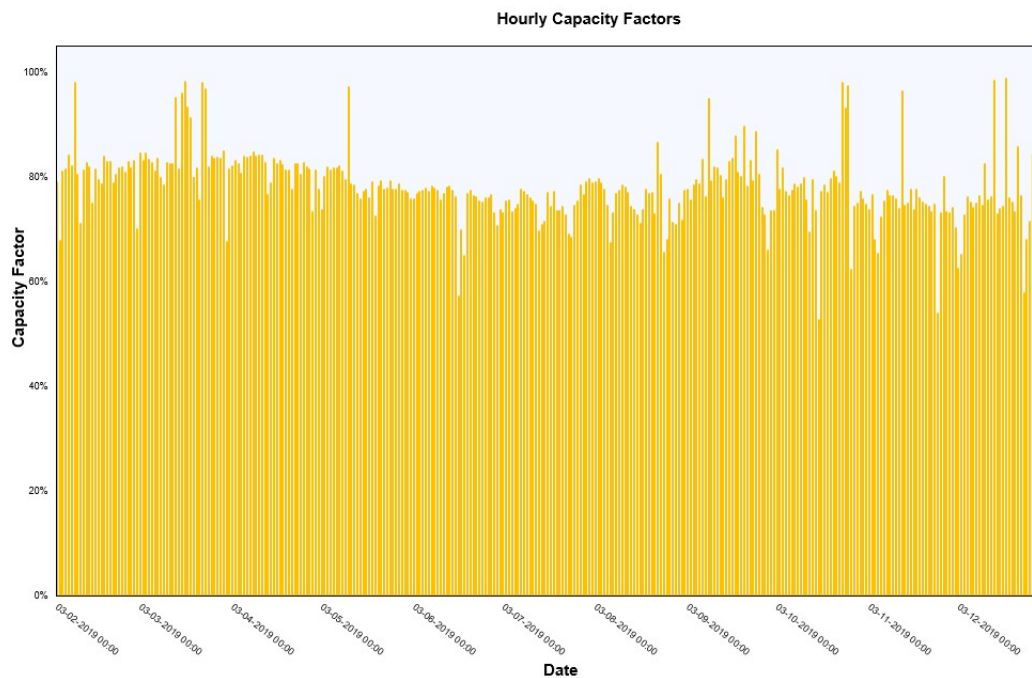
Figure 6.3: Capacity Factor as a function of time
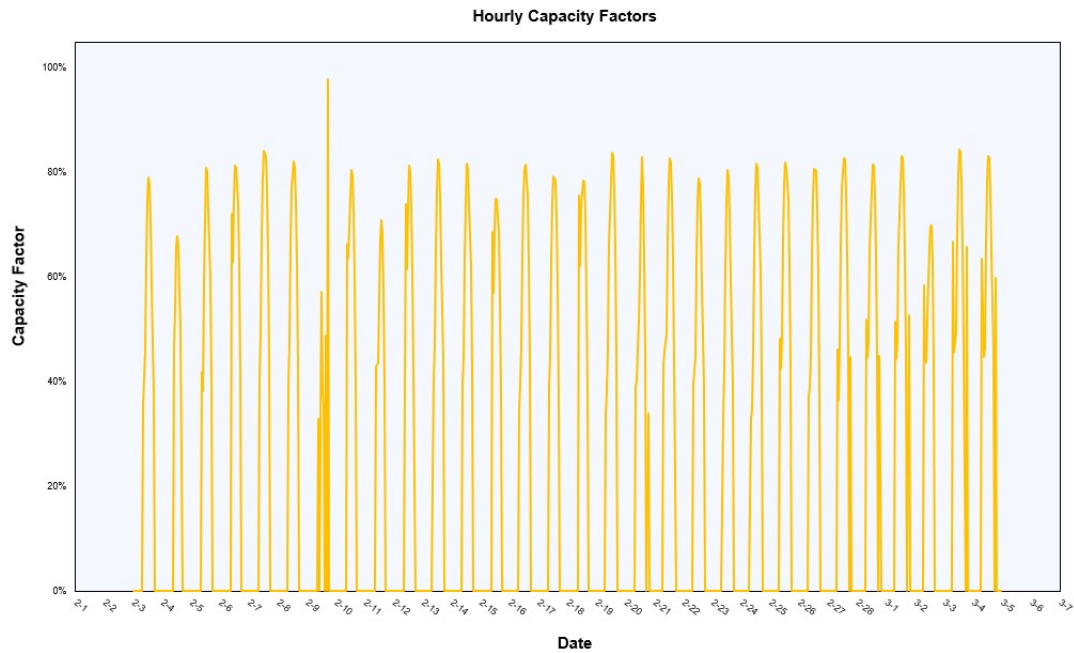
Figure 6.4: Hourly Capacity Factor for 30 days

The integrated solar PV generator and ammonia synthesis unit highlight significant aspects of its performance. The ammonia production plant exhibits a capacity factor of 22%. Due to the limited availability of the power supply , the total ammonia production per annum reduced from 9000 tonnes to 1900 tonnes, exhibiting a reduction in 80%. Additionally, the levelized cost of ammonia stands at USD 3.3/kg. Table 6.2 below shows the results obtained from the simulation.

Parameter	Value
Average Power Plant Capacity Factor	22%
Annual Capacity Factor of Ammonia Plant	20%
Average Total Time Ammonia Plant is in Operation	3220 hrs/yr
Ammonia Produced (TPA)	1900
LCOA (USD/kg)	3.3

Table 6.2: Solar PV connected Ammonia Production Plant Results

Table 6.3 shows a breakdown of capital costs associated with each of the components in the ammonia synthesis unit. In the transmission costs, the transmission distance is assumed to be 25 km. The indirect costs include the installation costs for the electrolyzer, ammonia synthesis unit, air separation unit, power plant installation and transmission line installation. It is observed that the total capital costs associated with setting up an ammonia production facility under solar PV generator is **USD 62 million**.

Component	Capital Cost (USD)
Power Plant	5.2 million
Transmission	8 million
Electrolyzer	8.1 million
Ammonia Plant	3.4 million
Air Separation Unit	1.3 million
Indirect Costs	35 million
Total Capital Costs	**62 million**

Table 6.3: Total Capital Costs for Solar PV Connected Ammonia Plant

6.4. Wind generator with Electrolyzer and Haber-Bosch unit

In the second scenario, a wind farm is connected to the electrolyzer, air separation unit and the ammonia synthesis unit. The size of the wind farm is the total amount of electricity that is determined in section 6.3 is 11 MW. Both the responses of the electrolyzer and ammonia synthesis plant are recorded and the results obtained are portrayed in each of the subsections.

Electrolyzer response to Wind generator:

In the figures below, the dynamic response of the electrolyzer when integrated with a wind generator is observed, along with the corresponding capacity factor achieved. Figure 6.5(a) provides a detailed view of response of the electrolyzer over a course of 30 days and Figure 6.5(b) portrays the electrolyzer's response and behaviour over the course of an entire year.
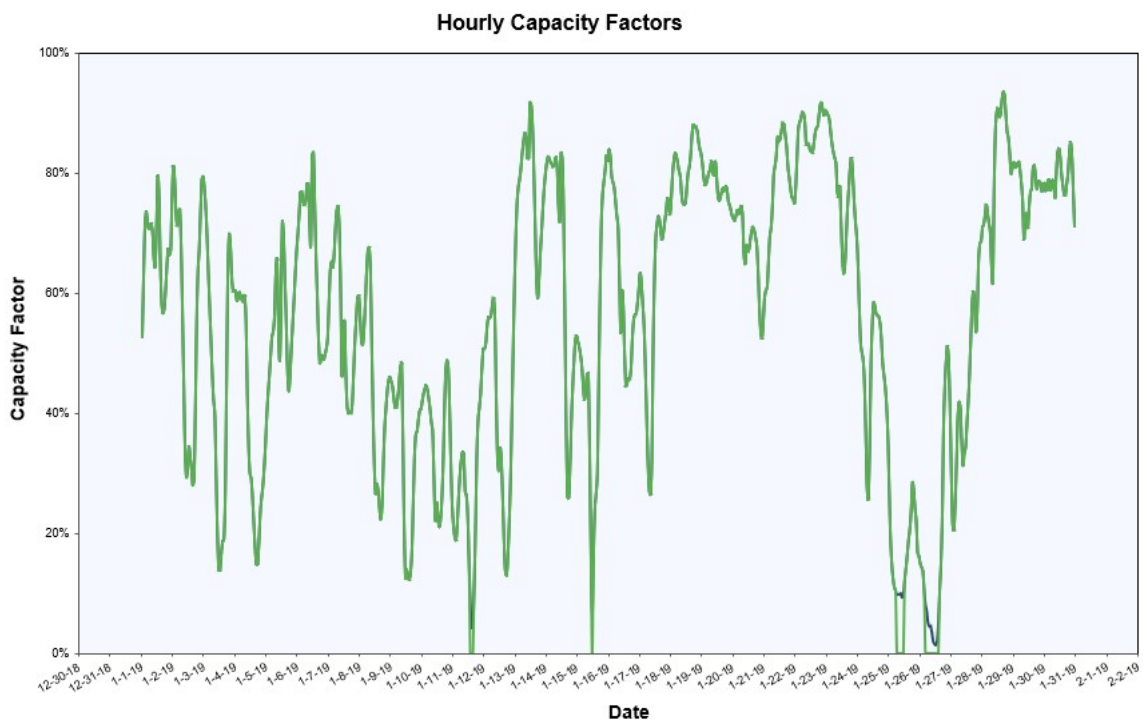
(a) Hourly Capacity Factor of Electrolyzer for 30 days
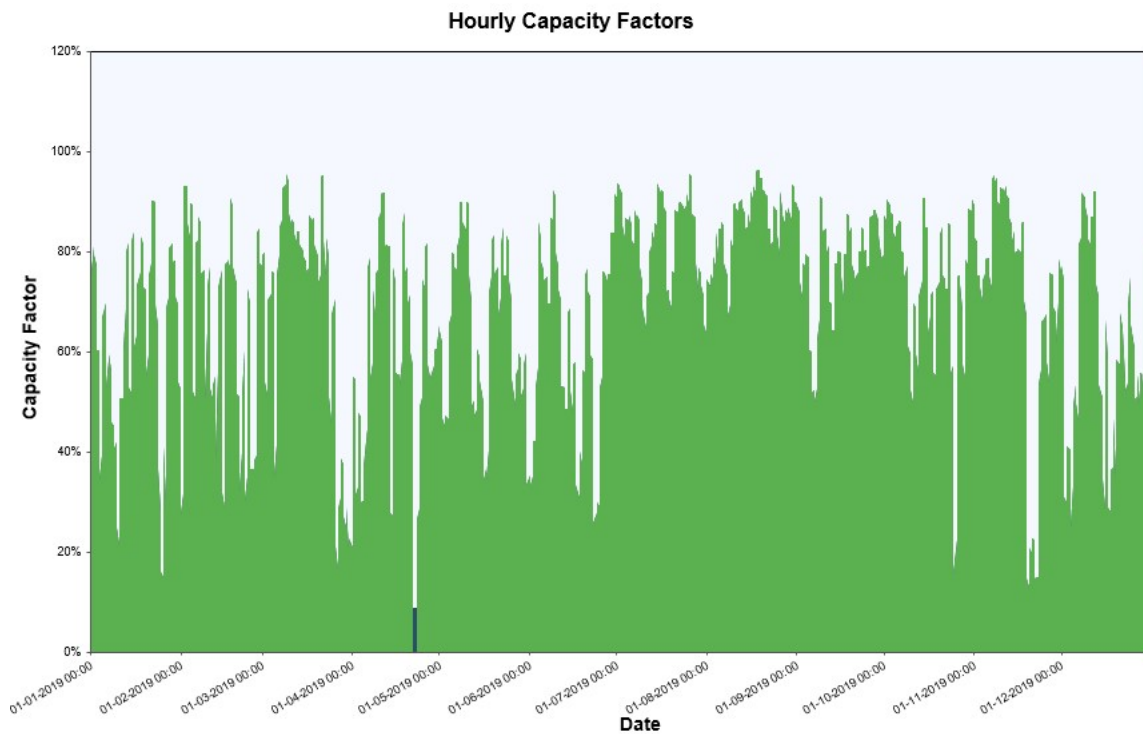
(b) Capacity Factor of Electrolyzer throughout the year

Figure 6.5: Capacity Factor vs Time for Wind Generator connected Electrolyzer

The figures above graphically demonstrate the significant impact of wind fluctuations on electrolyzer performance. Variability in wind-related elements such as wind speed and turbine height have a substantial impact on daily hydrogen generation, resulting in noticeable fluctuations. Despite this unpredictability, the electrolyzer's improved performance stands out, with a capacity factor improved to 70% when compared to a solar PV generator at 23%. Notably, this improvement in capacity factor results in a drop in the levelized cost of hydrogen, reaching an economically advantageous USD 3.16 per kg_{H_2} generated. Table 6.4 presents specific insights and comparative data, offering a thorough overview of the achieved results and showing the economic viability of this integrated system.

Parameter	Value
Total Time Electrolyzer is Operating	98%
Electrolyzer Capacity Factor Achieved	70%
Energy Consumed by Electrolyzer (MWh/yr)	63000
Hydrogen Output (TPA)	950
LCOH (USD)	3.16

Table 6.4: Wind Connected Electrolyzer Results

Haber-Bosch unit response to wind generator:

In the figures below, the dynamic response of the ammonia synthesis plant when integrated with wind generated electricity is observed, along with the corresponding capacity factor achieved and the amount of ammonia produced per year. Figure 6.6(a) provides a view of response of ammonia synthesis plant over a course of 30 days and Figure 6.6(b) shows the behavior of the Haber-Bosch unit for a span of entire one year.
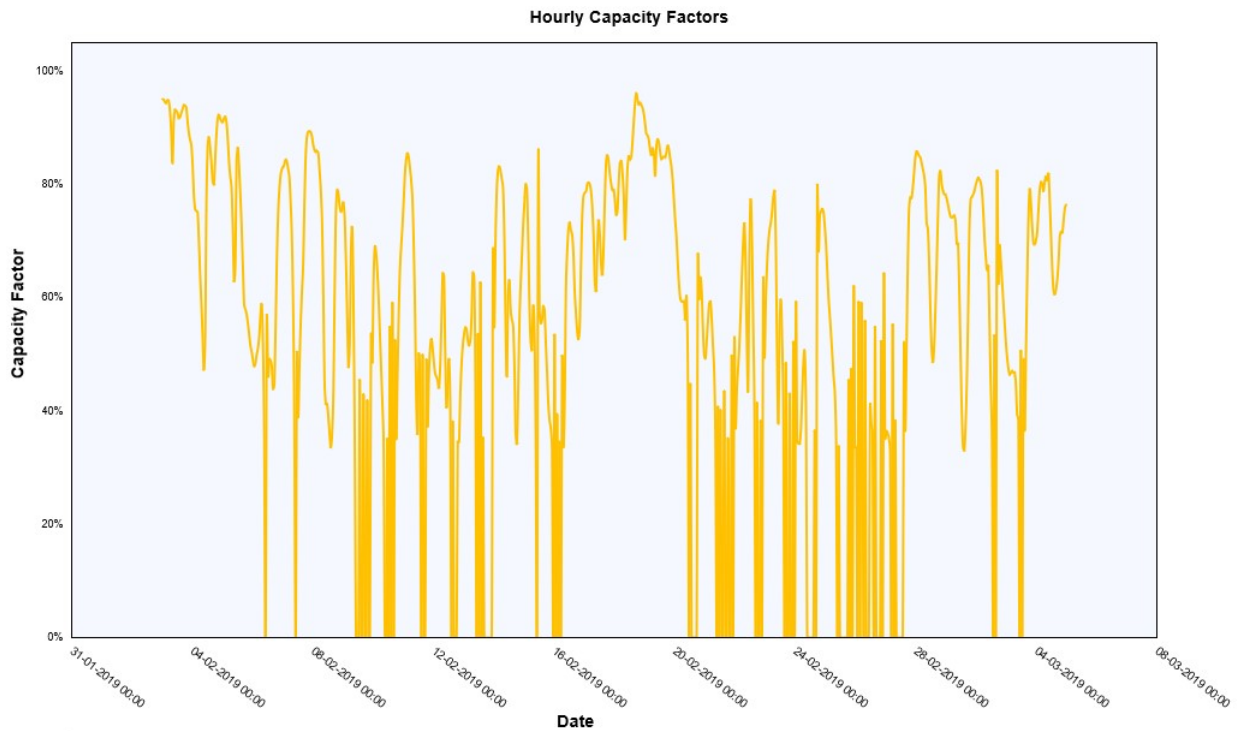
(a) Hourly Capacity Factor of Ammonia Synthesis Plant for 30 days
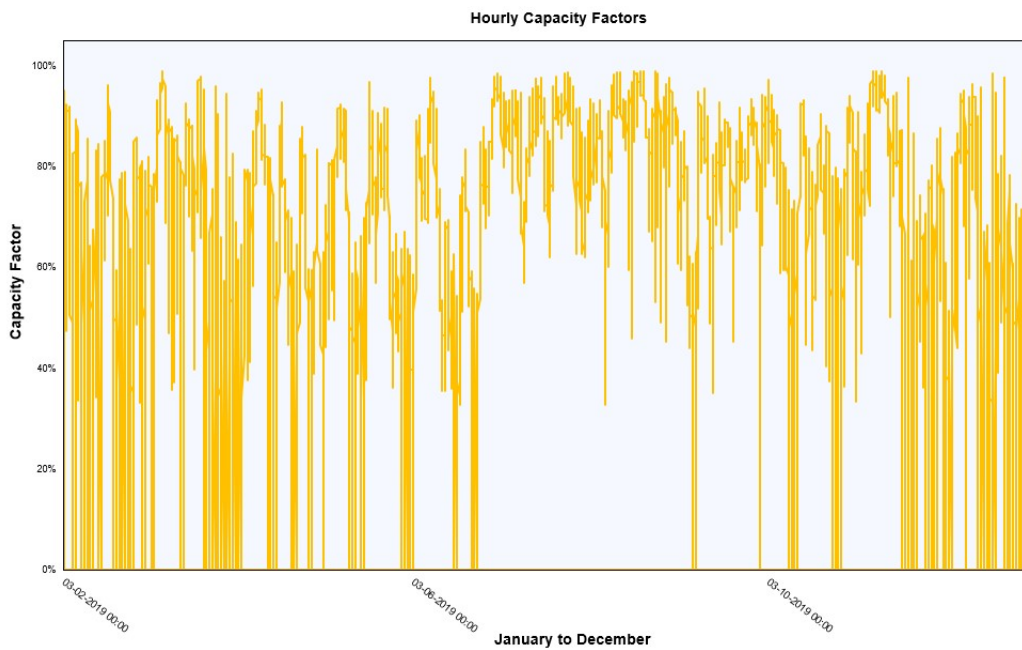
(b) Capacity Factor of Ammonia Synthesis Plant throughout the year

Figure 6.6: Capacity Factor vs Time for Wind Generator connected Haber-Bosch unit

Based on the graphs above and from the simulation, it has been observed that the capacity factor of the ammonia synthesis plant increased to 60% compared to solar PV generator. This is due to higher availability of wind energy with an average power plant capacity factor of 66%. The ammonia plant is observed to be running at maximum capacity for 3.5% of the entire time in an year with a production rate of 5300 TPA. Due to the availability of wind energy, the levelized cost of ammonia reaches USD 1.3 per kg NH_3.

Parameter	Value
Average Power Plant Capacity Factor	66%
Annual Capacity Factor of Ammonia Plant	60%
Average Total Time Ammonia Plant is in Operation	8050 hrs/yr
Ammonia Produced (TPA)	5300
LCOA (USD)	1.3

Table 6.5: Wind connected Ammonia Production Plant Results

Table 6.6 shows a breakdown of capital costs associated with each of the components in the ammonia synthesis unit. In the transmission costs, the transmission distance is assumed to be 25 km. The indirect costs include the installation costs for the electrolyzer, ammonia synthesis unit, air separation unit, power plant installation and transmission line installation. It is observed that the total capital costs associated with setting up an ammonia production facility under wind generator is **USD 65 million**.

Component	Capital Cost (USD)
Power Plant	8.1 million
Transmission	8 million
Electrolyzer	8.1 million
Ammonia Plant	3.4 million
Air Separation Unit	1.3 million
Indirect Costs	35.3 million
Total Capital Costs	**65 million**

Table 6.6: Total Capital Costs for Wind Connected Ammonia Plant

6.5. Hybrid Generator with Electrolyzer and Haber-Bosch unit

In the current section, a hybrid generator (combination of wind and solar) is connected to the electrolyzer and ammonia synthesis plant and the performance of the plants are observed. A hybrid system is usually considered since it provides a more reliable and consistent energy output. Since the optimization of renewable energy plants is out of the scope, 25% of the farm is considered solar and the rest 75% of the farm is considered wind. Based on the depicted hybrid generator split, the performance of electrolyzer and ammonia synthesis plant are shown below along with a cost estimation at the end of the current section.
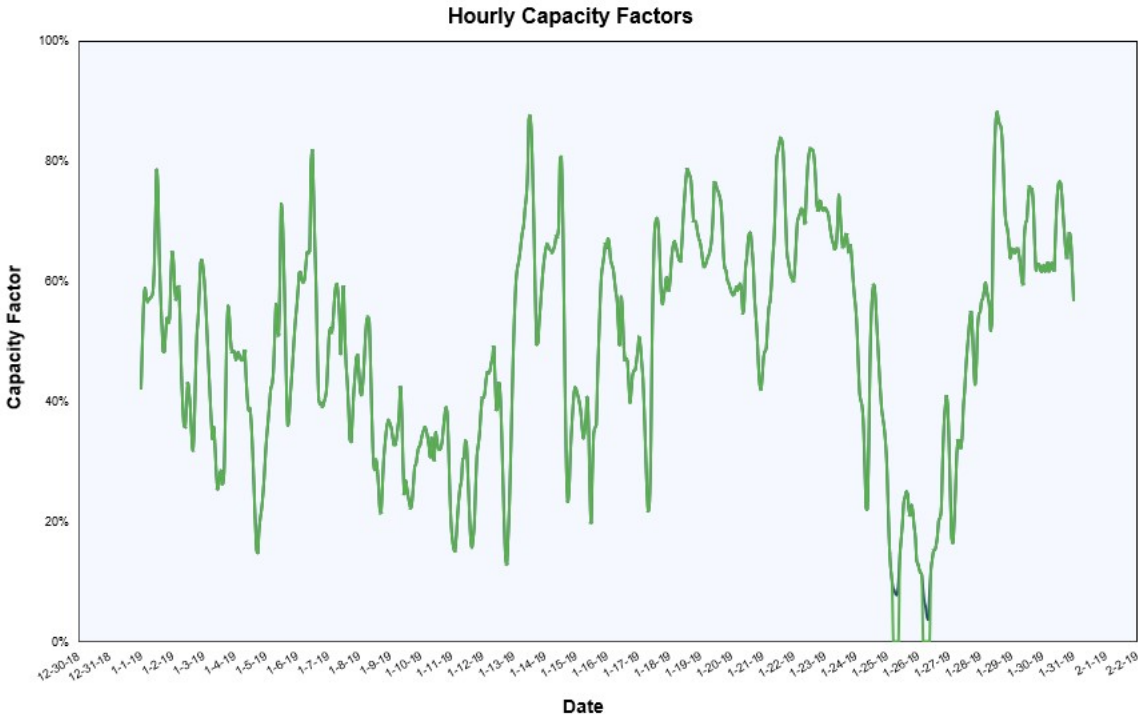
Electrolyzer Response to Hybrid Generator:

In the figuers below, the dynamic response of the electrolyzer when connected to a hybrid system is modelled and observed, along with the costs associated with it and capacity factor achieved. Similar to previous sections, Figure 6.7(a) shows the performance for 30 days and Figure 6.7(b) shows the response of the electrolyzer for the entire year.

(a) Hourly Capacity Factor of Electrolyzer for 30 days
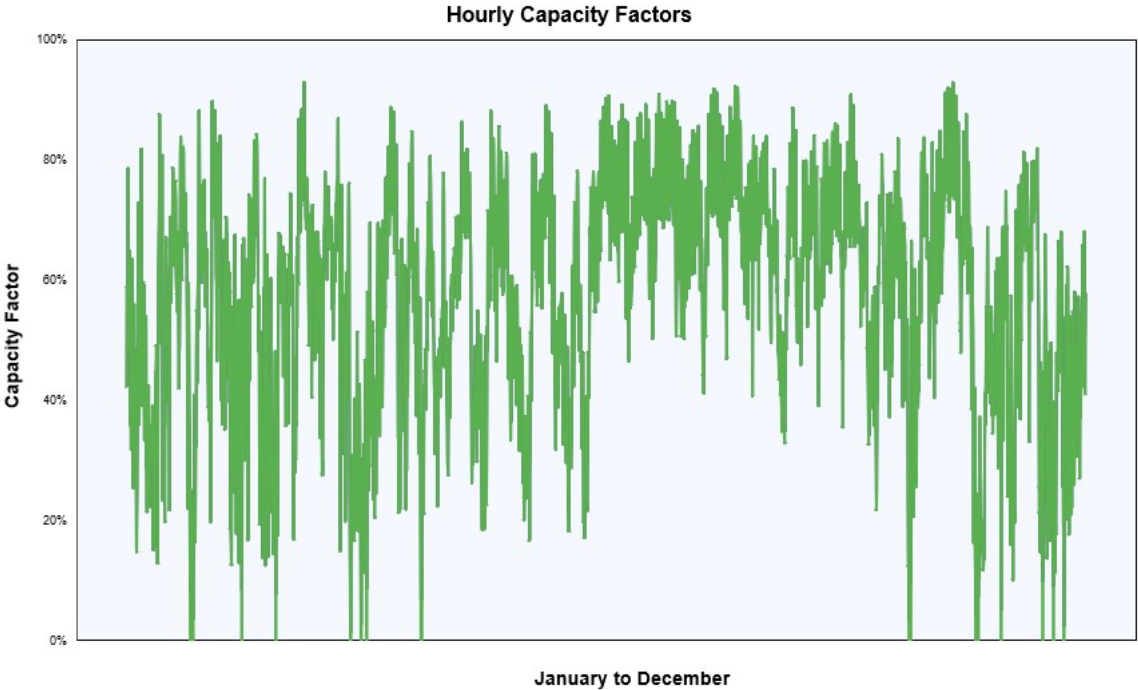
(b) Capacity Factor of Electrolyzer throughout the year

Figure 6.7: Capacity Factor vs Time for Hybrid Generator connected Electrolyzer

It has been observed from the results that the hybrid generator does not have a major impact on increase of electrolyzer performance. The electrolyzer capacity factor achieved was 57% with a total hydrogen

production of 830 tonnes per year. The levelized cost of hydrogen also increased to USD 3.5 per kg$_{H_2}$ compared to wind connected electrolyzer (USD 3.16/kg). The results obtained are demonstrated below in Table 6.7.

Parameter	Value
Total Time Electrolyzer is Operating	99.2%
Electrolyzer Capacity Factor Achieved	57%
Energy Consumed by Electrolyzer (MW/yr)	51500
Hydrogen Output (TPA)	830
LCOH (USD)	3.5

Table 6.7: Hybrid Connected Electrolyzer Results

Haber-Bosch unit Response to Hybrid Generator:

Based on the simulation results from the model analysis tool for ammonia, there has been a reduction in the annual capacity factor of ammonia production unit. The intermittent response of the ammonia synthesis plant to hybrid electricity generator is plotted in Figure 6.8.
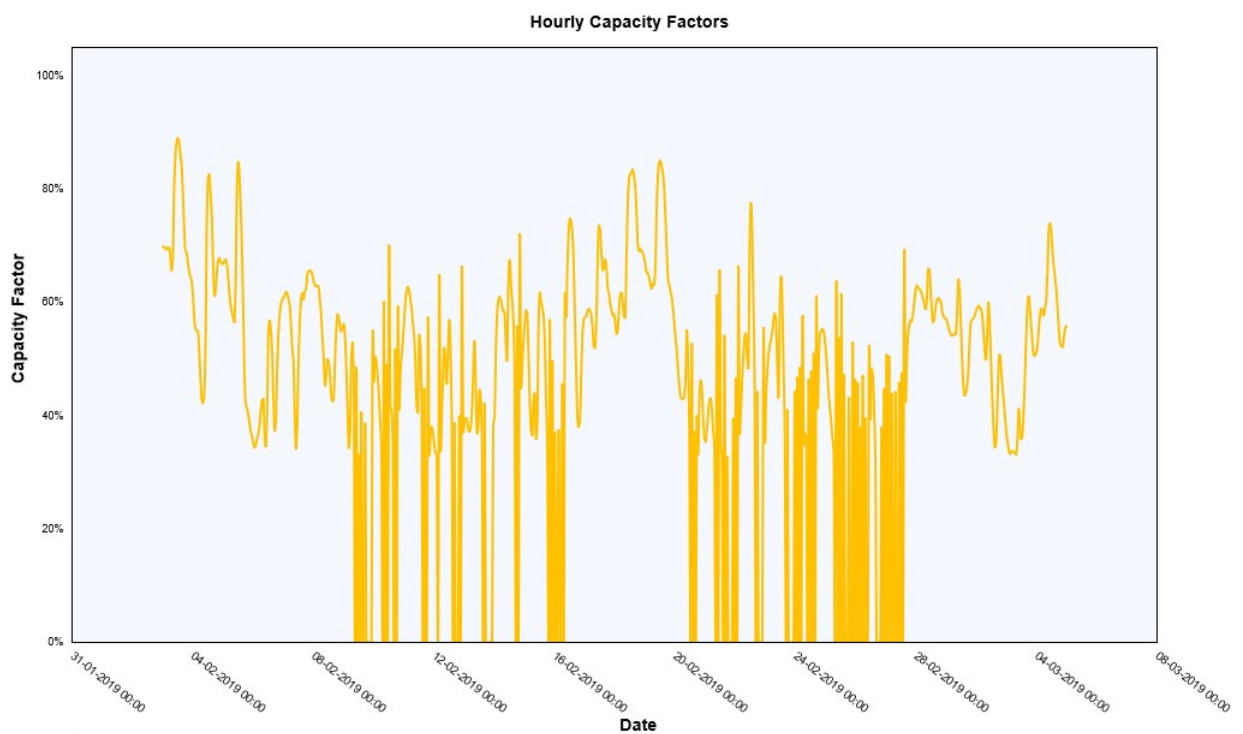
(a) Hourly Capacity Factor of Ammonia Synthesis Plant for 30 days
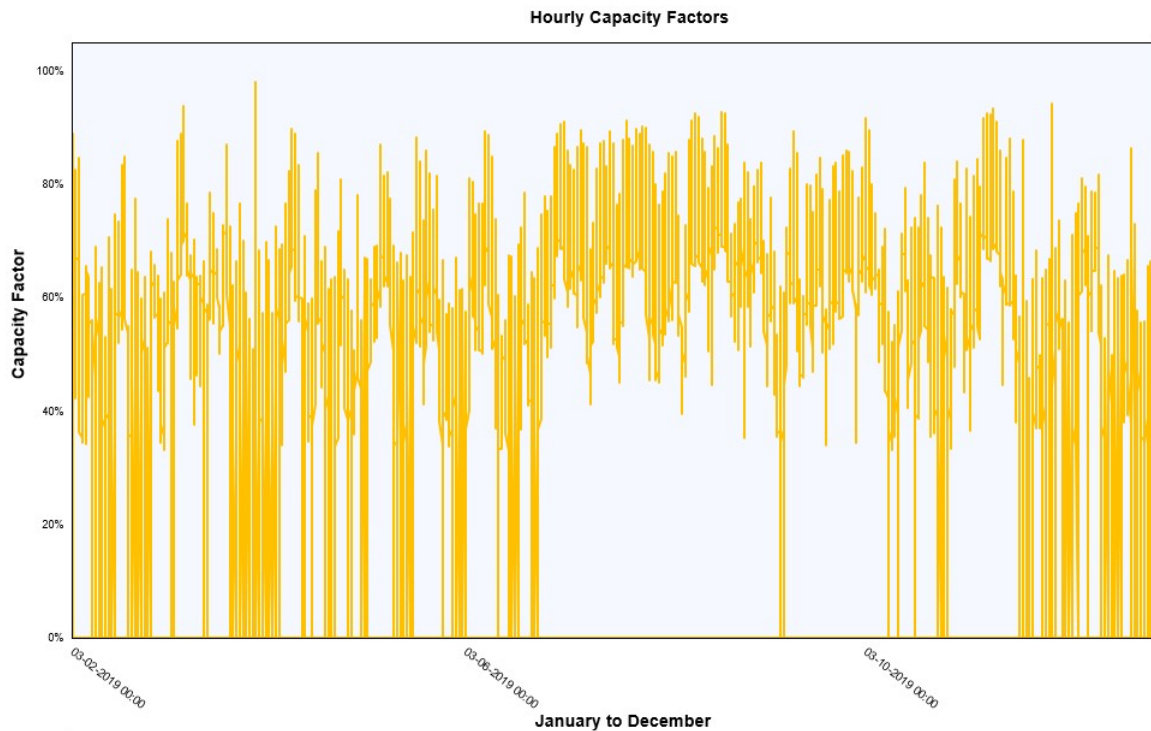
(b) Capacity Factor of Ammonia Synthesis Plant throughout the year

Figure 6.8: Capacity Factor vs Time for Hybrid Generator connected Haber-Bosch unit

Based on the results obtained, the average power plant capacity factor is 55% and the ammonia plant capacity factor achieved is 52%. These values are comparatively lower than those obtained from wind only connected ammonia plant. It has been observed that the annual ammonia production reduced by 48% compared to the nominal production capacity (9000 tonnes per year).

Parameter	Value
Average Power Plant Capacity Factor	55%
Annual Capacity Factor of Ammonia Plant	52%
Average Total Time Ammonia Plant is in Operation	7950 hrs/yr
Ammonia Produced (TPA)	4660
LCOA (USD)	1.55

Table 6.8: Hybrid connected Ammonia Production Plant Results

The capital costs of the hybrid connected ammonia production plant were found to be **USD 63 million**. This value is slightly lower than the total capital costs associated with wind operated ammonia plant. This is due to the partial usage of solar PV which result in reduction in reduction of capital costs due to low CAPEX/kW compared to wind. A breakdown of components is given in the Table 6.9 below.

Component	Capital Cost (USD)
Power Plant	7.3 million
Transmission	8 million
Ammonia Plant	3.4 million
Indirect Costs	35 million
Total Capital Costs	**63 million**

Table 6.9: Total Capital Costs for Hybrid Connected Ammonia Plant

Conclusion:

Boujdour in Morocco presents as exceptional wind profile, making it the ideal location for integrating wind power with the ammonia production unit. The wind-connected plant demonstrates the highest capacity factor the ammonia plant achieved at 60%. This shows the reliability of wind power in driving the ammonia production process. Moreover, the wind-connected plant showed the lowest levelized cost of ammonia (LCOA) signifying the cost effectiveness and competitiveness (USD 1.3/kg). However, the plant demonstrates that it cannot reach full capacity (100%) to produce 9000 tonnes of ammonia per year. Therefore, extra measures need to be considered in order to achieve maximum desired capacity. The measures stated below are applied to wind operated ammonia synthesis plant.

- Over-sizing of electrolyzer
- Introducing a hydrogen buffer between ammonia synthesis unit and the electrolyzer
- Usage of balancing technology (Batteries or Grid Electricity) to supply back-up electricity

6.6. Hydrogen Buffer Vessel

The use of a hydrogen buffer between the electrolyzer and the ammonia synthesis plant plays a crucial role in ensuring a smooth and consistent operation of the entire ammonia production process. Some of the benefits of implementing hydrogen buffer storage are:

1. **Stabilizing Hydrogen Supply:**

   - The hydrogen buffer acts as an intermediate storage facility, ensuring a continuous and stable supply of hydrogen to the ammonia synthesis plant. This is important as the electrolyzer produces hydrogen intermittently due to variation in renewable energy sources.

2. **Optimizing Electrolyzer Operations:**

   - The buffer storage allows the electrolyzer to operate at its optimal efficiency, irrespective of the variations in renewable energy availability. The excess hydrogen can be stored during periods of high production and utilized during low production, thereby enhancing the overall efficiency of the ammonia synthesis plant.

The hydrogen buffer vessel storage size is modelled as 8 hours of storage based on [76]. Eichman et al. [76] from National Renewable Energy Laboratory (USA) mentioned that the hydrogen storage size is 8 hours for all rated power of electrolyzer for all configurations except islanded. If the green ammonia plant is built in an island, then the hydrogen storage size would be 168 hours. But these values are subjected to change i.e., the size of the hydrogen buffer storage can be more or less than 8 hours based on the location and availability of renewable energy sources.

Cost of Hydrogen Buffer Storage:

In order to determine the size and cost of the hydrogen buffer vessel, the pressure of hydrogen gas plays a vital role. The higher the pressure of hydrogen, the lower the size of the vessel could be since the density increases when the pressure is increased. Based on literature data [83], the costs of compressor required to compressed hydrogen gas and the cost associated to store hydrogen per kg are shown in figure below.

(a) Costs of Compressor based on [83]
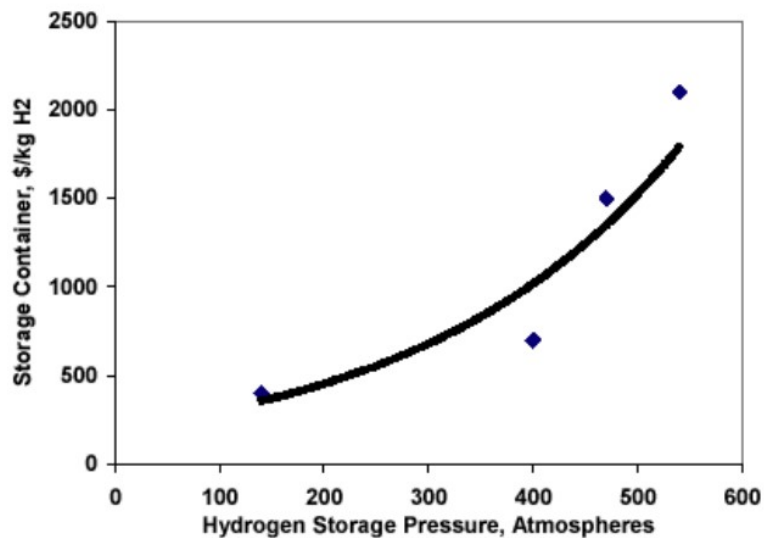
(b) Costs to Store Hydrogen in Pressurized Vessels [83]

Figure 6.9: Costs of Compressor to Compress Hydrogen Gas and Costs to Store Hydrogen

It is assumed that hydrogen is stored at room temperatures and the storage pressure is considered to be 200 bar. Therefore, the density of hydrogen at $25°$C and 200 bar is 14.48 kg/m^3. The amount of hydrogen produced for the chosen electrolyzer capacity and the ammonia production unit requirement is 190 kg/hr. Therefore, for 8 hours of storage the total hydrogen storage is 1520 kg. The size of the vessel is determined by:

$$Size = \frac{Total\ Hydrogen\ Storage\ in\ kg}{Density\ of\ hydrogen\ at\ 200\ bar}$$

The total size of the hydrogen buffer storage tank to store 1520 kg of hydrogen at 200 bar is **104.9 m^3**.

An aspen simulation has been carried out to determine the compressor work in order to pressurize the hydrogen gas to 200 bar. Giving an inlet pressure of 80 bar (assuming the outlet pressure of hydrogen from PEM electrolyzer is 80 bar) and a discharge pressure of 200 bar, the work required for compression is 100 kW. Therefore, based on the above graphs, the specific costs of compressor are $\sim$ 2100 USD/kW. For a 100 kW compressor power, the cost of compressor is 210,000 USD. Since the paper was published in the year 2003 and the values were reference points from the year 2003, an inflation rate of 3.6% per year is applied in order to calculate the cost of compressor in 2023. It is determined that in 2023 the **cost of compressor is USD 361,000**.

From the above graphs, the cost of compressed hydrogen storage container at a pressure of 200 bar is $\sim$ USD 500/kg H_2. Adding the inflation costs, the cost to store compressed hydrogen in 2030 is **USD 986 / kg H_2**. Therefore, to store 1520 kg hydrogen in a container, the cost of the buffer vessel is **USD 1,498,720**.
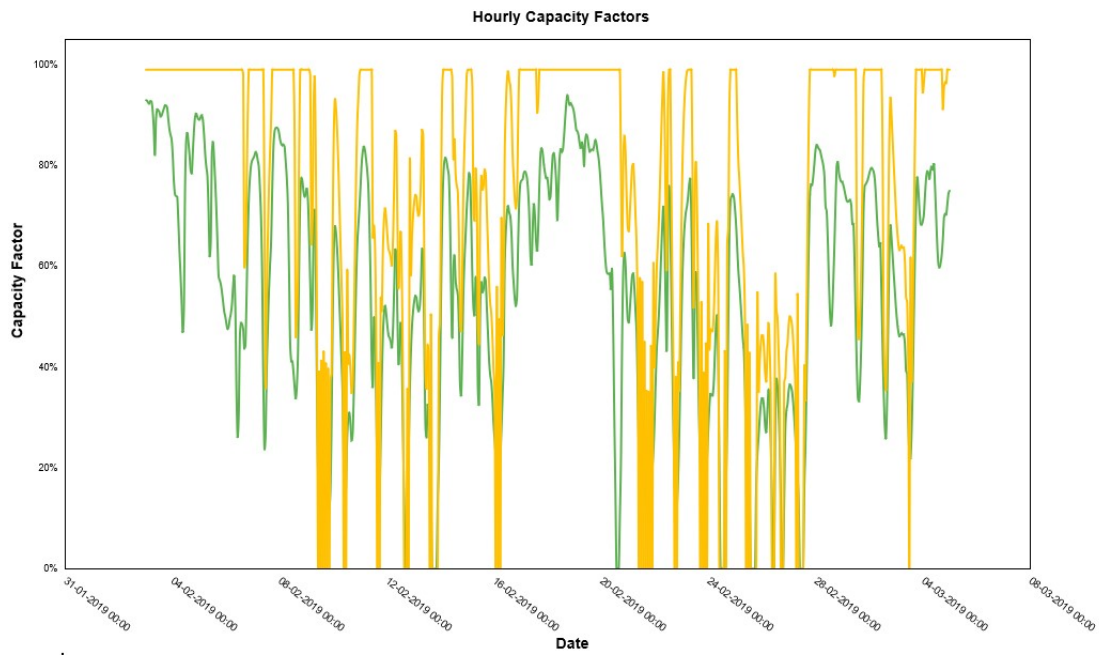
6.7. Electrolyzer Over-sizing

The current section illustrates the effect of over-sizing of the electrolyzer on the ammonia production. As discussed in section 6.6, the excess hydrogen required is 1520 kg when 8 hours of hydrogen buffer is considered. Thus, producing this excess hydrogen needs an electrolyzer capacity of 13.8 MW. For the current thesis project, the goal is to get the annual ammonia plant capacity factor to 80% since start-up and shut-down times were not modelled in the present study. However, the option of hot stand-by could be used and is discussed in section 6.8.

Based on the new electrolyzer capacity required to store 8 hours of hydrogen buffer, the electrolyzer needs to be over sized by 34%. This value is given as input parameter to the ammonia cost tool. It has been observed that the ammonia plant capacity factor achieved increases to 82% with an additional increase in capital costs by 14.7 million USD. A breakdown of results and costs is given below in Table 6.10

Component	Value
Ammonia plant annual capacity factor achieved	82%
Time ammonia plant is at maximum capacity	63%
LCOH (USD/kg)	3.15
LCOA (USD/kg)	1.19
Electrolyzer Cost (USD)	10.8 million
Hydrogen Storage Costs (USD)	1.5 million
Total Capital Costs	**79.7 million**

Table 6.10: Results of Wind Connected Ammonia Plant with 34% Electrolyzer Over-Sized

Figure 6.10: Capacity factor of Electrolyzer and Ammonia Plant in 30 days for 34% Oversized Electrolyzer (Green: Electrolyzer, Yellow: Ammonia)
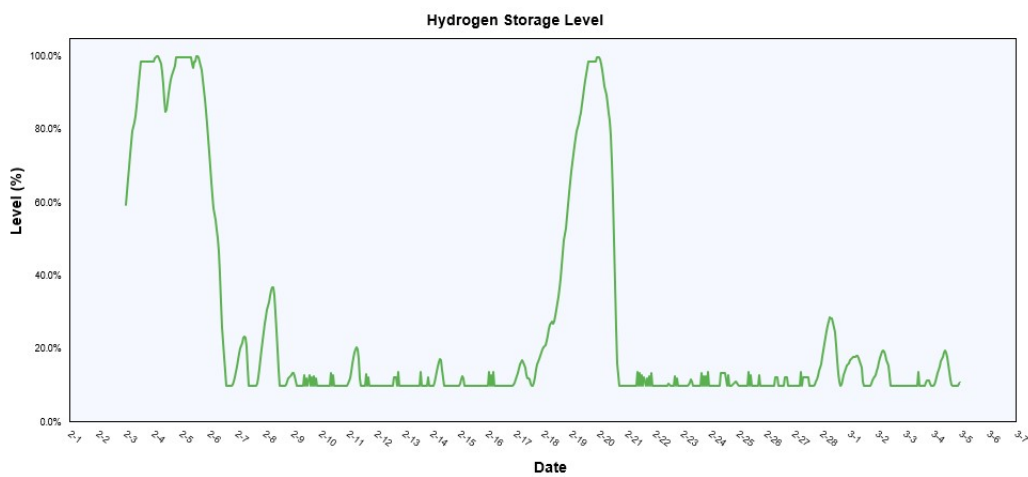
Figure 6.11: Hydrogen Buffer Vessel Storage Level

The capacity factor profile of both electrolyzer and ammonia production plant is shown in Figure 6.10 above and Figure 6.11 shows the level of hydrogen storage tank. It can be observed that there is not much of excess hydrogen produced and therefore, there are instances in the year where the ammonia plant goes to a capacity factor of 0. This could be solved either by over-sizing the electrolyzer more or by providing more electricity.

It can also be seen from the hydrogen storage level that the tank is at its 100% level only for a very few days in average. This shows that the hydrogen produced from electrolyzer is directly used by the ammonia plant and huge amounts of excess hydrogen is not produced. Therefore, the size of the hydrogen storage tank can be reduced. For the current thesis project, an overall ammonia production capacity factor of 80% is targeted considering the cost optimization.

In order to achieve a capacity factor of 80%, the size of the hydrogen storage tank can be reduced to 300 kg. This value is obtained by doing trial and error input in the open-source ammonia tool. The profile of the hydrogen storage tank level of 300 kg size as a function of time is shown in Figure D.1. The overall capital costs of 76 million is observed considering 34% oversized electrolyzer. The LCOA calculated is **USD 1.15/kg**.

Based on the above results, the following conclusion have been drawn:

1. **Effect of Electrolyzer Over-Sizing on Ammonia Production**

   - Achieving an annual ammonia production capacity factor of 80%, the electrolyzer capacity is increased by 34% than nominal capacity. In order to store the excess the excess hydrogen produced by oversized electrolyzer, a hydrogen storage tank of 1520 kg was considered leading to an increase in capital costs by **USD 14.7 million** compared to wind connected ammonia synthesis plant.

2. **Efficient Hydrogen Storage and Cost Savings**

   - It has been observed that the hydrogen produced by the electrolyzer is utilized by the ammonia synthesis unit without any excess hydrogen produced. This showed that the hydrogen storage tank size can be reduced to 300 kg to optimize the cost savings. This led to a reduction in capital costs by **USD 3.7 million** compared to using 1520 kg of hydrogen storage tank. The total capital costs calculated are **USD 76 million** and the reduced size of hydrogen storage tank is **20.7 m^3**.

3. **LCOA and LCOH**

   - The LCOA where 300 kg of hydrogen storage used is found to be minimum at **USD 1.15/kg** compared to USD 1.3/kg for wind connected Haber-Bosch unit where an 11% reduction is levelized cost of ammonia is observed. The LCOH reduced from 3.16 USD/kg to **3.02 USD/kg**.

6.8. Balancing Technology

Balancing technology is crucial in managing and mitigating fluctuations in renewable intermittent electricity, ensuring a stability and reliability in the electrical power grid. Renewable energy sources like wind and solar are intermittent and variable in nature which are influenced by weather conditions. This intermittency can cause imbalances between electricity supply and demand, leading to instability in the grid. Therefore, balancing technology is used as back-up electricity in order to supply electricity under renewable electricity unavailability.

Some of the balancing technologies usually used are batteries, gas turbines, grid electricity etc [13]. For the current thesis project, batteries and grid electricity have been considered and the cost analysis has been carried out. The capacity of the batteries and grid electricity is determined by finding the energy required to heat the catalyst bed in the ammonia synthesis reactor to maintain it in hot stand-by and the heat loss from the reactor to the surroundings. Based on the calculation, it was observed that the electricity input to the heater in the reactor is 233 kWhr. The detailed calculation of the derivation of the exact number is shown in section D.1.

Batteries

Lithium-ion batteries are considered for the current application of balancing technology. According to **BloombergNEF** [80], the cost of batteries is considered to be $151/kWh as an input to the cost analysis model. In addition, a battery rated power of 0.116 MW is considered with 2 hours of charge/discharge time. Therefore, the rated energy capacity of the battery is 0.233 MWh. Using the model with 34% oversized electrolyzer with 300 kg hydrogen buffer storage, it has been observed that the total capital costs associated with usage of batteries increase by **USD 90,000**

Grid Electricity

Grid electricity could also be used to mitigate the fluctuations in intermittent renewable electricity but at a cost. This grid electricity is produced results in emission of carbon with a carbon footprint of 296 kg CO_2 per MWh [84]. The cost of grid connection is USD 44.5/kW [85] and the cost of electricity in Morocco is USD 106/MWh for businesses [82]. This leads to an overall increase in capital costs to **USD 10,600**. This is significantly cheaper than using batteries as a balancing technology. But the carbon emissions related to using 0.23 MW of grid electricity is estimated to be 68 kg CO_2.
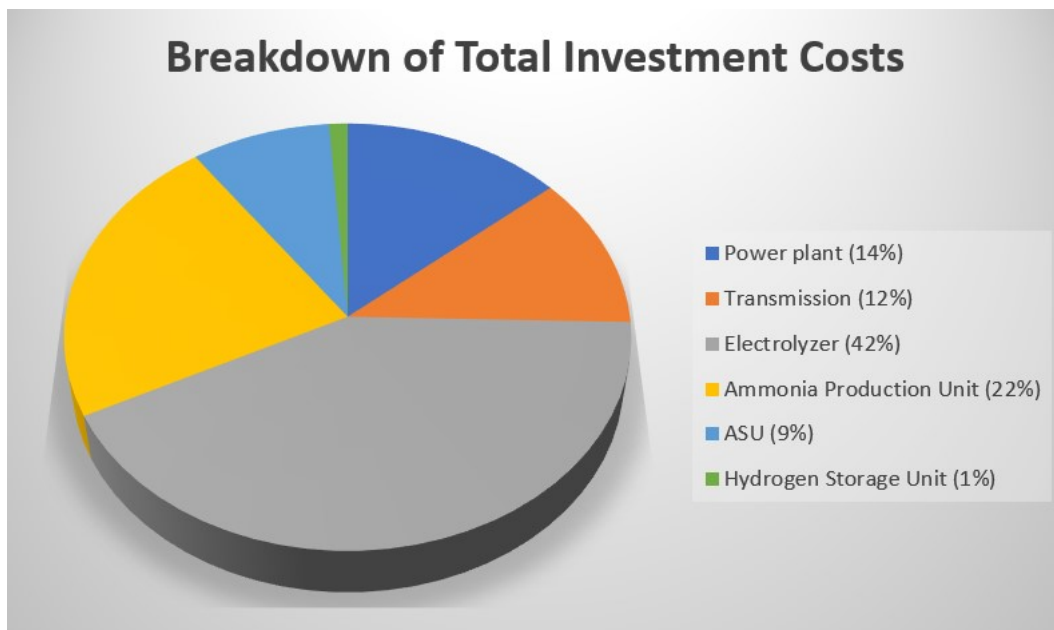
6.9. LCOH Comparison

The following table below shows the LCOH values reported by various sources and are compared to the current work.

Source	Value (USD/kg H2)
PV Magazine [86]	2.75-4.08
[87]	3.23-13.70
NREL [88]	4.50
IEA [89]	3.20-7.70
Bloomberg NEF [90]	4.30
GEP [91]	3-6
Current Work	3.02-7.20

Table 6.11: LCOH comparison from different sources

An overall breakdown of total investment costs is shown in the pie chart (Figure 6.12) below:

Breakdown of Total Investment Costs

- Power plant (14%)
- Transmission (12%)
- Electrolyzer (42%)
- Ammonia Production Unit (22%)
- ASU (9%)
- Hydrogen Storage Unit (1%)

Figure 6.12: Overall breakdown of Investment Costs

7

Conclusions and Recommendations

This chapter summarizes the main conclusion of the study and provides recommendations for future work.

7.1. Conclusions

This section answers the research questions that were presented in chapter 1.

1. How can a stable ammonia synthesis process be maintained under varying hydrogen feed flow rates?

(a) **How can the dynamic behavior of the system be modelled?**

The dynamic behaviour of the system is captured through Aspen Plus Dynamics, a simulation tool for dynamic interactions. Initially, a steady-state model is created in Aspen Plus by determining the boundaries and operating conditions. This steady-state model is transferred to dynamic mode and the model is sent to Aspen Plus Dynamics. For this purpose, the dynamics of electricity input are translated into fluctuations in hydrogen feed flow rate, as the electrolyzer is connected to renewable energy source.

Three distinct scenarios were simulated, each representing a linear and step reduction of 20%, 50% and 70% in the hydrogen feed flow rate. These scenarios provided an understanding about the response of the plant to the changes in hydrogen feed flow rate.

(b) **What are the suitable control philosophies to maintain pressure under dynamic input?**

As the hydrogen feed flow rate reduces due to intermittent electricity, there is a direct impact on the pressure within the system. Effective control strategies were implemented to main stable pressure levels during these variations in order to prevent the damaging of production unit and ensure consistent operation of ammonia synthesis process.

Three different control strategies were implemented and each strategy is designed to efficiently regulate system pressure under dynamic input conditions. The components used to control the system pressure in three different control strategies were

- cooling duty of condenser
- brake power of recycle compressor
- nitrogen feed flow rate

It has been observed that all three control strategies perform till 70% reduction of hydrogen feed flow rate. The challenge associated when controlling the system pressure using brake power of compressor is that the compressor is not as flexible as it is assumed to be for simulation purposes. The compressor does not work where the brake power is too low, resulting in instabilities. The challenge associated with using nitrogen to substitute deficit hydrogen is that the recycle flow rate increases drastically. Therefore, the control strategy involving usage of cooling duty of compressor in terms of stability and flexibility in controlling pressure of the system.

2. How can the complete ammonia plant be optimized by introducing a hydrogen buffer for realistic renewable power availability scenarios?

(a) **What renewable power source can be considered to ensure ammonia production with reduced levelized cost of ammonia?**

Various possibilities were explored to achieve the desired operation and maximize ammonia production. The analysis revealed that connecting the plant to wind power exhibited exceptional results due to Boujdour in Morocco having high mean capacity factor for wind. The overall ammonia production capacity factor achieved is 60% with a LCOA of USD 1.3/kg ammonia produced.

A 0.23 MW of back-up electricity is considered to maintain the reactor in hot stand-by during times when the renewable power production is insufficient. This step could ensure several advantages such as reduction in start-up times, process flexibility, reduction in thermal stress and improved energy efficiency. This 0.23 MW electricity is provided either by batteries or grid electricity. It has been observed that batteries cause an increase in capital costs by USD 90,000 whereas grid electricity results in increase of capital costs by USD 10,600. But this comes with carbon emissions of 68 kg.

It was also observed from dynamic simulations that by using control strategy 1 for pressure stabilization, the system responds to stabilizing the initial conditions within 100 minutes. Therefore, the system can be shut down during times when there is no wind and can be made run again in 100 minutes. It can also be said that hydrogen buffer storage is not necessary if the system responds instantly to changes in feed flow rates.

(b) **What is the optimum amount of hydrogen storage capacity required for the selected ammonia production capacity?**

The hydrogen buffer acts as a storage unit that can stock excess hydrogen during periods of abundant electricity, which can later be utilized when there is a deficit in power supply. This ensures a consistent hydrogen availability for the ammonia synthesis plant. An 8 hours of hydrogen buffer is considered resulting in the requirement of oversizing of electrolyzer by 34%. However, it is observed that 8 hours of excess hydrogen storage cannot be incorporated when the electrolyzer is oversized by 34% due to all hydrogen being utilized by ammonia synthesis plant. This required hydrogen buffer is specific to location and production capacity. Therefore, a 300 kg of hydrogen buffer is found to be beneficial for the selected ammonia capacity plant to achieve a capacity factor of 80% with a reduction of levelized cost of ammonia by 11% from USD 1.3/kg to USD 1.15/kg.

However, designing an efficient and cost-effective storage system is a key challenge. Due to the lower densities of hydrogen gas at standard temperatures and pressures, there is a need for compression. This balance of costs between the required compressor work and size of hydrogen buffer vessel is crucial. Other than costs associated with compression and storage vessel, safety is another predominant factor that should be considered when storing hydrogen at high pressures.

7.2. Recommendations for Future Work

The following section discusses about the recommendations for future study based on the current research.

- **Control Philosophies:**

    - Examining and fine tuning of the control parameters within the controllers would be a recommendation since the tuning was out of the scope. This provides a deeper insights in the system behaviour and performance by better understanding and reproducing realistic dynamics in the ammonia plant under varied inputs.
    - Investigate and execute a control method that focuses on managing the feed-to-recycle ratio. Understanding and adjusting this ratio has the potential to improve ammonia production efficiency.

- Considering compressor curves to get an in detail understanding on the dynamics associated with change in brake power of compressor in the control strategy

- Extend the techno-economic analysis to study the scalability of the production unit and analyze the economic viability, costs, and benefits associated with scaling up the ammonia production plant, considering different sizes and capacities

- **Pressure Drop and Dynamic Effects:**

    - Implement a pressure drop correlation study to fully understand how different pressure drops effect the ammonia production plant's dynamics. This is essential for improving and stabilizing the system's performance.

- **Start-Up and Shut-Down Dynamics:**

    - Conducting a detailed analysis focusing on the start up and shut down times would be beneficial. This could be possible by modelling parallel Haber-Bosch reactors with different configurations. Using parallel reactors provides a high turn-down ratio of ammonia production and therefore, a further cost optimization can be carried out.

- **Optimization in Hydrogen Storage Compression:**

    - Optimize the hydrogen storage compression process by finding an appropriate balance between compression work and hydrogen storage costs. Energy reductions and cost-effectiveness in hydrogen storage can be achieved through efficient compression.

References

[1] Jos Delbeke et al. "The paris agreement". In: *Towards a Climate-Neutral Europe: Curbing the Trend* (2019), pp. 24–45. DOI: `10.4324/9789276082569-2`.

[2] J S Wallace and C A Ward. "H Y D R O G E N As a Fuel". In: *Int. J. Hydrogen Energy,* 8.4 (1983), pp. 255–268.

[3] Muhammad Aziz, Agung TriWijayanta, and Asep Bayu Dani Nandiyanto. "Ammonia as effective hydrogen storage: A review on production, storage and utilization". In: *Energies* 13.12 (2020), pp. 1–25. ISSN: 19961073. DOI: `10.3390/en13123062`.

[4] International Energy Agency. "Ammonia Technology Roadmap Towards more sustainable nitrogen fertiliser production". In: (). URL: `www.iea.org/t&c/`.

[5] *Direct CO☐ emissions from ammonia production, 2020-2050 – Charts – Data & Statistics - IEA*. URL: `https://prod.iea.org/data-and-statistics/charts/direct-co-emissions-from-ammonia-production-2020-2050`.

[6] Yoshitsugu Kojima and Masakuni Yamaguchi. "Ammonia as a hydrogen energy carrier". In: *International Journal of Hydrogen Energy* 47.54 (2022), pp. 22832–22839. ISSN: 03603199. DOI: `10.1016/j.ijhydene.2022.05.096`. URL: `https://doi.org/10.1016/j.ijhydene.2022.05.096`.

[7] Collin Smith, Alfred K. Hill, and Laura Torrente-Murciano. "Current and future role of Haber-Bosch ammonia in a carbon-free energy landscape". In: *Energy and Environmental Science* 13.2 (2020), pp. 331–344. ISSN: 17545706. DOI: `10.1039/c9ee02873k`.

[8] Muhammad Heikal Hasan et al. *A comprehensive review on the recent development of ammonia as a renewable energy carrier*. 2021. DOI: `10.3390/en14133732`.

[9] Zhijian Wan et al. "Ammonia as an effective hydrogen carrier and a clean fuel for solid oxide fuel cells". In: *Energy Conversion and Management* 228.September 2020 (2021), p. 113729. ISSN: 01968904. DOI: `10.1016/j.enconman.2020.113729`. URL: `https://doi.org/10.1016/j.enconman.2020.113729`.

[10] Grigorii Soloveichik. "Ammonia as a virtual Hydrogen Carrier". In: *US Department of Energy* 95.5 (2016), pp. 364–370. ISSN: 0916-8753. URL: `https://www.energy.gov/sites/prod/files/2016/12/f34/fcto_h2atscale_workshop_soloveichik.pdf`.

[11] H. Ishaq and I. Dincer. "Design and simulation of a new cascaded ammonia synthesis system driven by renewables". In: *Sustainable Energy Technologies and Assessments* 40.April (2020), p. 100725. ISSN: 22131388. DOI: `10.1016/j.seta.2020.100725`. URL: `https://doi.org/10.1016/j.seta.2020.100725`.

[12] *Global Wind Atlas*. URL: `https://globalwindatlas.info/en`.

[13] Jack Shepherd et al. "Open-source project feasibility tools for supporting development of the green ammonia value chain". In: *Energy Conversion and Management* 274.June (2022), p. 116413. ISSN: 01968904. DOI: `10.1016/j.enconman.2022.116413`. URL: `https://doi.org/10.1016/j.enconman.2022.116413`.

[14] Hirokazu Kojima et al. "Influence of renewable energy power fluctuations on water electrolysis for green hydrogen production". In: *International Journal of Hydrogen Energy* 48.12 (2022), pp. 4572–4593. ISSN: 03603199. DOI: `10.1016/j.ijhydene.2022.11.018`. URL: `https://doi.org/10.1016/j.ijhydene.2022.11.018`.

[15] M. Anvari et al. "Short term fluctuations of wind and solar power systems". In: *New Journal of Physics* 18.6 (2016). ISSN: 13672630. DOI: `10.1088/1367-2630/18/6/063027`.

[16] Phebe Asantewaa Owusu and Samuel Asumadu-Sarkodie. *A review of renewable energy sources, sustainability issues and climate change mitigation*. 2016. DOI: `10.1080/23311916.2016.1167990`.

[17] *Solar Panel Tilt Angle Calculator - Footprint Hero*. URL: `https://footprinthero.com/solar-panel-tilt-angle-calculator`.

[18] Siemens Gamesa renewable energy. "SG 4.5-145 New SGRE turbine with the best-in-class LCoE >4 MW". In: (). URL: `https://www.siemensgamesa.com/en-int/-/media/siemensgamesa/downloads/en/products-and-services/archive/siemens-gamesa-onshore-wind-turbine-sg-4-5-145-en.pdf`.

[19] *Renewables.ninja*. URL: `https://www.renewables.ninja/`.

[20] Mengdi Ji and Jianlong Wang. *Review and comparison of various hydrogen production methods based on costs and life cycle impact assessment indicators*. 2021. DOI: `10.1016/j.ijhydene.2021.09.142`.

[21] Marcus Newborough and Graham Cooley. "Developments in the global hydrogen market: The spectrum of hydrogen colours". In: *Fuel Cells Bulletin* 2020.11 (2020). ISSN: 14642859. DOI: `10.1016/S1464-2859(20)30546-0`.

[22] S. Shiva Kumar and V. Himabindu. *Hydrogen production by PEM water electrolysis – A review*. 2019. DOI: `10.1016/j.mset.2019.03.002`.

[23] Md Mamoon Rashid et al. "Hydrogen Production by Water Electrolysis: A Review of Alkaline Water Electrolysis, PEM Water Electrolysis and High Temperature Water Electrolysis". In: *International Journal of Engineering and Advanced Technology* 3 (2015), pp. 2249–8958.

[24] Diogo M.F. Santos, César A.C. Sequeira, and José L. Figueiredo. "Hydrogen production by alkaline water electrolysis". In: *Quimica Nova* 36.8 (2013). ISSN: 01004042. DOI: `10.1590/S0100-40422013000800017`.

[25] Jörn Brauns and Thomas Turek. "Alkaline water electrolysis powered by renewable energy: A review". In: *Processes* 8.2 (2020). ISSN: 22279717. DOI: `10.3390/pr8020248`.

[26] L. W. Hourng, T. T. Tsai, and M. Y. Lin. "The analysis of energy efficiency in water electrolysis under high temperature and high pressure". In: *IOP Conference Series: Earth and Environmental Science*. Vol. 93. 1. 2017. DOI: `10.1088/1755-1315/93/1/012035`.

[27] Marko Vuksic, Siniša Zorica, and Ivan Zulim. "Evaluation of DC-DC Resonant Converters for Solar Hydrogen Production Evaluation of DC-DC resonant converters for solar hydrogen production based on load current characteristics". In: *Contemporary Issues in Economy and Technology* June 2014 (2014), pp. 121–133. URL: `https://www.researchgate.net/publication/263470190_Evaluation_of_DC-DC_Resonant_Converters_for_Solar_Hydrogen_Production_Based_on_Load_Current_Characteristics`.

[28] Yujing Guo et al. "Comparison between hydrogen production by alkaline water electrolysis and hydrogen production by PEM electrolysis". In: *IOP Conference Series: Earth and Environmental Science* 371.4 (2019), pp. 0–5. ISSN: 17551315. DOI: `10.1088/1755-1315/371/4/042022`.

[29] Xiufu Sun et al. "Durability of Solid Oxide Electrolysis Cells for Syngas Production". In: *Journal of The Electrochemical Society* 160.9 (2013), F1074–F1080. ISSN: 0013-4651. DOI: `10.1149/2.106309jes`.

[30] Meilin Liu et al. "Understanding the phase formation and compositions of barium carbonate modified NiO-yttria stabilized zirconia for fuel cell applications". In: *International Journal of Hydrogen Energy* 40.45 (2015). ISSN: 03603199. DOI: `10.1016/j.ijhydene.2015.09.092`.

[31] Greg Gege Tao, Anil Virkar, and Roxanne Garland. "A Reversible Planar Solid Oxide Fuel-Assisted Electrolysis Cell and Solid Oxide Fuel Cell for Hydrogen and Electricity Production Operating on Natural Gas/Biogas". In: *FY Annual Progress Report* (2006).

[32] Pierre Millet and Sergey Grigoriev. "Water Electrolysis Technologies". In: *Renewable Hydrogen Technologies: Production, Purification, Storage, Applications and Safety*. 2013. DOI: `10.1016/B978-0-444-56352-1.00002-7`.

[33] Aldo Vieira da Rosa and Aldo Vieira da Rosa. "Chapter 10 – Hydrogen Production". In: *Fundamentals of Renewable Energy Processes*. 2009.

[34] Greig Chisholm, Tingting Zhao, and Leroy Cronin. *Hydrogen from water electrolysis*. Elsevier Inc., 2022, pp. 559–591. ISBN: 9780128245101. DOI: `10.1016/B978-0-12-824510-1.00015-5`. URL: `http://dx.doi.org/10.1016/B978-0-12-803440-8/00016-6`.

[35] S. Shiva Kumar and Hankwon Lim. "An overview of water electrolysis technologies for green hydrogen production". In: *Energy Reports* 8 (2022), pp. 13793–13813. ISSN: 23524847. DOI: `10.1016/j.egyr.2022.10.127`. URL: `https://doi.org/10.1016/j.egyr.2022.10.127`.

[36] Agustin Valera-Medina and Rene Banares-Alcantara. *Techno-Economic Challenges of Green Ammonia as an Energy Vector*. 2020, pp. 41–52. DOI: `10.1016/B978-0-12-820560-0.01001-8`. URL: `https://books.google.nl/books?id=W2XRDwAAQBAJ&lpg=PA27&dq=DOI%3A10.1016%2FB978-0-12-820560-0.00003-5&pg=PP1#v=onepage&q&f=false`.

[37] Yu Wang et al. "Storage system of renewable energy generated hydrogen for chemical industry". In: *Energy Procedia* 29.February 2014 (2012), pp. 657–667. ISSN: 18766102. DOI: `10.1016/j.egypro.2012.09.076`.

[38] Joakim Andersson and Stefan Grönkvist. "Large-scale storage of hydrogen". In: *International Journal of Hydrogen Energy* 44.23 (2019), pp. 11901–11919. ISSN: 03603199. DOI: `10.1016/j.ijhydene.2019.03.063`.

[39] Patrick Preuster, Alexander Alekseev, and Peter Wasserscheid. "Hydrogen storage technologies for future energy systems". In: *Annual Review of Chemical and Biomolecular Engineering* 8 (2017), pp. 445–471. ISSN: 19475438. DOI: `10.1146/annurev-chembioeng-060816-101334`.

[40] *Hydrogen Storage Underground?* URL: `https://fuelcellsworks.com/subscribers/hydrogen-storage-underground/`.

[41] M L Williams. "CRC Handbook of Chemistry and Physics, 76th edition". In: *Occupational and Environmental Medicine* 53.7 (1996). ISSN: 1351-0711. DOI: `10.1136/oem.53.7.504`.

[42] W. F. Castle. "Air sepration and liquefaction: Recent developments and prospects for the beginning of the new millennium". In: *International Journal of Refrigeration* 25.1 (2002), pp. 158–172. ISSN: 01407007. DOI: `10.1016/S0140-7007(01)00003-2`.

[43] *Cryogenic Process of Air Separation – IspatGuru*. URL: `https://www.ispatguru.com/cryogenic-process-of-air-separation/`.

[44] Ahmed Khalil, Ahmed M Khalil, and Ahmed Mohame Khalil. "Production Of Nitrogen from the Air During Cryogenic Process". In: January (2018).

[45] N. K. Mohalik et al. "Application of nitrogen as preventive and controlling subsurface fire - Indian context". In: *Journal of Scientific and Industrial Research* 64.4 (2005). ISSN: 00224456.

[46] Mehran Moazeni Targhi, Mohammadreza Malek, and Pooyan Shams. "Simulation, Sensitivity Analysis and Introducing New Valid Process Cases in Air Separation Units". In: *Journal of Applied Chemistry* 10.September (2017), pp. 45–60. DOI: `10.9790/5736-1009024560`.

[47] C. R. Reid and K. M. Thomas. "Adsorption of gases on a carbon molecular sieve used for air separation: Linear adsorptives as probes for kinetic selectivity". In: *Langmuir* 15.9 (1999). ISSN: 07437463. DOI: `10.1021/la981289p`.

[48] *Generating Nitrogen with Pressure Swing Adsorption (PSA) Technology - Atlas Copco UK*. URL: `https://www.atlascopco.com/en-uk/compressors/wiki/compressed-air-articles/pressure-swing-adsorption-generator`.

[49] Svetlana Ivanova and Robert Lewis. "Producing nitrogen via pressure swing adsorption". In: *Chemical Engineering Progress* 108.6 (2012), pp. 38–42. ISSN: 03607275.

[50] K. Seshan. "Pressure swing adsorption". In: *Applied Catalysis* 46.1 (1989), p. 180. ISSN: 01669834. DOI: `10.1016/S0166-9834(00)81410-4`.

[51] Zykamilia Kamin, Mohd H V Bahrun, and Awang Bono. "A short review on pressure swing adsorption (PSA) technology for nitrogen generation from air A Short Review on Pressure Swing Adsorption (PSA) Technology for Nitrogen Generation from Air". In: 050006.August (2022).

[52] Soonchul Kwon et al. *CO2 Sorption*. Elsevier Inc., 2011, pp. 293–339. ISBN: 9780815520498. DOI: `10.1016/b978-0-8155-2049-8.10010-5`. URL: `http://dx.doi.org/10.1016/B978-0-8155-2049-8.10010-5`.

[53] Lei Wang, Cheng Shao, and Hai Wang. "Operation optimization of a membrane separation process through auto-controlling the permeate gas flux". In: *Separation and Purification Technology* 55.1 (2007). ISSN: 13835866. DOI: 10.1016/j.seppur.2006.10.015.

[54] *Nitrogen & Oxygen Gas Generators - Pneumatic Engineering*. URL: https://www.pneumatic.com.au/gases/nitrogen-and-oxygen-gas-generators/.

[55] Moises A. Carreon. *Molecular sieve membranes for N2/CH4 separation*. 2018. DOI: 10.1557/jmr.2017.297.

[56] Lakshminarayana Kudinalli Gopalakrishna Bhatta et al. "Progress in hydrotalcite like compounds and metal-based oxides for CO2 capture: A review". In: *Journal of Cleaner Production* 103 (2015). ISSN: 09596526. DOI: 10.1016/j.jclepro.2014.12.059.

[57] M. G. Kaganer et al. "Vessels for the storage and transport of liquid oxygen and nitrogen". In: *Chemical and Petroleum Engineering* 3.12 (1967). ISSN: 15738329. DOI: 10.1007/BF01136404.

[58] *Cryogenic Dewar Flasks*. URL: https://www.tedpella.com/cryo-supplies_html/cryo-dewar.aspx.

[59] Max Appl. "The Haber-Bosch Process and the Development of Chemical Engineering". In: *A Century of Chemical Engineering*. 1982. DOI: 10.1007/978-1-4899-5289-9{_}3.

[60] G. Ertl. "Primary steps in catalytic synthesis of ammonia". In: *Journal of Vacuum Science & Technology A: Vacuum, Surfaces, and Films* 1.2 (1983). ISSN: 0734-2101. DOI: 10.1116/1.572299.

[61] Max Appl. "Chapter 4 Production". In: *Ullmann's Encyclopedia of Industrial Chemistry: Ammonia [M]*. 2006.

[62] *Home | ARENHA*. URL: https://arenha.eu/.

[63] *Role of Promoters in Haber's Process*. URL: https://unacademy.com/content/jee/study-material/chemistry/role-of-promoters-in-habers-process/.

[64] Jayant M Modak. "Haber Process for Ammonia Synthesis". In: August (2002).

[65] *Ammonia - Properties at Gas-Liquid Equilibrium Conditions*. URL: https://www.engineeringtoolbox.com/ammonia-gas-liquid-equilibrium-condition-properties-temperature-pressure-boiling-curve-d_2013.html.

[66] Mahdi Malmali et al. "Better Absorbents for Ammonia Separation". In: *ACS Sustainable Chemistry and Engineering* 6.5 (2018), pp. 6536–6546. ISSN: 21680485. DOI: 10.1021/acssuschemeng.7b04684.

[67] Matthew J. Kale et al. "Optimizing Ammonia Separation via Reactive Absorption for Sustainable Ammonia Synthesis". In: *ACS Applied Energy Materials* 3.3 (2020), pp. 2576–2584. ISSN: 25740962. DOI: 10.1021/acsaem.9b02278.

[68] Marlinda Bauer. "Dynamic behavior of a flexible smallscale ammonia synthesis process". In: (2022). URL: http://repository.tudelft.nl/..

[69] K.H.R. Rouwenhorst et al. *Ammonia Production Technologies*. Elsevier Inc., 2021, pp. 41–83. ISBN: 9780128205600. DOI: 10.1016/b978-0-12-820560-0.00004-7. URL: http://dx.doi.org/10.1016/B978-0-12-820560-0.00004-7.

[70] Cheng Liang. "First Workshop ARENHA project : " Introduction to novel technologies related to ammonia- based energy storage " Advanced Ammonia Synthesis Technologies Overview Index 1 . About Proton Ventures BV". In: (2022), pp. 1–18. URL: https://arenha.eu/content/consortium-workshops/.

[71] Huazhang Liu. "Ammonia synthesis catalyst 100 years: Practice, enlightenment and challenge". In: *Cuihua Xuebao/Chinese Journal of Catalysis* 35.10 (2014), pp. 1619–1640. ISSN: 02539837. DOI: 10.1016/S1872-2067(14)60118-2. URL: http://dx.doi.org/10.1016/S1872-2067(14)60118-2.

[72] Antonio Araújo and Sigurd Skogestad. "Control structure design for the ammonia synthesis process". In: *Computers and Chemical Engineering* 32.12 (2008), pp. 2920–2932. ISSN: 00981354. DOI: 10.1016/j.compchemeng.2008.03.001.

[73]   Bent Wiencke. "Fundamental principles for sizing and design of gravity separators for indus-
       trial refrigeration". In: *International Journal of Refrigeration* 34.8 (2011), pp. 2092–2108. ISSN:
       01407007. DOI: `10.1016/j.ijrefrig.2011.06.011`. URL: `http://dx.doi.org/10.1016/j.`
       `ijrefrig.2011.06.011`.

[74]   Simon Learman. "Horizontal Gas-Liquid Separator Calculator". In: (2011). URL: `www.blackmonk.`
       `co.uk`.

[75]   Rajiv Mukherjee. "TEMA designations for shell-and-tube heat exchangers". In: February (1998).
       URL: `http://www.torr-engenharia.com.br/wp-content/uploads/2011/05/exchanger.pdf`.

[76]   Joshua. D. Eichman et al. "Optimizing an Integrated Renewable-Electrolysis System". In: *United*
       States National Renewable Energy Laboratory March (2020). URL: `https://www.nrel.gov/`
       `docs/fy20osti/75635.pdf%0Ahttp://www.osti.gov/servlets/purl/1606147/`.

[77]   *Lang Factor and Return on Investment – Foundations of Chemical and Biological Engineering I*.
       URL: `https://pressbooks.bccampus.ca/chbe220/chapter/lang-factor-and-return-on-`
       `investment/`.

[78]   Ryan Wiser, Mark Bolinger, and Joachim Seel. "Benchmarking Utility-Scale PV Operational Ex-
       penses and Project Lifetimes: Results from a Survey of U.S. Solar Industry Professionals". In:
       Eletricity Markets & Policy 1.34078 (2020), pp. 1–8. URL: `https://eta-publications.lbl.`
       `gov/sites/default/files/solar_life_and_opex_report.pdf`.

[79]   Tyler Stehly and Patrick Duffy. "2020 Cost of Wind Energy Review". In: *Nrel* December (2021),
       p. 68.

[80]   *Lithium-ion Battery Pack Prices Rise for First Time to an Average of $151/kWh | BloombergNEF*.
       URL: `https://about.bnef.com/blog/lithium-ion-battery-pack-prices-rise-for-first-`
       `time-to-an-average-of-151-kwh/`.

[81]   Brian Cory. "Pricing in electricity transmission and distribution". In: *Proceedings of the Mediter-*
       ranean Electrotechnical Conference - MELECON 1.April (1996), pp. 19–25. DOI: `10.1109/`
       `melcon.1996.550955`.

[82]   *Morocco electricity prices, December 2022 | GlobalPetrolPrices.com*. URL: `https://www.globa`
       `lpetrolprices.com/Morocco/electricity_prices/`.

[83]   Peteves Stathis. *HYDROGEN STORAGE : STATE-OF-THE-ART AND FUTURE PERSPECTIVE*
       HYDROGEN STORAGE : STATE-OF-THE-ART AND FUTURE PERSPECTIVE. April. 2016. ISBN:
       9289469501. URL: `https://www.researchgate.net/publication/255636014_HYDROGEN_`
       `STORAGE_STATE-OF-THE-ART_AND_FUTURE_PERSPECTIVE`.

[84]   Nicolae Scarlat, Matteo Prussi, and Monica Padella. "Quantification of the carbon intensity of
       electricity produced and used in Europe". In: *Applied Energy* 305 (2022). ISSN: 03062619. DOI:
       `10.1016/j.apenergy.2021.117901`.

[85]   *How much does it cost to sign up for an electricity or gas supply?| Endesa*. URL: `https://www.`
       `endesa.com/en/advice/processes-contracts/doubts-with-your-contract/how-much-`
       `does-it-cost-to-register-for-a-new-contract`.

[86]   *The Hydrogen Stream: LCOH of subsidized green hydrogen under $2/kg – pv magazine Interna-*
       tional. URL: `https://www.pv-magazine.com/2023/04/14/the-hydrogen-stream-lcoh-of-`
       `subsidized-green-hydrogen-under-2-kg/`.

[87]   Leonhard Povacz and Ramchandra Bhandari. "Analysis of the Levelized Cost of Renewable
       Hydrogen in Austria". In: *Sustainability 2023, Vol. 15, Page 4575* 15.5 (Mar. 2023), p. 4575. ISSN:
       2071-1050. DOI: `10.3390/SU15054575`. URL: `https://www.mdpi.com/2071-1050/15/5/4575/`
       `htm%20https://www.mdpi.com/2071-1050/15/5/4575`.

[88]   T. Ramsden, D. Steward, and J. Zuboy. ""Análisis del costo nivelado de producción de hidrógeno
       centralizado y distribuido"". In: September (2009). URL: `www.nrel.gov/docs/fy09osti/46267.`
       `pdf`.

[89]   *Global average levelised cost of hydrogen production by energy source and technology, 2019 and*
       2050 – Charts – Data & Statistics - IEA. URL: `https://www.iea.org/data-and-statistics/`
       `charts/global-average-levelised-cost-of-hydrogen-production-by-energy-source-`
   `and-technology-2019-and-2050`.

[90] *2023 Hydrogen Levelized Cost Update: Green Beats Gray | BloombergNEF*. URL: `https://about.bnef.com/blog/2023-hydrogen-levelized-cost-update-green-beats-gray/`.

[91] *Green & Blue Hydrogen: Current Levelized Cost of Production & Outlook | GEP Blog*. URL: `https://www.gep.com/blog/strategy/Green-and-blue-hydrogen-current-levelized-cost-of-production-and-outlook`.

[92] *Heat Capacities for Some Select Substances*. URL: `https://gchem.cm.utexas.edu/data/section2.php?target=heat-capacities.php`.

A
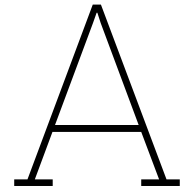
Control Philosophy-1

A.1. Step Change in Hydrogen Feed Flow Rate

Without the addition of controllers to the control philosophy-1, when the hydrogen feed flow rate was reduced by 50%, a pressure reduction of 46 bar was observed. Figure A.1 shows the behaviour of control philosophy-1 under 50% reduction in hydrogen feed flow rate and the response is plotted below:
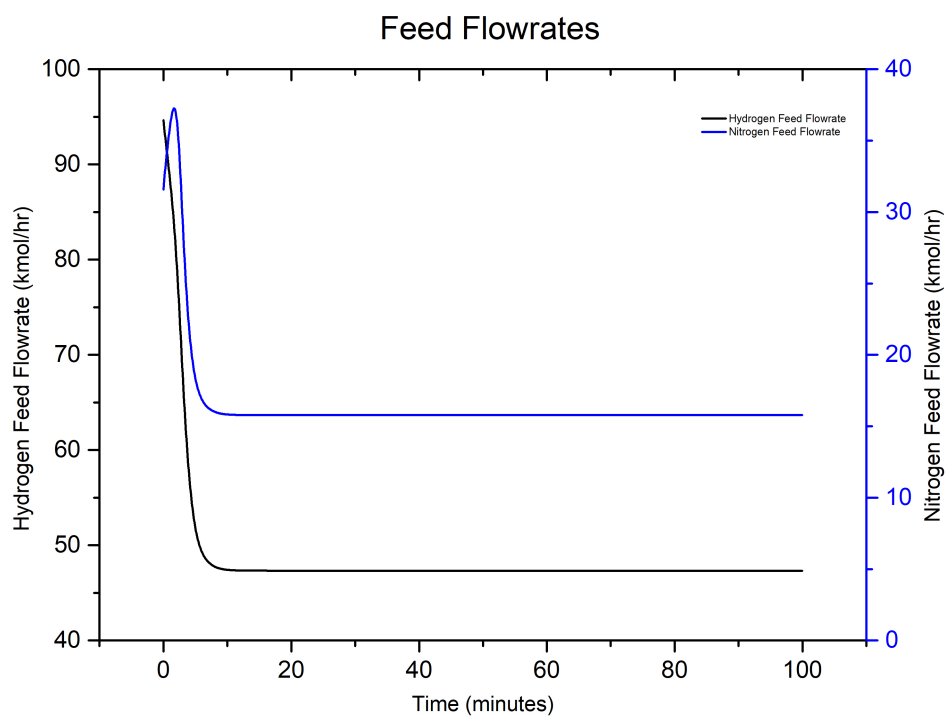
(a) Hydrogen and Nitrogen Feed Flow Rates
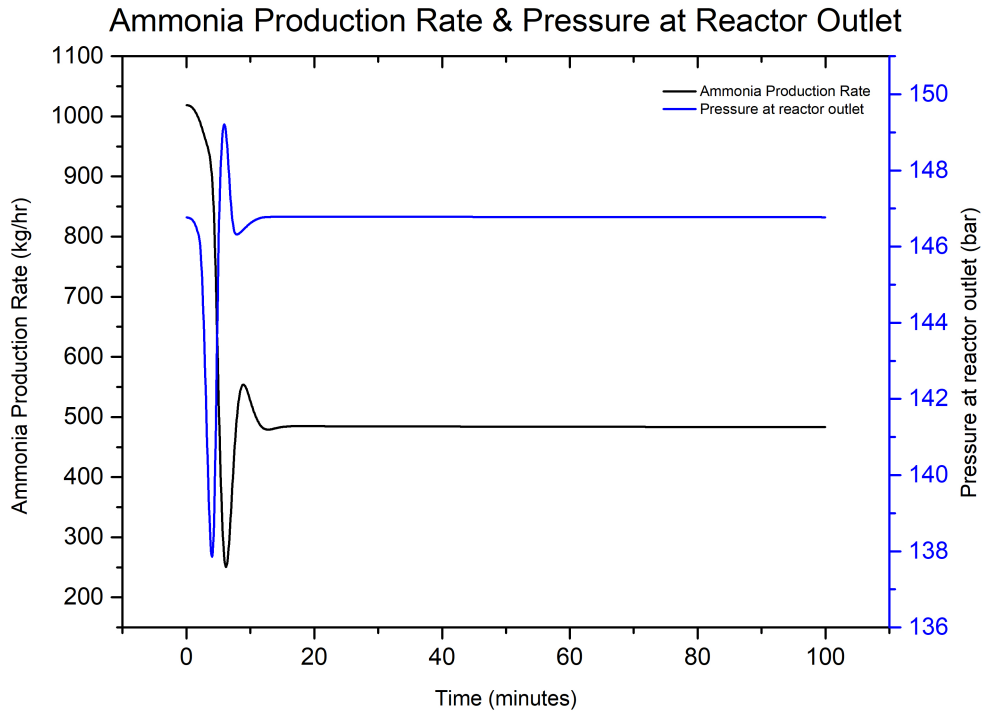
Ammonia Production Rate & Pressure at Reactor Outlet

(b) Ammonia Production Rate and Pressure at Reactor Outlet

Cooling Duty & Separator feed Temperature
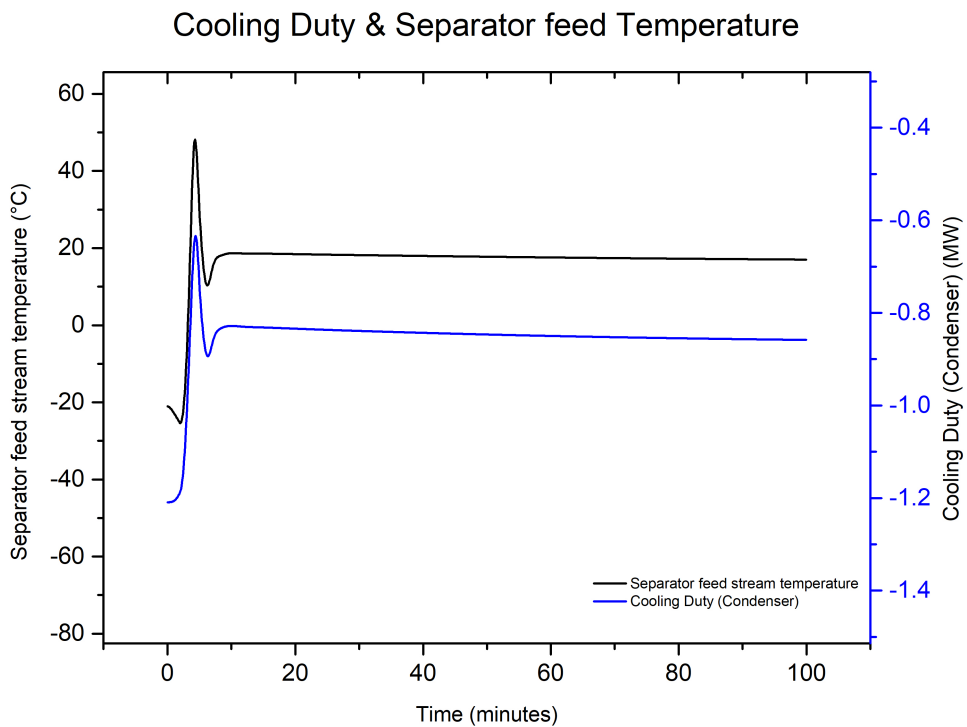
(c) Cooling Duty of Condenser and Temperature of Condenser Outlet Stream

Figure A.1: Control Philosophy-1 response to 50% step change in hydrogen feed flow rate

Results:

- As observed in Figure A.1 (a), the nitrogen flow rate reduces when the hydrogen feed flow rate is reduced and reaches steady state value where the stoichiometric ratio of $H_2 : N_2$ is maintained to a value of 3. The small peak in the nitrogen feed in the beginning could be due to slower response of ratio controller.
- A pressure reduction of $\sim$ 9 bar is observed and then increases back to the desired set point in around 15-20 minutes. A small overshoot is also observed. As expected, 50% reduction in hydrogen feed flow rate resulted in 50% of ammonia production rate.
- The condenser cooling duty reduces from 1.2MW to 0.85MW i.e., a reduction of 29% is observed. Hence, the outlet stream of condenser increases from -20°C to 17°C.

For 70% reduction in hydrogen feed flow rate, a pressure reduction of 68 bar was observed before the addition of controllers in control philosophy-1. Figure A.2 shows the behaviour of the model under 70% reduction in hydrogen feed flow rate.
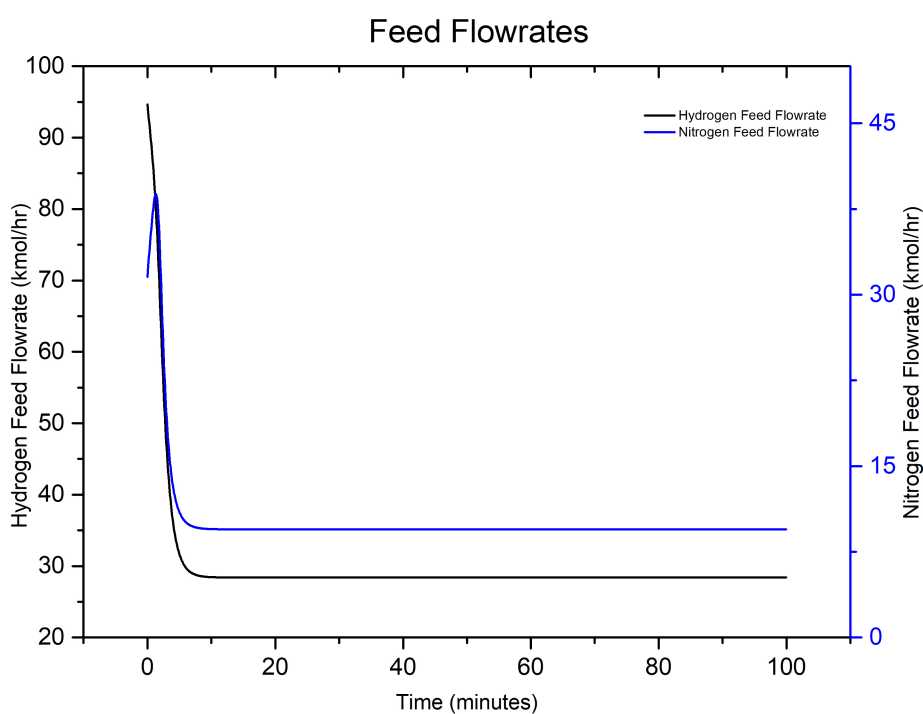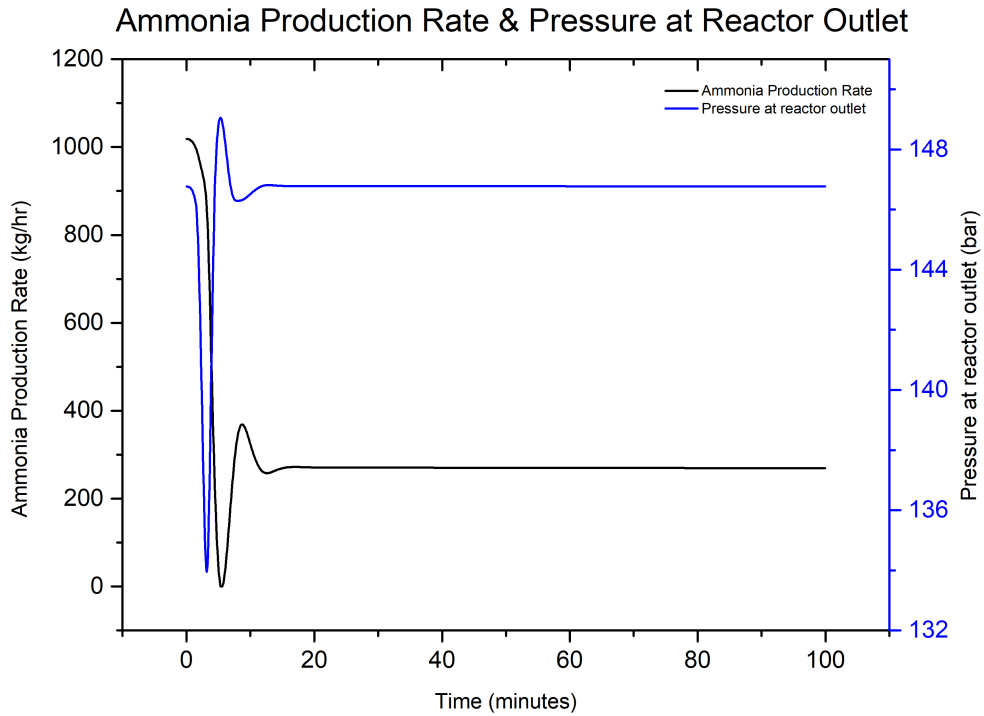
(a) Hydrogen and Nitrogen Feed Flow Rates

Ammonia Production Rate & Pressure at Reactor Outlet

(b) Ammonia Production Rate and Pressure at Reactor Outlet

Cooling Duty & Separator Feed Inlet Temperature
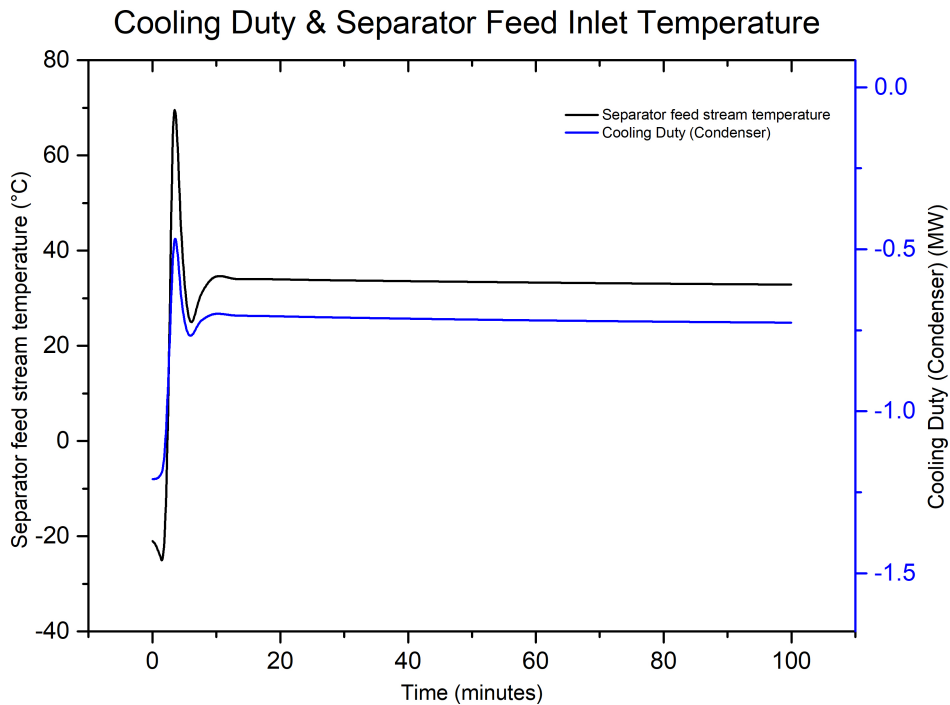
(c) Cooling Duty of Condenser and Temperature of Condenser Outlet Stream

Figure A.2: Control Philosophy-1 response to 70% step change in hydrogen feed flow rate

Results:

- Based on the data shown in Figure A.2 (a) it can be observed that when the hydrogen feed flow rate is reduced there is a decrease, in the nitrogen flow rate. Eventually it reaches a point where the stoichiometric ratio of hydrogen to nitrogen ($H_2 : N_2$) remains at 3.
- A pressure drop of $\sim$ 13 bar is observed, then rises again to the desired set point within 10-15 minutes. As expected, reducing the hydrogen supply by 70% resulted in a reduction ammonia production rate of 70%.
- In a similar way as the other two scenarios, the temperature of condenser outlet stream is increased to increase the pressure in the loop. The cooling duty reduces from 1.2MW to 0.72MW and the temperature increases from -20°C to 33°C.

A.2. Linear Change in Hydrogen Feed Flow Rate

Figure A.3 shows the response of control philosophy-1 to 50% gradual change in hydrogen feed flow rate.
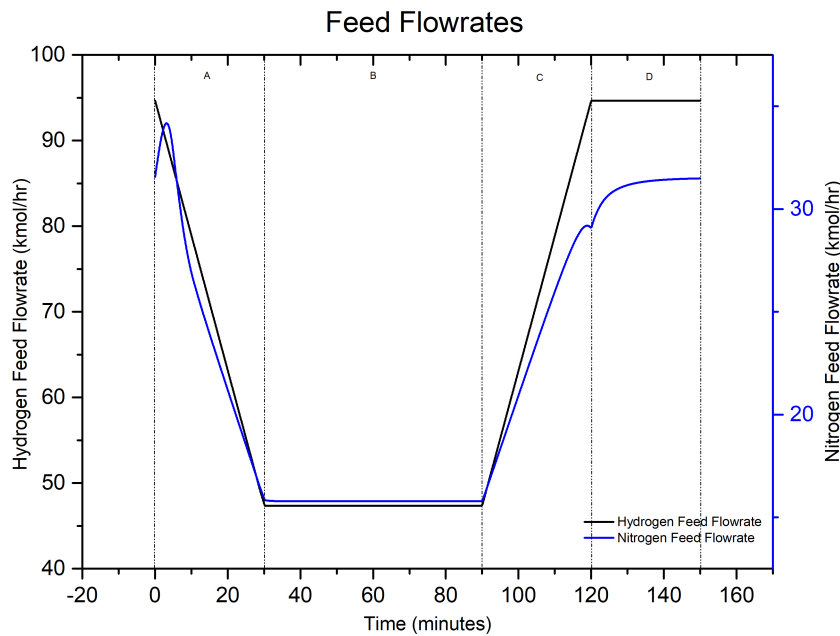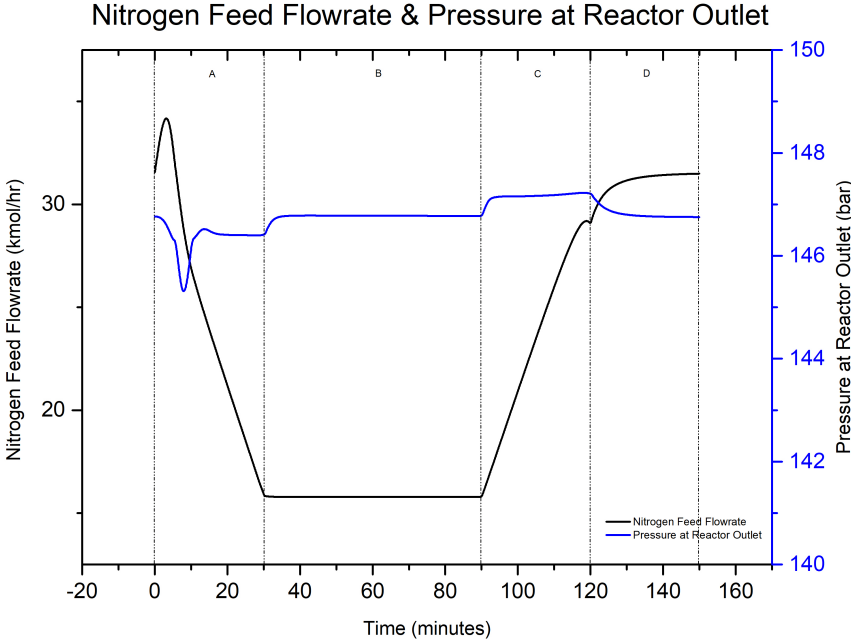
(a) Hydrogen and Nitrogen Feed Flow Rates

Nitrogen Feed Flowrate & Pressure at Reactor Outlet

(b) Nitrogen Feed Flowrate and Pressure at Reactor Outlet

Temperature at Reactor Outlet & Ammonia Production Rate
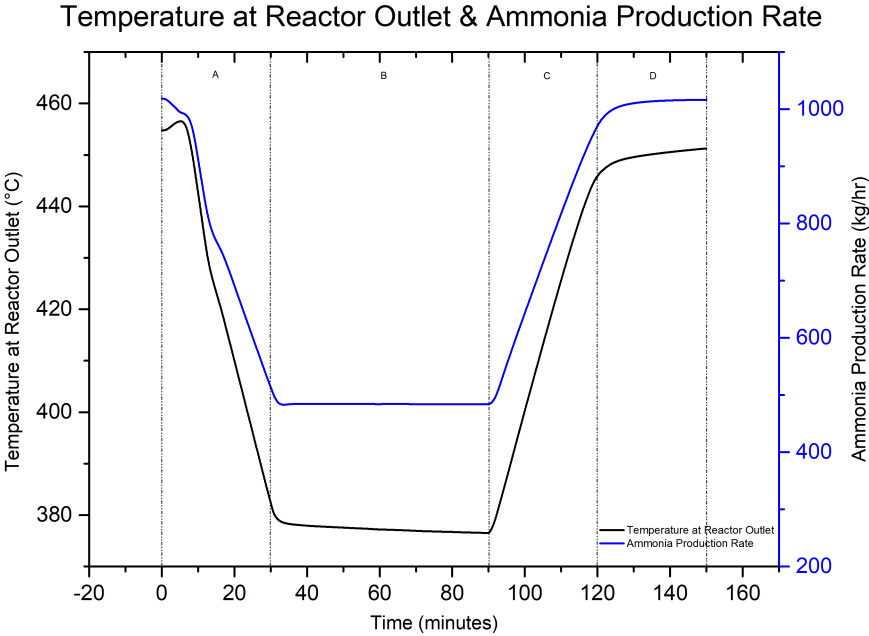
(c) Ammonia Production Rate and Temperature at Reactor Outlet
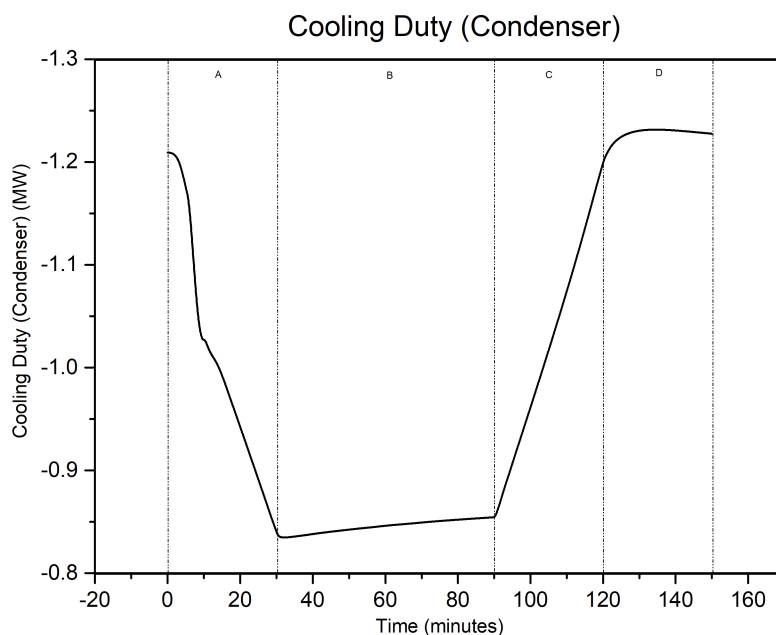
(d) Cooling Duty of Condenser

Figure A.3: Control Philosophy-1 response to 50% linear change in hydrogen feed flow rate

Discussion:

- **Region A:** When the controller detects a change in the ratio, it immediately closes the nitrogen valve, resulting in a decrease in the nitrogen supply flow rate. A small peak is observed in the nitrogen feed flow rate due to delay in controller response and a pressure reduction of 1 bar is observed. The cooling duty of condenser is reduced to increase the pressure.

- **Region B:** Both the nitrogen and hydrogen feed flow rates are unchanging during this period, maintaining a stoichiometric ratio of 3 ($H_2 : N_2$) while the system's pressure remained constant as well. The temperature of outlet of reactor reduces from $455°C$ to $375°C$ along with ammonia production reduced by 50%.

- **Region C:** The hydrogen feed flow rate is gradually ramped up again to its original value for a 30 minute time interval. In this process, the nitrogen feed flow rate also increases proportionally to uphold the stoichiometric ratio. As a result in increased feed flow rates, there is a very negligible amount of deviation in pressure from the set point. During this phase, the system responds to increase in pressure and therefore, the temperature of the outlet condenser stream is reduced by increasing the cooling duty again.

- **Region D:** The simulation was run for 30 minutes more, allowing the system to gradually return to its original steady-state conditions. During this period, the system's pressure was maintained at constant level, ensuring that it remains stable. The simulation was stopped after 30 mins. It was observed that the system requires more than 30 minutes to reach the initial steady state conditions.
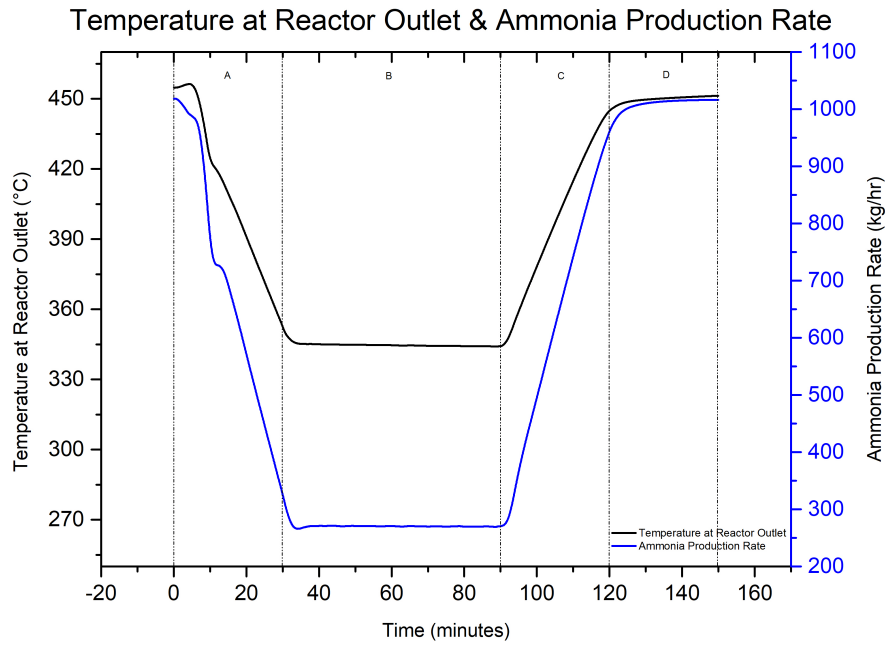
Figure A.4 shows the response of control philosophy-1 to 70% linear reduction in hydrogen feed flow rate.
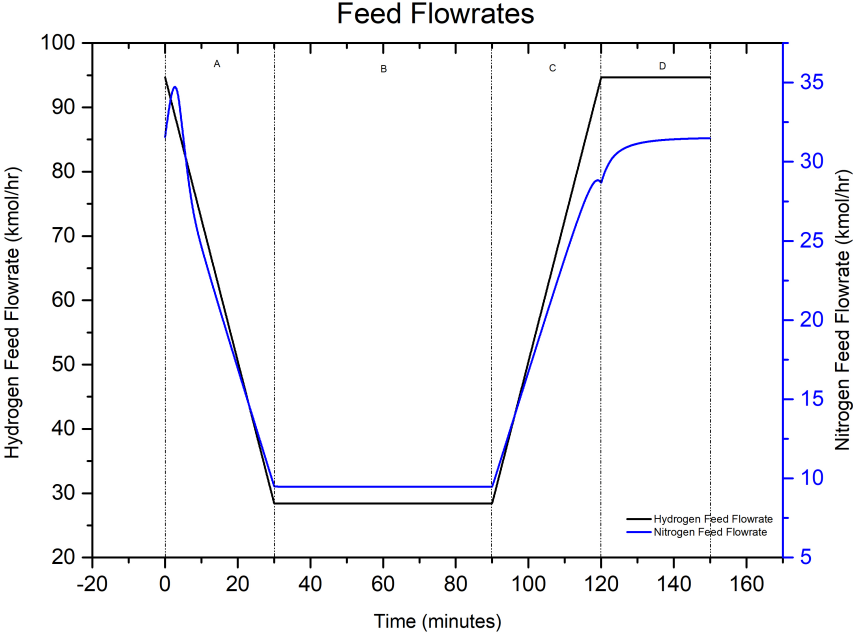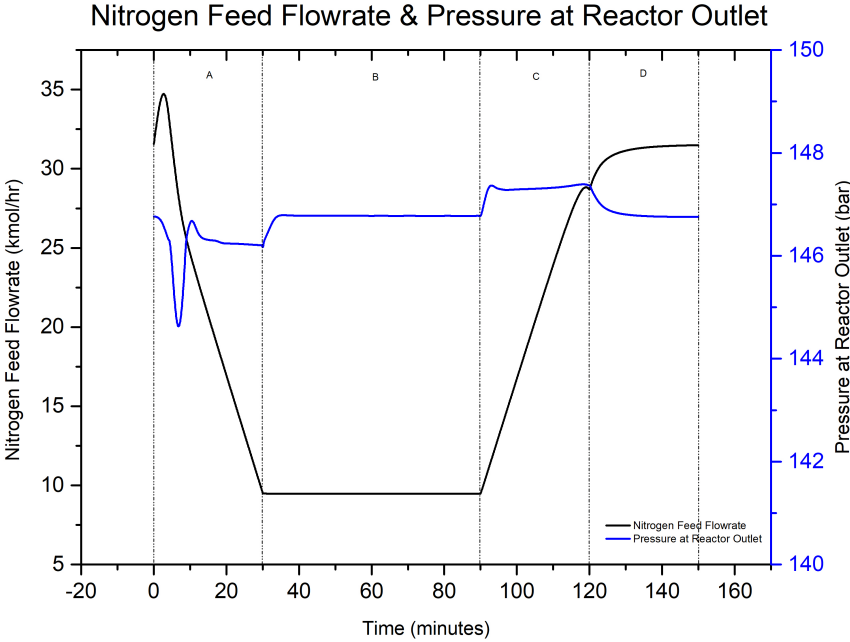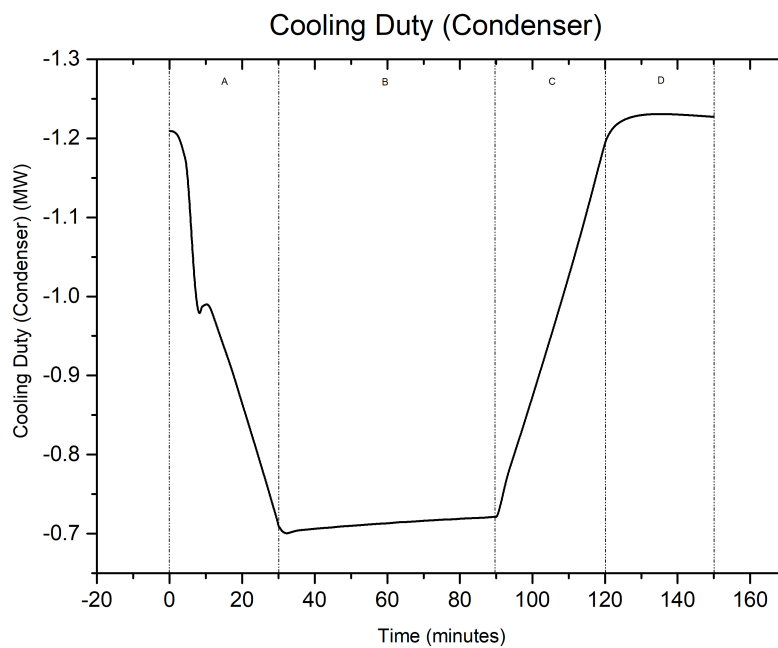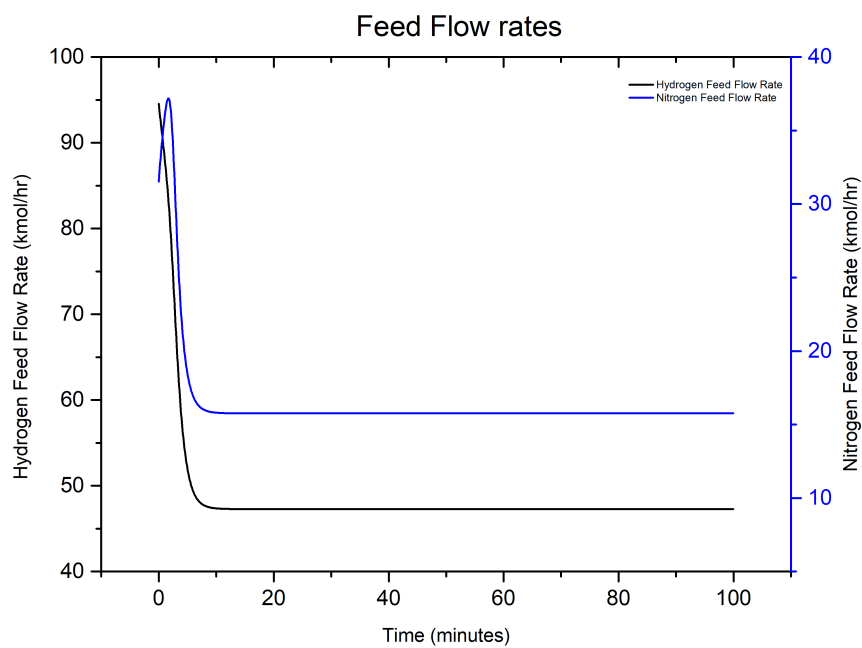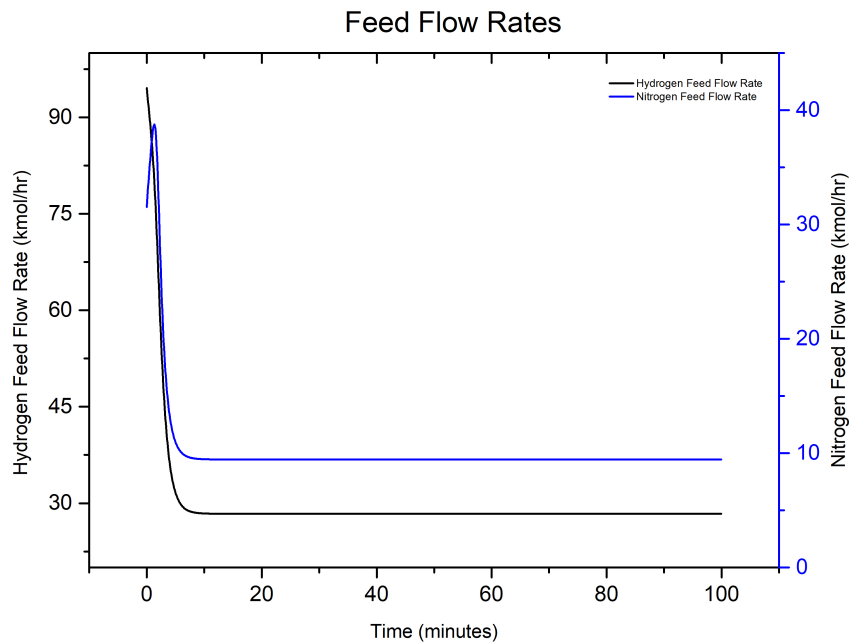
(a) Hydrogen and Nitrogen Feed Flow Rates

(b) Nitrogen Feed Flowrate and Pressure at Reactor Outlet

Temperature at Reactor Outlet & Ammonia Production Rate

(c) Ammonia Production Rate and Temperature at Reactor Outlet

Cooling Duty (Condenser)

(d) Cooling Duty of Condenser

Figure A.4: Control Philosophy-1 response to 70% linear change in hydrogen feed flow rate

Similar to 20% and 50% reduction in hydrogen feed flow rates, the system responds to 70% linear reduction in hydrogen feed flow rate. The temperature of the outlet reactor stream drops from $455°$C to $345°$C. The reduction in hydrogen feed flow rate also led to 70% reduction in ammonia production rate. The cooling duty of condenser goes to -0.7MW thereby increasing the condenser outlet stream temperature by $50°$C.

B

Control Philosophy-2

B.1. Step Change in Hydrogen Feed Flow Rate

The following Figure B.1 shows the response of the control philosophy-2 to a 50% reduction in hydrogen feed flow rate.

(a) Hydrogen and Nitrogen Feed Flow Rate

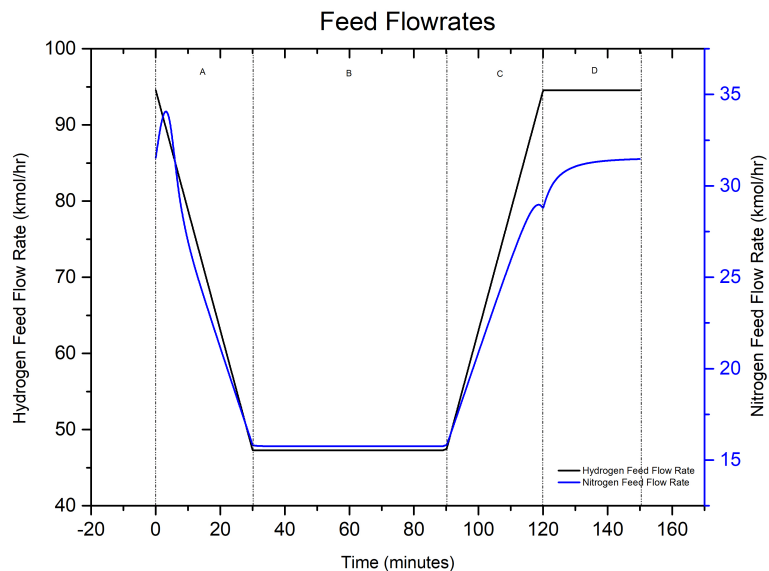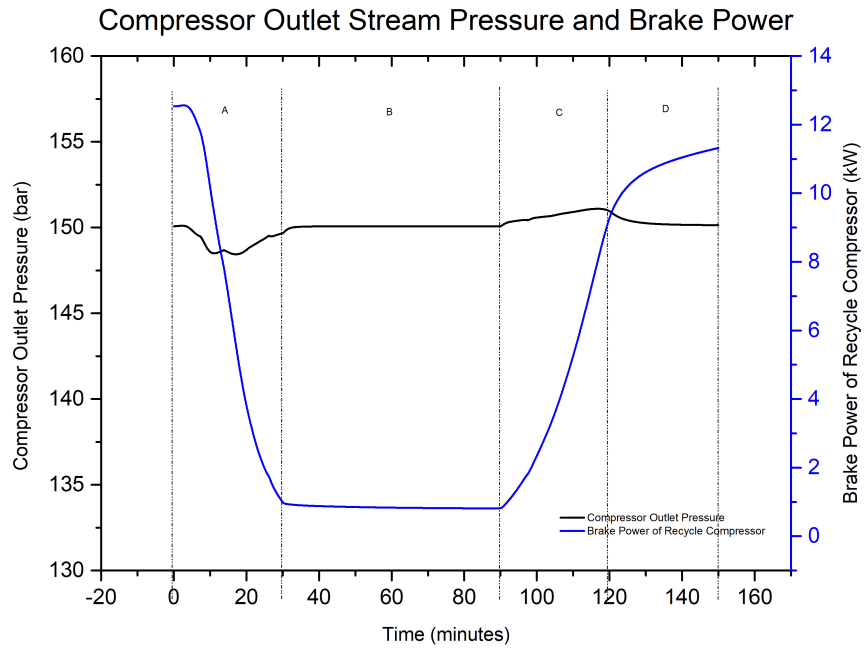## Recycle Compressor Outlet Stream Pressure and Brake Power
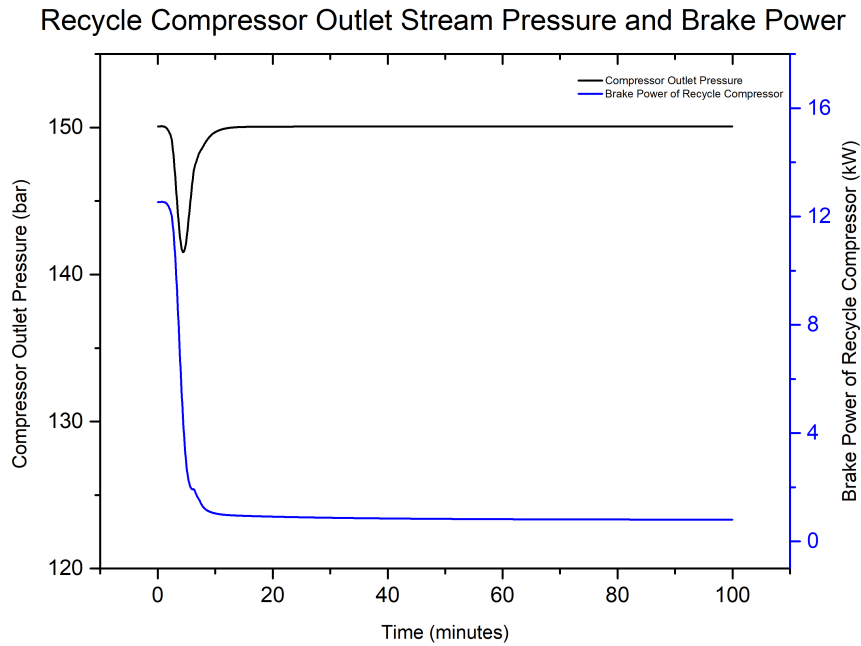
(b) Recycle Compressor Outlet Pressure and Brake Power

Figure B.1: Control Philosophy-2 response to 50% step change in hydrogen feed flow rate

It was observed that there is an initial pressure reduction of ~ 8 bar. The controller responds to change in pressure and therefore rectifies the pressure back to the set point in ~ 15 min. To increase the pressure back to the initial value, the recycle compressor brake power reduces from 12.5kW to 1kW.

The following Figure B.2 shows the response of control philosophy-2 to 70% reduction in hydrogen feed flow rate.

Feed Flow Rates

(a) Hydrogen and Nitrogen Feed Flow Rate

Recycle Compressor Outlet Stream Pressure and Brake Power
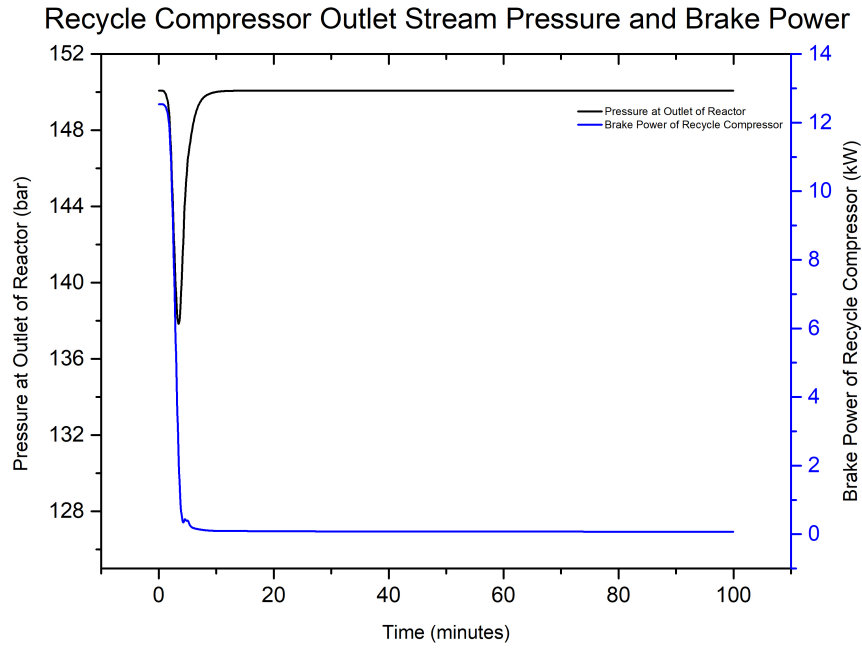
(b) Recycle Compressor Outlet Pressure and Brake Power

Figure B.2: Control Philosophy-2 response to 70% step change in hydrogen feed flow rate

It was noticed that for 70% reduction in hydrogen feed flow rate, the brake power of the compressor almost reaches to a negligible value. For the current scenario, a pressure reduction of ~ 12 bar was observed. To retain the system pressure, the brake power of the recycle compressor reduces from 12.5kW to 0.15kW.

B.2. Linear Change in Hydrogen Feed Flow Rate

Feed Flowrates

(a) Hydrogen and Nitrogen Feed Flow Rates

Compressor Outlet Stream Pressure and Brake Power

(b) Compressor Outlet Pressure and Brake Power

Recycle Flowrate and Ammonia Production Rate
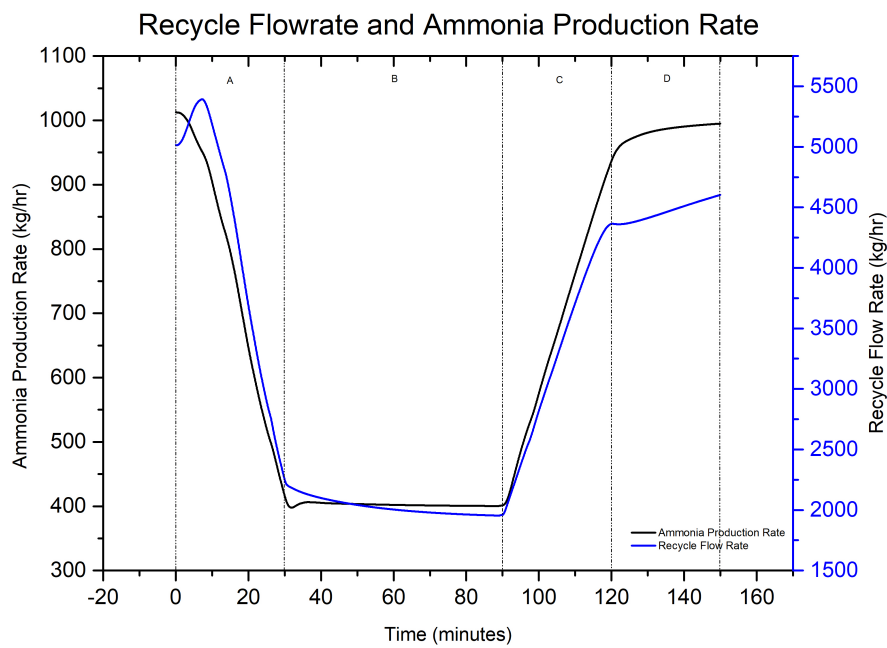
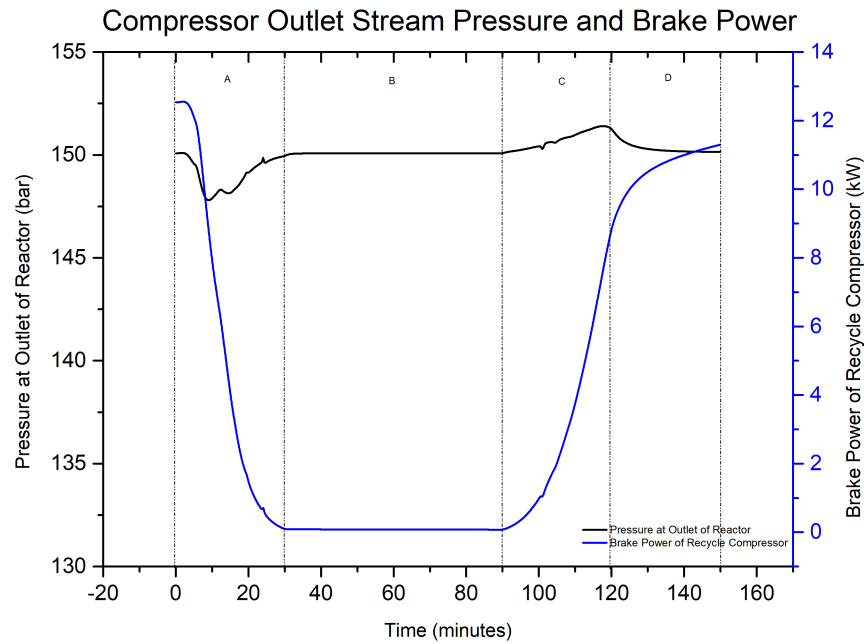**(c)** Recycle stream Flow Rate and Ammonia Production Rate

Figure B.3: Control Philosophy-2 response to 50% linear change in hydrogen feed flow rate
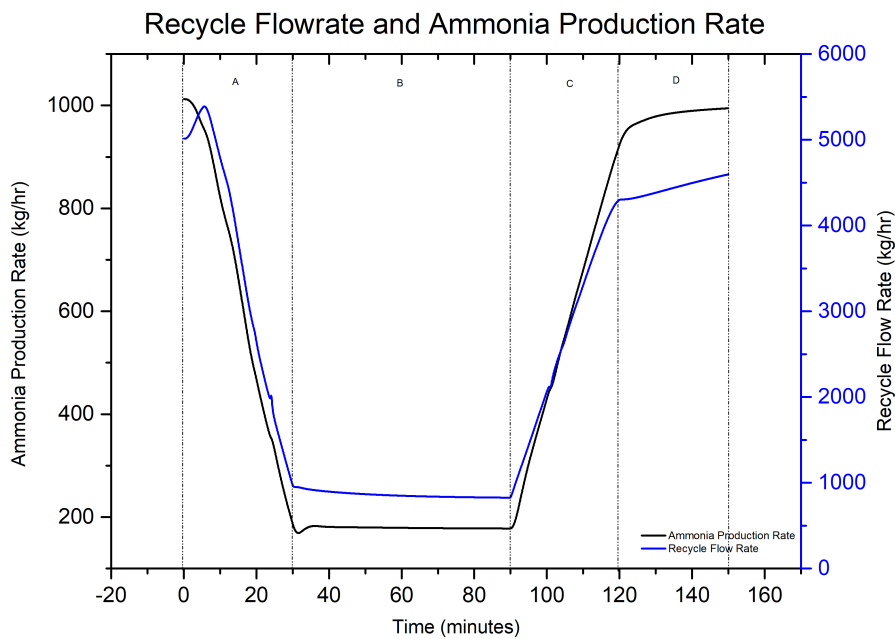
Results:

- **Region A:** A similar trend has been identified when observing reduction in hydrogen and nitrogen flow rates, as depicted in Figure A.3 of control philosophy-1. When there is a linear reduction in hydrogen feed flow rate by 50%, there is a gradual decrease in compressor brake power. This reduction in compressor power correlates with a decrease in flow rate, resulting in a less inflow of gas into the system. Therefore, the reduction in system pressure remains minimal and exhibits only minor fluctuations. The ammonia production also reduces by 50% due to reduction in feed flow rates. It is also observed that the brake power of the compressor also reduces gradually to 1 kW thereby, reducing the recycle flow rate too.

- **Region B:** For a span of 60 minutes, the hydrogen and nitrogen feed flow rates have been maintained constant in order to make the system reach its new steady-state as described in Table 5.1. The pressure of the system remains constant during this phase of simulation, but the recycle flow rate did not emerge to a steady-state value. This shows that the system requires more than 60 minutes to reach new steady-state conditions. The ammonia production rate also reduced by 50%.

- **Region C:** Hydrogen feed flow rate is ramped up back to original value for 30 mins and as a result, the recycle flow rate also increases. In order to compress this increased recycle flow rate, the brake power of the compressor also increases. The pressure in the system does not fluctuate a lot.

- **Region D:** The system is left for 30 minutes to reach its original steady-state conditions. The current model requires more time than simulated since the steady-state conditions are not reached within 150 minutes.
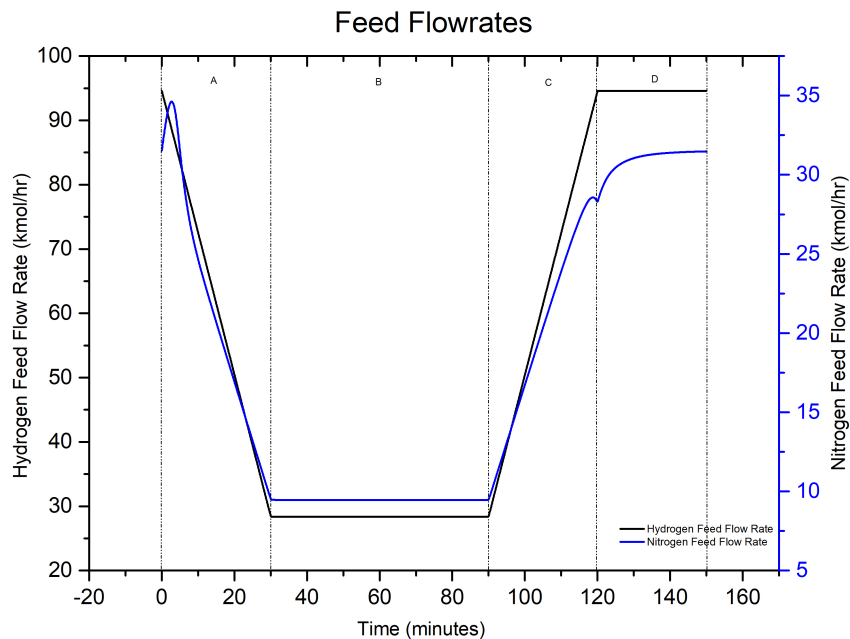
(a) Hydrogen and Nitrogen Feed Flow Rates

(b) Compressor Outlet Pressure and Brake Power

(c) Recycle stream Flow Rate and Ammonia Production Rate

Figure B.4: Control Philosophy-2 response to 70% linear change in hydrogen feed flow rate

A similar set of results are obtained as observed in 50% gradual reduction in hydrogen feed flow rate. It has been observed that the brake power of the compressor almost reaches to 0 kW indicating the compressor is shut down. The pressure in the system is regulated by this reduction in brake power and the recycle flow rate also reduces. The flow rate of the recycle stream also reduces from 5000 kg/hr to 1000 kg/hr.

C

Control Philosophy-3
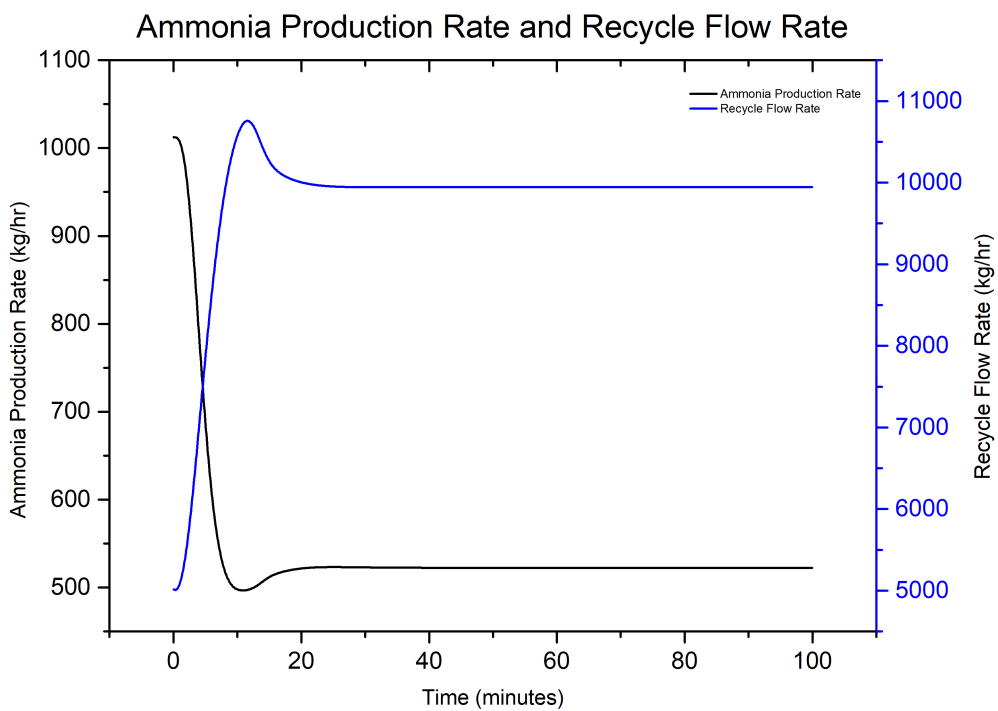
C.1. Step-Change in Hydrogen Feed Flow Rate

A step-change in reduction of hydrogen feed flow rate is implemented to examine the behaviour of the system. This step-change is carried out by reducing hydrogen feed flow rate by 50% and 70%. The response time of the controller and the effect of control action are noticed and plotted below in Figure C.1.
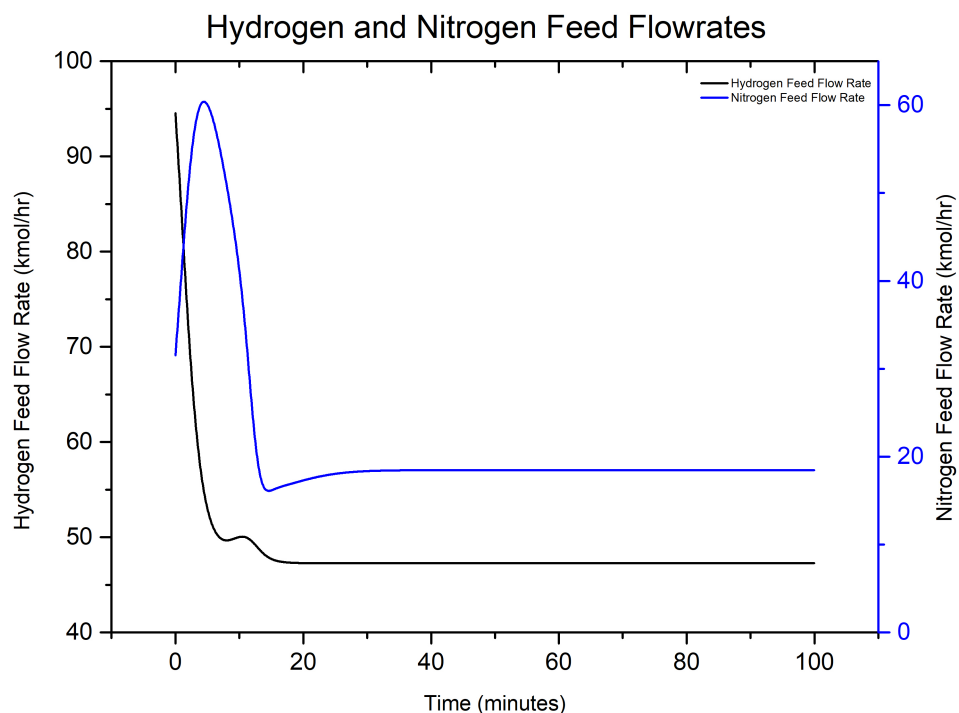
(a) Hydrogen and Nitrogen Feed Flow Rates
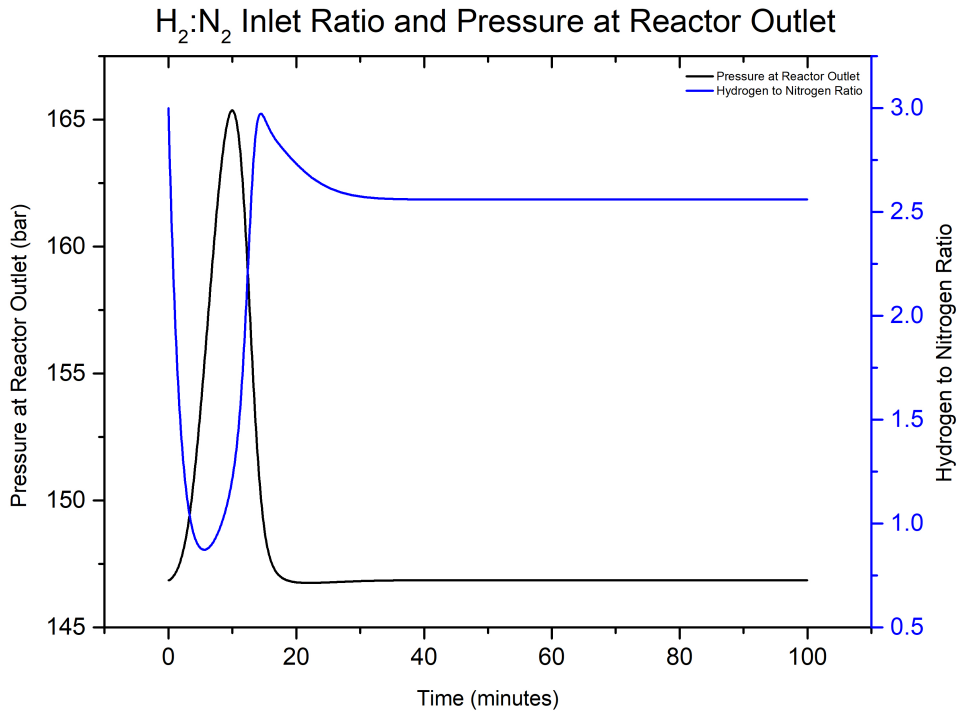
H$_2$:N$_2$ Inlet Ratio and Pressure at Reactor Outlet

(b) Inlet Feed Ratio and Pressure at Reactor Outlet

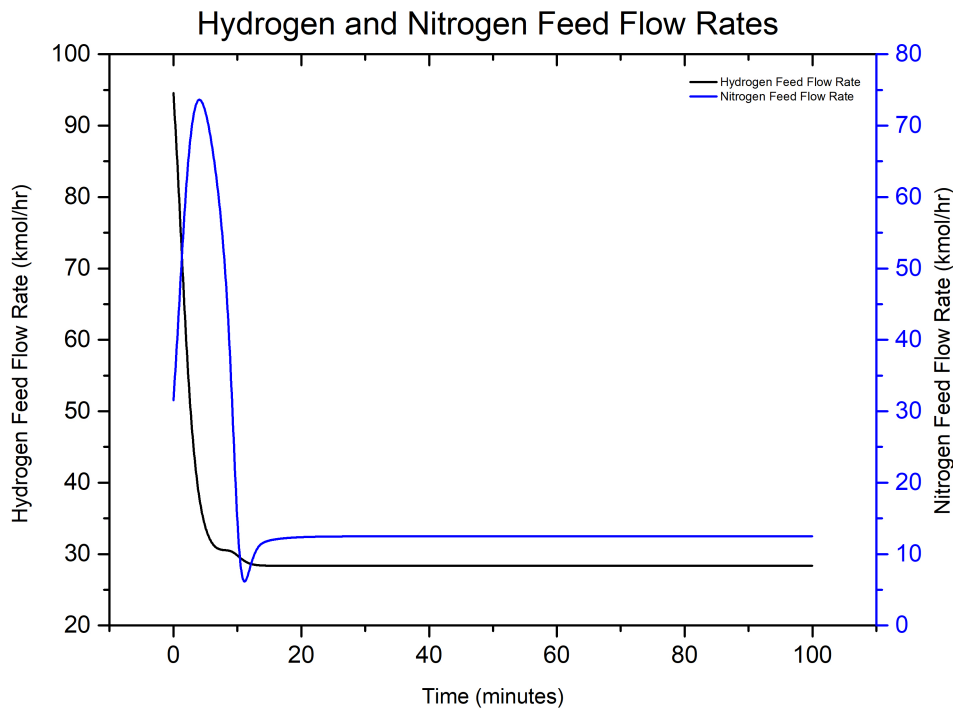## Ammonia Production Rate and Recycle Flow Rate

(c) Recycle stream Flow Rate and Ammonia Production Rate

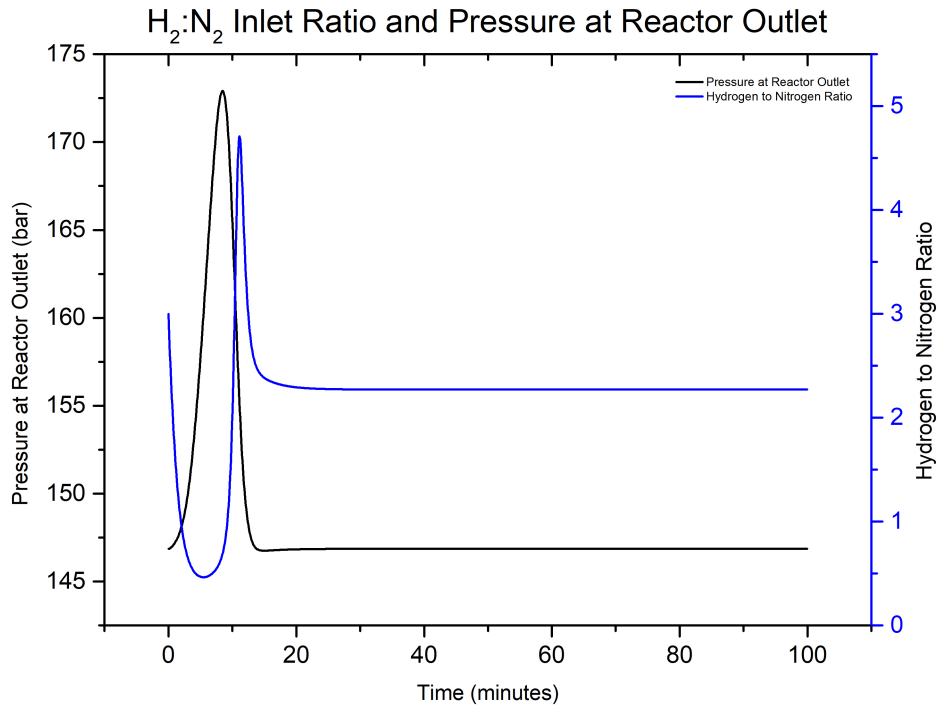**Figure C.1:** Control Philosophy-3 response to 50% step change in hydrogen feed flow rate

Results:

- When a 50% reduction in hydrogen feed flow rate is imposed, the nitrogen feed flow rate increases by 30 kmol/hr initially and again reduces. This response is observed as nitrogen is pumped to cover up the deficiency in hydrogen in the system.
- Due to this initial increase in the nitrogen feed flow rate, a peak in the pressure of the system is also observed. A pressure increase of 19 bar is observed but later the pressure stabilizes to its initial value.
- After the pressure is stabilized, the stoichiometric inlet ratio of hydrogen to nitrogen reduces from 3 to 2.56. This causes an increase in the nitrogen gas in the ammonia synthesis loop. Additionally, the recycle flow rate increases by 5000 kg/hr due to excess nitrogen in the system.
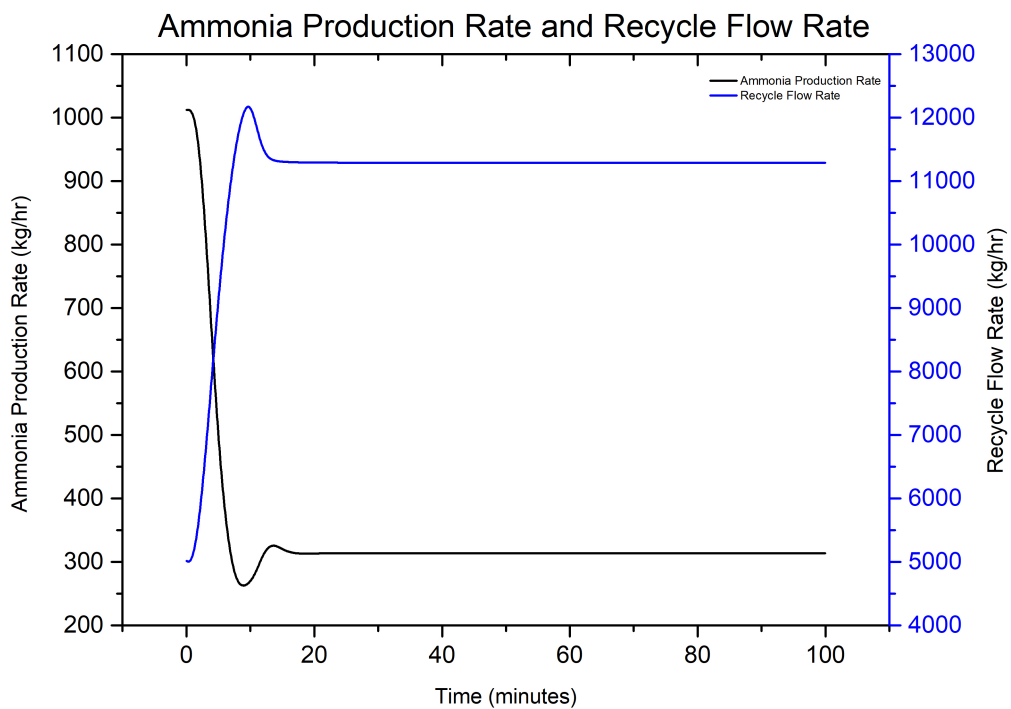
In a similar way, a step change of reduction of reduction of 70% of hydrogen feed flow rate is carried out and the results are shown below in Figure C.2.

(a) Hydrogen and Nitrogen Feed Flow Rates

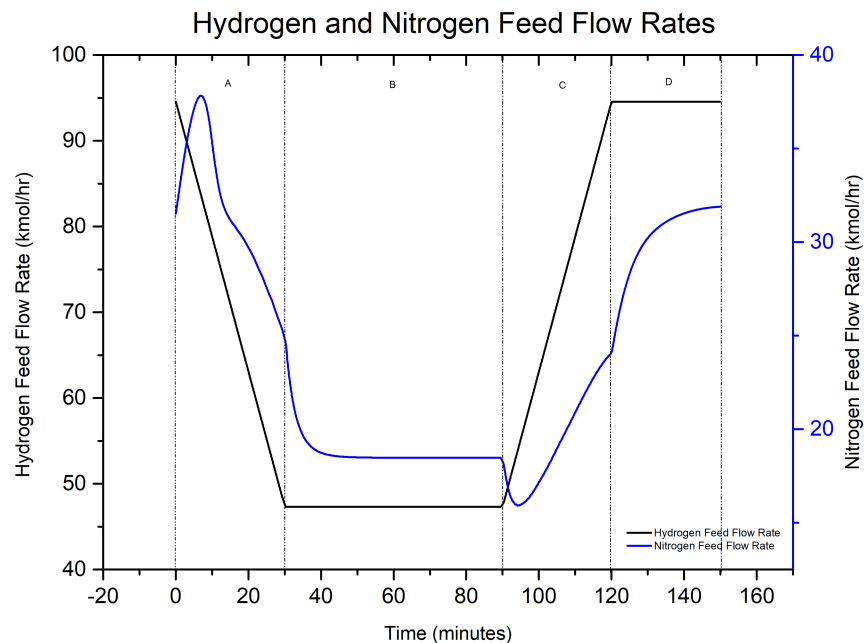**(b)** Inlet Feed Ratio and Pressure at Reactor Outlet

(c) Recycle stream Flow Rate and Ammonia Production Rate

Figure C.2: Control Philosophy-3 response to 70% step change in hydrogen feed flow rate

A similar pattern is observed compared to 20% and 50% step reduction in hydrogen feed flow rate. The nitrogen feed flow rate peaks its value to 75 kmol/hr from 31.5 kmol/hr in order to replace the deficit hydrogen in the beginning. As the system gets adapted to reduced hydrogen feed flow rate, the nitrogen feed flow rate again reduces to $\sim$ 12.5 kmol/hr. An initial pressure increase of 26.5 bar is observed and thereafter, the pressure is maintained constant after the reduction in nitrogen feed flow rate. Ammonia production rate also reduces by 70% due to less amount of reactants present. The stoichiometric ratio of $H_2 : N_2$ in the inlet changes from 3 to 2.27 in order to maintain the pressure in the ammonia synthesis loop. Due to the excess nitrogen, the recycle flow rate increases significantly by 6200 kg/hr which possesses a challenge to performance of the system.

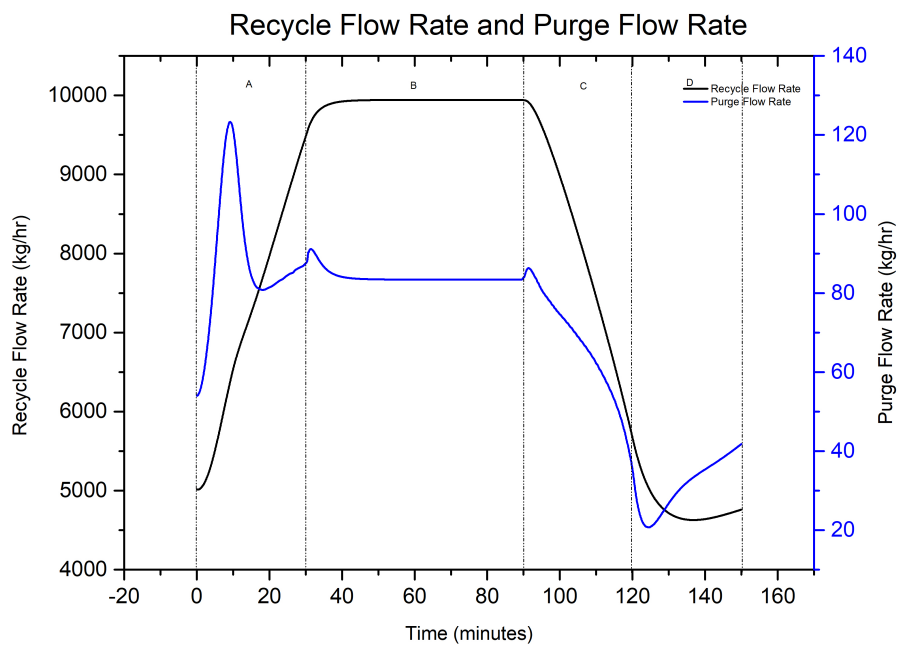## C.2. Linear-Change in Hydrogen Feed Flow Rate

The effect of 50% and 70% gradual reduction in hydrogen feed flow rates are shown in the following section. Figure C.3 shows the effect of 50% gradual reduction in hydrogen feed flow rate.
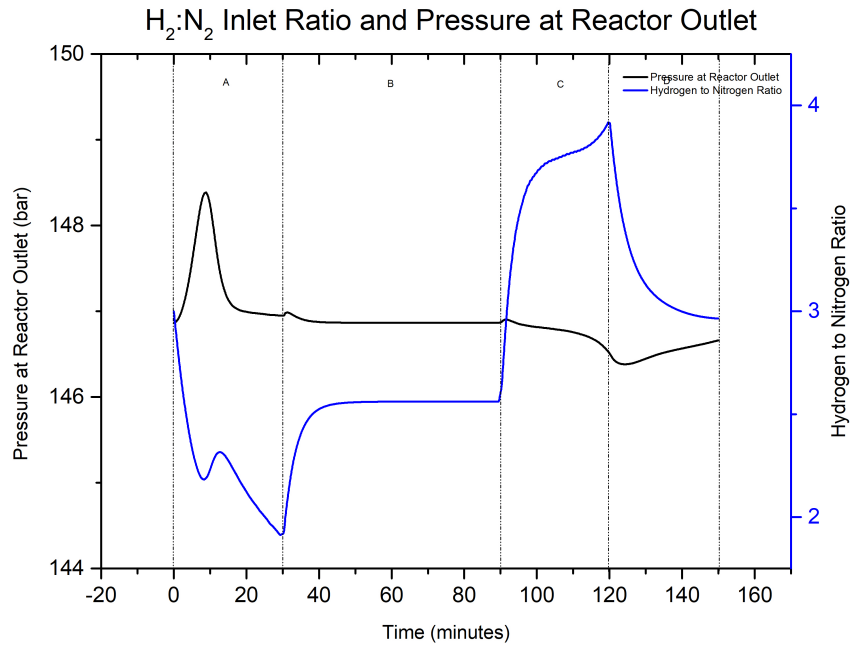
(a) Hydrogen and Nitrogen Feed Flow Rates

H$_2$:N$_2$ Inlet Ratio and Pressure at Reactor Outlet

(b) Inlet $H_2 : N_2$ Ratio and Pressure at Reactor Outlet

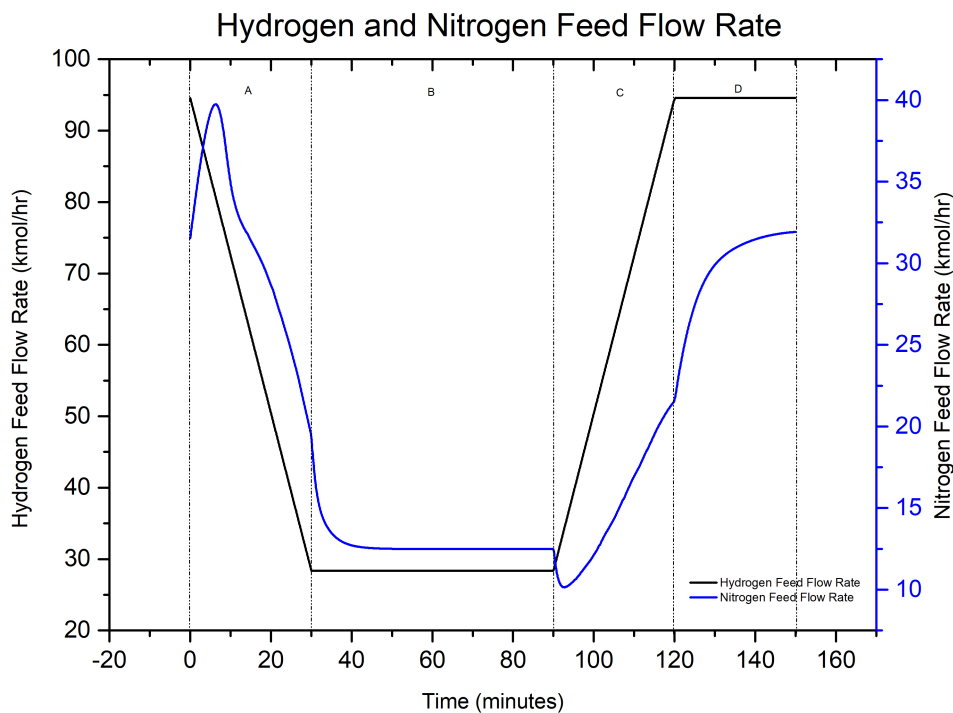## Recycle Flow Rate and Purge Flow Rate

(c) Recycle stream Flow Rate and Purge Flow Rate

Figure C.3: Control Philosophy-3 response to 50% linear change in hydrogen feed flow rate
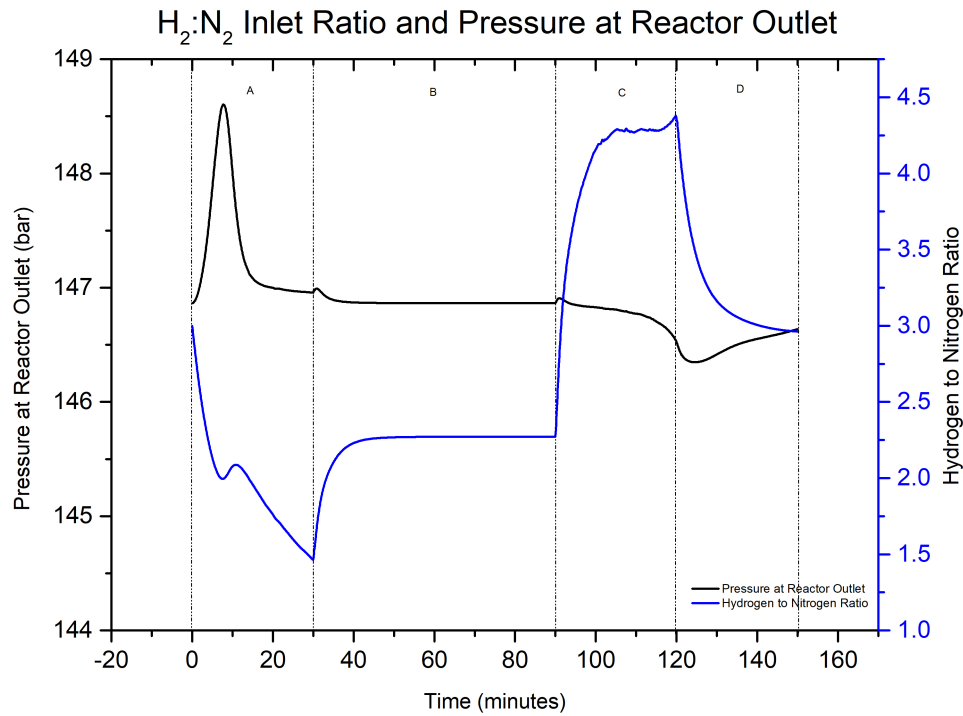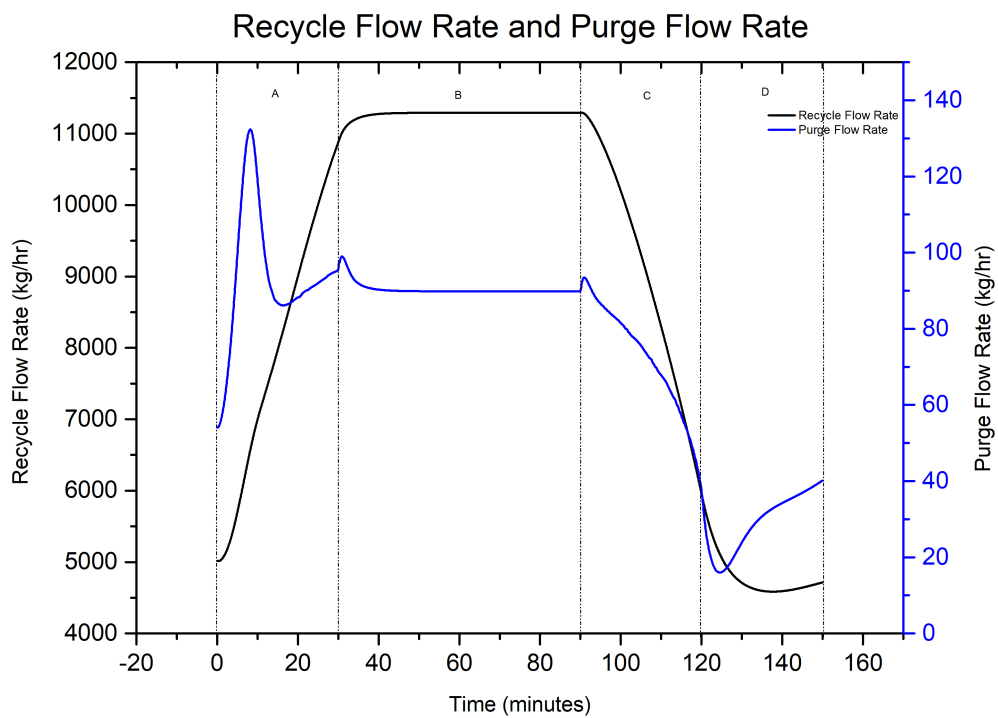
Discussion:

- **Region A:** A small increase in nitrogen feed flow rate is observed similar to the system's response to step change in hydrogen feed flow rate. After 10 minutes, the system again reduces the nitrogen feed flow rate. A 1.5 bar pressure increase in observed and in 20 minutes the controller stabilizes the pressure to its original value.

- **Region B:** When the feed is kept at a steady rate, the pressure in the system remains constant, suggesting a stable system response. The input hydrogen to nitrogen ratio stabilizes at 2.55 resulting in excess nitrogen in the system than at normal conditions. The recycle flow rate increases by 5000 kg/hr.

- **Region C:** With only a minor decrease in pressure, the pressure practically remains constant. The inlet ratio rises from 2.8 to 4, indicating an adjustment to the changing hydrogen supply flow rate. Both the recycle and purge flow rates drop in reaction to the increasing hydrogen feed flow rate.

- **Region D:** All the parameters do not reach to their initial values and therefore, a 150 minute simulation timeline is not sufficient for the system to reach the original steady state conditions.

The model's response to 70% gradual reduction in hydrogen feed flow rate is shown the Figure C.4 below.

(a) Hydrogen and Nitrogen Feed Flow Rates

(b) Inlet $H_2 : N_2$ Ratio and Pressure at Reactor Outlet

(c) Recycle stream Flow Rate and Purge Flow Rate

Figure C.4: Control Philosophy-3 response to 70% linear change in hydrogen feed flow rate

Discussion:

- **Region A:** A small increase in nitrogen feed flow rate is observed similar to all other responses. After 10 minutes, the system again reduces the nitrogen feed flow rate. A 2 bar pressure increase in observed and in about 15 minutes the pressure reduces and the controller stabilizes the pressure to its original value

- **Region B:** When the feed is kept at a steady rate, the pressure in the system remains constant, suggesting a stable system response. The input hydrogen to nitrogen ratio stabilizes at 2.27 resulting in excess nitrogen in the system than at normal conditions. The recycle flow rate increases by 6500 kg/hr.

- **Region C:** The pressure practically remains constant with minor fluctuations. The inlet ratio rises from 2.8 to 4.3, indicating an adjustment to the changing hydrogen supply flow rate. The recycle flow rate drops due to hydrogen being pumped into the system and almost reaches to its initial value.

- **Region D:** The simulation needs to be carried out for more than 150 minutes since the parameters do not reach their initial steayd state conditions. In this region the inlet ratio reduces from 4.5 to 3 due to the response of the ratio controller.

D

Economic Evaluation

D.1. Determination of Required Back-Up Electricity

The amount of heat gained/lost by a substance or sample is represented as:

$$Q = m \times C_p \times (T_{operating} - T_{ambient}) \tag{D.1}$$

The above Equation D.1 is used to calculate the amount of heat required to heat the catalyst bed in the reactor where m is the mass of the catalyst in kg and C_p is the specific heat capacity of the catalyst. In order to calculate the amount of heat required to heat the catalyst, the mass of catalyst present in the reactor should be determined. This is calculated by:

$$W_c = \rho_B \times V_R \tag{D.2}$$

where,

$$\rho_B = (1 - \epsilon)\rho_p$$

ρ_B is the bed density of catalyst

ρ_p is the particle density of catalyst (2200 kg/m^3)

ϵ is the bed voidage which is the percentage of bed volume uncovered by the particles (0.33)

V_R is the volume of the reactor (= 4.58 m^3 with 0.9 m diameter and 7.2 m length of reactor)

Substituting the above values in the above Equation D.2, the mass of catalyst is 6751 kg.

The thermal conductivity of iron is 0.451 kJ/kg°C [92]. The operating temperature of the reactor is 300°C and ambient temperature is considered as 25°C. Substituting all the values in the Equation D.1, the heat required to heat up the iron catalyst bed in the reactor from 25°C to 300°C is 835436.25 KJ which translates into **232 kWhr**.

The heat transfer between the reactor and surroundings i.e., the heat loss is calculated by:

$$Q = U \times A \times (T_{operational} - T_{ambient}) \tag{D.3}$$

where,

"U" is the heat transfer coefficient of insulation material. Glass wool is considered as insulation material with a thickness of 150 mm (0.2 W/m^{2}K) (thermal conductivity of glass wool is 0.023-0.040 W/mK)

"A" is the surface area of the reactor (21.62 m^2)

Substituting the above values in Equation D.3, the total heat lost is 1189.6 W, i.e., 1.18 kW. It is assumed that the dispersion of heat inside the reactor is much faster than loss of heat to the surroundings. Therefore, the total amount of back-up electricity required to keep the reactor warm is **233.18 kW**

D.2. Hydrogen Storage Tank Level

The following image below shows the storage level of the 300 kg hydrogen buffer considered as a function of time for 30 days.
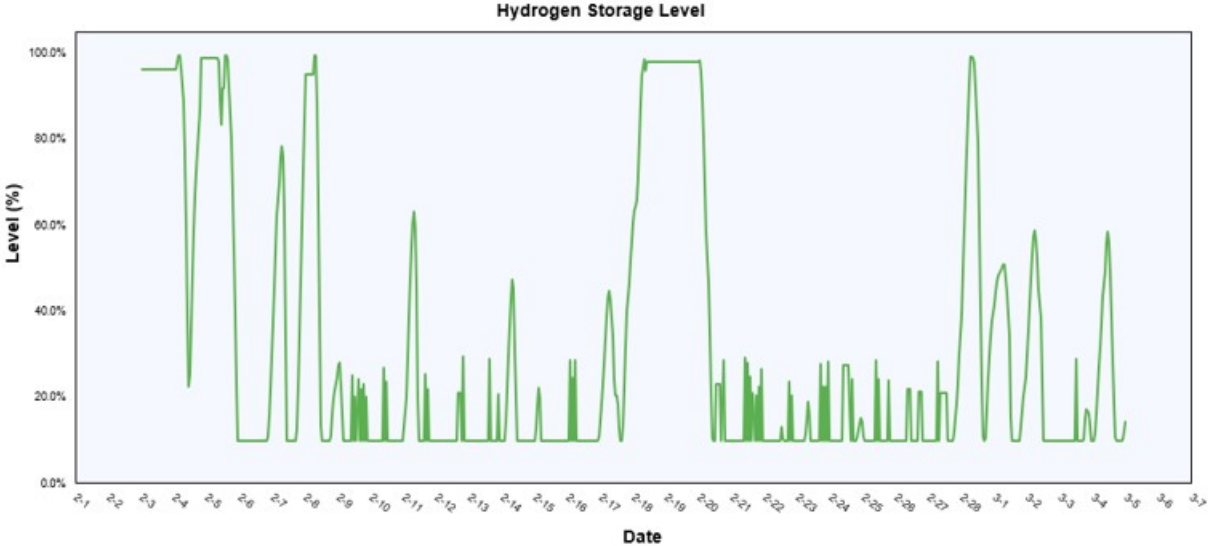

Figure D.1: Hydrogen Tank Storage Level (300 kg)